

AD-A110 561

RHODE ISLAND UNIV KINGSTON DEPT OF OCEAN ENGINEERING  
DESIGN OF AN ARTICULATED SPAR BUOY. (U)  
FEB 80 J W CUTLER

F/G 13/10

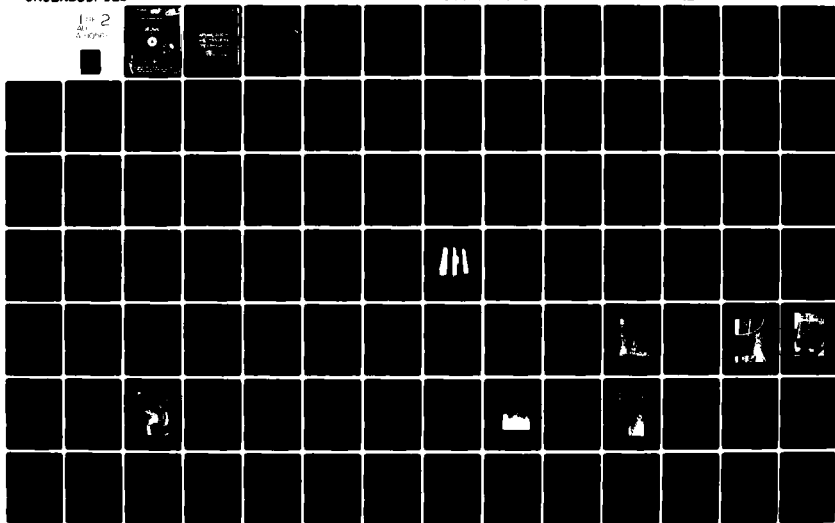
DOT-C8-81-78-1882

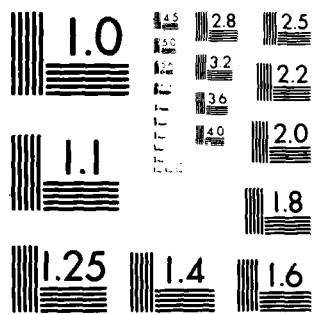
UNCLASSIFIED

USCG-D-71-81

NL

Fig 2  
Buoy





AD A110561



1. Report No. CG-D-71-81	2. Government Accession No. AD-A110 561	3. Recipient's Catalog No.	
4. Title and Subtitle  DESIGN OF AN ARTICULATED SPAR BUOY		5. Report Date FEBRUARY 1980	6. Performing Organization Code
		8. Performing Organization Report No.	
7. Author(s) JOHN W. CUTLER, JR.		10. Work Unit No. (TRAIS)	
9. Performing Organization Name and Address Department of Ocean Engineering University of Rhode Island Kingston, Rhode Island 02881		11. Contract or Grant No. DOT-CG-81-78-1882	
		13. Type of Report and Period Covered  FINAL REPORT	
12. Sponsoring Agency Name and Address United States Coast Guard Research and Development Center Avery Point Groton, Connecticut 06340		14. Sponsoring Agency Code CGR&DC 22/81	
15. Supplementary Notes  167			
16. Abstract  A generalized analytical model of the wind, current, and wave forces on an elliptical cylinder is presented with specific application to predicting the list angle of an articulated spar buoy. The major physical and environmental parameters present in the system are then analyzed to determine their relative influence on these forces and moments.  Data to validate this analytical model was obtained from both laboratory and field experiments. Model tests performed in a circulating water channel revealed that directional stability was a significant factor in determining the overall performance of elliptically cross-sectioned spars. Of the shapes investigated, only a circular cylinder with splitter plate was found to be stable and to return to an equilibrium position if displaced. Laboratory measurements of the circular cylinder list angle for various current velocities showed generally good agreement with that predicted by the analytical model.  Using a nominal 6 inch (16.83 cm) diameter, 1/2 inch aluminum spar 18 feet (5.49 m) in length with a splitter plate, field tests were obtained over a broad range of current and water depth conditions. Data from this field experiment also showed good agreement with that predicted by the analytical model.  On the basis of these results, it was concluded that for spars of circular cross-section, the analytical model is a good predictor of an articulated spar's behavior and, consequently, a useful design aid. Possible improvements to both the laboratory and field tests are suggested.			
17. Key Words  Articulated Spar List Angle Hydrodynamics Spar Buoys		18. Distribution Statement  This document is available to the U.S. public through the National Technical Information Service, Springfield, Virginia 22161	
19. Security Classif. (of this report)  UNCLASSIFIED	20. Security Classif. (of this page)  UNCLASSIFIED	21. No. of Pages	22. Price

# METRIC CONVERSION FACTORS

## Approximate Conversions to Metric Measures

Symbol	When You Know	Multiply by	To Find	Symbol
<b>LENGTH</b>				
in	inches	2.5	centimeters	cm
ft	feet	30	centimeters	cm
yd	yards	0.9	meters	m
mi	miles	1.6	kilometers	km
<b>AREA</b>				
sq in	square inches	6.5	square centimeters	cm <sup>2</sup>
sq ft	square feet	0.09	square meters	m <sup>2</sup>
sq yd	square yards	0.8	square meters	m <sup>2</sup>
sq mi	square miles	2.6	square kilometers	km <sup>2</sup>
acres	acres	0.4	hectares	ha
<b>MASS (weight)</b>				
oz	ounces	28	grams	g
lb	pounds	0.45	kilograms	kg
	short tons (2000 lb)	0.9	tonnes	t
<b>VOLUME</b>				
1/2 p	teaspoons	5	milliliters	ml
1/4 p	tablespoons	15	milliliters	ml
fl oz	fluid ounces	30	milliliters	ml
c	cups	0.24	liters	l
p	pints	0.47	liters	l
qt	quarts	0.96	liters	l
gal	gallons	3.8	liters	l
cu ft	cubic feet	0.03	cubic meters	m <sup>3</sup>
cu yd	cubic yards	0.76	cubic meters	m <sup>3</sup>
<b>TEMPERATURE (exact)</b>				
°F	Fahrenheit temperature	5/9 (after subtracting 32)	Celsius temperature	°C

\* 1 in = 2.54 centimeters. For other exact conversion factors and more detailed tables, see NBS Mon. Publ. 286, Guide for Weight and Measure, Price \$2.25, SO Catalog No. C13.10.286.

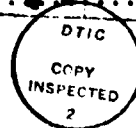
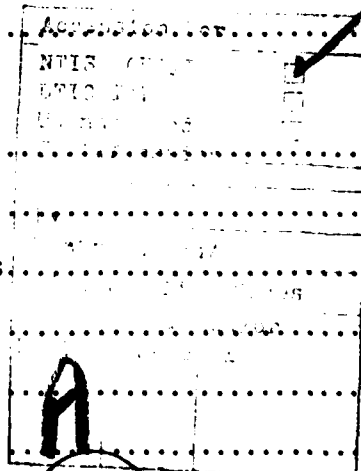
## Approximate Conversions from Metric Measures

Symbol	When You Know	Multiply by	To Find	Symbol
<b>LENGTH</b>				
mm	millimeters	0.04	inches	in
cm	centimeters	0.4	inches	in
m	meters	3.3	feet	ft
km	kilometers	0.6	miles	mi
<b>AREA</b>				
cm <sup>2</sup>	square centimeters	0.16	square inches	in <sup>2</sup>
m <sup>2</sup>	square meters	1.2	square yards	yd <sup>2</sup>
ha	hectares (10,000 m <sup>2</sup> )	0.4	square miles	mi <sup>2</sup>
ha	hectares (10,000 m <sup>2</sup> )	2.5	acres	ac
<b>MASS (weight)</b>				
g	grams	0.035	ounces	oz
kg	kilograms	2.2	pounds	lb
t	tonnes (1000 kg)	1.1	short tons	ton
<b>VOLUME</b>				
ml	milliliters	0.03	fluid ounces	fl oz
l	liters	2.1	pints	p
l	liters	1.06	quarts	qt
m <sup>3</sup>	cubic meters	0.26	gallons	gal
m <sup>3</sup>	cubic meters	35	cubic feet	ft <sup>3</sup>
m <sup>3</sup>	cubic meters	1.3	cubic yards	yd <sup>3</sup>
<b>TEMPERATURE (exact)</b>				
°C	Celsius temperature	9/5 (then add 32)	Fahrenheit temperature	°F



# TABLE OF CONTENTS

	Page
Acknowledgment.....	ii
List of Figures.....	iii
List of Tables.....	v
Nomenclature.....	vi
Chapter I. Background	
I-1 Introduction.....	1
I-2 Review of Relevant Literature.....	3
Chapter II. The Analytical Model	
II-1 Introduction.....	8
II-2 Overview.....	8
II-2.1 Theoretical Considerations.....	8
II-2.2 Steady Flow Forces.....	12
II-2.3 Wave Induced Forces.....	13
II-2.4 Drag Coefficient Determination.....	16
II-3 Computer Model Description.....	21
II-4 Sensitivity Analysis.....	25
II-4.1 Introduction.....	25
II-4.2 Analysis of Forces.....	25
Chapter III. Prototype Testing	
III-1 Introduction.....	34
III-2 Description of Facilities.....	34
III-3 Description of Prototype Models.....	35
III-4 Results.....	39
III-5 Additional Testing Results.....	49
III-6 Field Model Selection.....	50



## Chapter IV. The Field Study

IV-1 Spar Description.....	52
IV-2 Siting Considerations.....	54
IV-3 Data Collection.....	55
IV-4 Results.....	62
IV-4.1 Configuration #1.....	62
IV-4.2 Configuration #2.....	66
IV-4.3 Splitter Plate Removal.....	71

## Chapter V. Summary

V-1 Review of Results.....	75
V-2 Conclusions.....	77
V-3 Suggestions for Future Study.....	78
V-3.1 A Better Shape.....	78
V-3.2 Field Test Modifications.....	79

References.....	81
-----------------	----

## Appendices

A. Listing of the Computer Model, ASB1.....	A-1
B. User Manual for the Computer Model, ASB1.....	B-1
C. Design Drawings of the Field Test.....	C-1



#### ACKNOWLEDGMENT

The author also wishes to express his appreciation to Dr. Frank M. White for his overall support and critical insight with regard to certain phases of this work; most notably the effects of fluid flow past a non-rigid body.

The members of the U.S. Coast Guard Academy's Department of Applied Science and Marine Engineering especially CDR Bruce Skinner, LCDR Ted Colburn and LCDR Ron Marcolini are to be commended for allowing use of their circulating water channel, without which the successful completion of this work would not have been possible. Further, their questions, comments and suggestions with regard to the development of a successful prototype were invaluable. LCDR Colburn deserves special mention for his critical insight and timely suggestions during all phases of this work.

The author wishes to thank the staff of the University of Rhode Island's Academic Computer Center for providing the computing facilities necessary to develop this simulation model, plot various data, and produce this report.

The author is deeply indebted to members of the Ocean Engineering branch at the U.S. Coast Guard Research & Development Center; Groton, Connecticut, especially, Mr. Ken Bitting and Mr. Richard Walker who deserve special recognition for their unselfish assistance and encouragement throughout the duration of this contract.

The author also wishes to thank the members of the Department of Environmental Management's Marine Experiment Station where the field testing phase of this project took place for their support and assistance.

# LIST OF FIGURES

	Page
I-1 Diagram of the Brega, Libya Single Anchor Leg Mooring.....	5
II-1 Definition Sketch of the Coordinate System.....	9
II-2 The Shore Protection Manual Recommended Design Curve for the Variation in Drag Coefficient with Reynolds Number for Circular Cylinders (U.S. Army Corps of Engineers, 1973).....	18
II-3 Summary Flowchart of the Analytical Model.....	22
II-4 Influence of Current Velocity on Circular Cylinders of Various WPL/BPL ratios; $L/h = 1.3$ .....	30
II-5 Influence of Current Velocity on Circular Cylinders of Various $L/h$ ratios; WPL/BPL 0.446.....	31
II-6 List Angle vs. Current Velocity for Various (A/B) Ratios; Constant Projected Area, WPL/BPL = 0.446, $L/h = 1.3$ .....	33
III-1 The Three Spar Shapes Used in the Circulating Water Channel Tests.....	36
III-2 Scale Drawings of the Three Prototype Spar Cross-Sections....	38
III-3 The Elliptical Spar Being Tested in the Circulating Water Channel.....	43
III-4 The Circular Spar in the Circulating Water Channel with a Splitter Plate.....	46
III-5 Circulating Water Channel Theoretical and Observed List Angles for a Circular Cylinder, WPL/BPL = 0.094, $L/h = 1.25$ ..	48
III-6 Foppl Vortices Formed Behind a Circular Cylinder with a Splitter Plate.....	50
IV-1 The Field Prototype Articulated Spar.....	53
IV-2 The Field Prototype Anchor Attachment Point.....	55
IV-3 The Anchor Used for Testing the Field Prototype.....	56
IV-4 Map of Point Judith Pond and Vicinity.....	57
IV-5 Inclinometers Used in the Field Prototype Spar.....	59
IV-6 Inclinometer and Load Cell Wiring Diagram.....	60
IV-7 The Field Articulated Spar Anchored in Configuration # 1.....	65

IV-8 The Field Articulated Spar Anchored in Configuration # 2.....	67
IV-9 List Angle vs. Depth Curves for Various Current Velocities...	72
IV-10 Parity Plot of the Measured vs. Computed List Angle.....	73

## LIST OF TABLES

	Page
II-1 Influence of Various Parameters on the Spar's List Angle.....	28
III-1 List Angle Data for a 2.83 inch (7.19 cm.) Diameter Spar, 30 inches (76.20 cm.) in Length With a Splitter Plate.....	47
IV-1 Configuration # 1 Field Data.....	63
IV-2 Configuration # 2 Field Data.....	68
IV-3 Field Test Measurement Errors.....	69

# NOMENCLATURE

A	Major Axis Length of an Ellipse
$A_c$	Cross-sectional Area
$A_p$	Projected area
a	Wave Amplitude
B	Minor Axis Length of an Ellipse
$C_D$	Dimensionless Drag Coefficient
$C_I$	Dimensionless Inertia Coefficient
$C_M$	Hydrodynamic Mass Coefficient
D	Characteristic Width (diameter in the case of a circle)
d	Depth From Mean Sea-Level
$\frac{dv}{dt}$	Time Rate of Change of Velocity
$\vec{F}_B$	Buoyant Force
BPL	Buoyant Force per Unit Length
$\vec{F}_{current}$	Current Force
$\vec{F}_D$	Drag Force
$\vec{F}_H$	Hydrodynamic Force
$\vec{F}_I$	Inertia Force
$\vec{F}_{wa}$	Wave Force
$\vec{F}_{wind}$	Wind Force
f	Spar Oscillation Frequency
g	Gravitational constant
h	Total Water Depth ( d + n )
k	Wave Number
L	Characteristic Length
$M_B$	Moment Resulting From the Buoyant Force
$M_H$	Moment Resulting From the Hydrodynamic Force
$M_O$	Moment about the anchor attachment point, o

$M_{\text{Wgt}}$	Moment Resulting From the Spar Weight
$m_v$	Virtual Mass (1 + hydrodynamic mass)
$Re$	Reynolds Number
$S$	Strouhal Number
$T$	Wave Period
$\vec{U}, \vec{V}, \vec{W}$	Directed Fluid Velocities
$\vec{V}_c$	Current Velocity
$\vec{V}_n$	Velocity Normal to the Spar
$\vec{V}_{\text{wind}}$	Wind Velocity
$\vec{V}_{\text{wa}}$	Wave Particle Velocity
$\vec{V}_{\text{wp}}$	Water Particle Velocity
$W_{\text{gt}}$	Spar Weight
$W_{\text{PL}}$	Spar Weight per Unit Length
$X, Y, Z$	Orthogonal Coordinate System; Z positive upwards
$z_0$	Effective Roughness Parameter
$\rho$	Fluid Density
$\theta$	Angle of Inclination
$\eta$	Free Surface Elevation
$\sigma$	Wave Frequency

## CHAPTER I

### BACKGROUND

#### I-1 Introduction

The U.S. Coast Guard presently has over 24,000 lighted and unlighted buoys serving as aids to marine navigation in harbors, rivers, lakes and coastal areas across the United States. In addition, a multitude of fixed structures ranging in size from small daymarks to offshore towers are used to "warn the navigator of dangers and oostruction." (U.S. Coast Guard, 1972). While the nature of these fixed aids varies widely, buoy classification has been standardized based upon their maximum **diameter** and overall length. Standard lighted buoys are generally made of steel plate and range in size from the small 3 1/2 x 8 feet (1.07 x 2.44 m.) buoy to the large 9 x 32 feet (2.74 x 9.75 m.) shape. Typically, these buoys are held on station by a rectangular concrete block anchor which is connected to the surface floating buoy by an iron chain. In an ideal situation, the length of this mooring chain would be equivalent to the local water depth. Such a mooring system, however, would not be very secure as any horizontal forces resulting from either wind, waves or current would quickly move the buoy off station or, if the sinker were large enough, cause it to submerge. Since neither of these alternatives is desirable, the length of a buoy's mooring chain always exceeds the water depth. The length of the mooring chain is dependent upon a host of factors including the average water depth, the maximum current velocity and the size of the buoy itself. The ratio between the mooring chain length and the water depth, or scope, has been found to generally be about 2.5:1. (Bitting, 1976). There are, however, certain high current areas where the scope necessary to securely anchor a buoy

is considerably larger than this nominal value. Such increases in scope result in a subsequent enlargement of a buoy's watch circle (the area on the sea surface whose perimeter is defined by the maximum excursion of a buoy from its anchor). Aside from the economic considerations, increasing a scope and consequently the area of a buoy's watch circle limits the effectiveness of the aid to navigation in assisting "the navigator in determining his position." (U.S. Coast Guard, 1976).

Fixed aids are preferred to buoys because of the positional stability they provide the mariner. Unfortunately, however, floating debris and ice occasionally strike these pilings or fixed aids with sufficient force to damage them. Furthermore, in some instances the lower portion of the broken pile remains submerged while still implanted in the seabed thus imposing a potential hazard to vessel traffic in the area. More frequently, however, these pilings are struck and subsequently broken by barges and other large cargo carrying vessels. That such accidents take place is not surprising when one considers the rather confined quarters of a river or shipping channel as compared with the open ocean, and that barges are frequently rafted together around one tugboat for transport. The effect of such rafting means that both barges and tug move as one massive vessel. Even under the best of conditions, the maneuvering of this assemblage is difficult. When moving downstream, relative to the earth, the relative flow of water past the tug's rudder is reduced by the velocity of the current and consequently steering control of this tug-barge system becomes all the more difficult. Considering that these piles are often placed in locations where there is a change in the direction of the channel, it is not surprising that these aids are frequently struck or grazed. Besides barge traffic, strong currents have a tendency to scour the bottom thereby creating the possibility



that it will erode the pile where it enters the seabed.

As an alternative, an articulated spar which combines the most desirable features of both standard buoys and conventional fixed aids might be used as a functional aid to navigation in these situations. Such an aid would consist of an anchor, a universal joint or similar attachment mechanism and a rigid member extending from just above the channel bottom through the water column to a relatively short distance above the sea surface. Being free to rotate about its attachment point, such an aid would tilt when grazed by a passing vessel. In addition, debris or flowing ice which might cause a pile to break would simply push the articulated spar aside and continue to move downstream or else force the spar underwater while passing above it. Although such a spar would be free to rotate about its attachment point, its rigidity would restrict its watch circle to a very small area.

#### I-2 Review of Relevant Literature

The concept of an articulated spar is relatively new to the field of Ocean Engineering, the first of such devices being the product of oil company research. The Elf-Ocean Experimental Oscillating platform is a massive cylindrical articulating structure 21 feet (6.40 m.) in diameter and over 300 feet (91.44 m.) in length. (Villian, 1970). Originally placed on station in August of 1968 in the Bay of Biscay, this platform was designed primarily for oil exploration purposes. In addition, six large cylindrical subsurface floats provide a sufficient amount of buoyancy to make the platform stable enough for general offshore research and data collection purposes as well.

Although considerably smaller in size, another articulated tower which had its origin at about the same time was the Single Point Mooring

(S.P.M.). Also the product of oil company research, these moorings were developed for the loading and unloading of large tankers in severe environments and relatively deep water. Such moorings were designed for the purpose of being a much less expensive and more easily constructed alternative to the deep water berthing facilities necessary to accommodate Very Large Crude Carriers (V.L.C.C.). (Gruy and Kiely, 1977). While somewhat similar in concept to the articulated spar, S.P.M.'s also have some fundamental differences. The first S.P.M. installed at Breqa, Libya in October of 1969 for the Exxon Company serves as an example. (Synodis and Flory, 1977). This S.P.M. essentially consists of an anchor, a universal joint, a riser section, a subsurface buoyancy chamber, a mooring float and some connecting chain. In addition, one or a series of hose sections leads from the swivel joints located at the top of the buoyancy chamber to either the vessel being loaded or, when not in use, to the mooring buoy itself. This configuration is shown in Figure I-1. From this sketch it can be seen that the upper portion of the S.P.M. with its flexiole anchor chain more closely resembles a standard mooring system.

In the early 1970's a series of light beacons known as Sarus Towers were constructed and installed in several countries including Australia, Papua, New Guinea and Indonesia. The Sarus Tower design combines the reliability of a fixed structure with the low capital cost, ease of installation and flexibility of a lighted buoy. Unlike the articulated spar, the main body of the Sarus tower is composed of not one, but three rigid members which are welded together end to end. While the exact dimensions of these towers may vary from site to site, the installation at Port Hedland, on the western coast of Australia serves as an example. (Whitaker, 1975). At this location, the lower

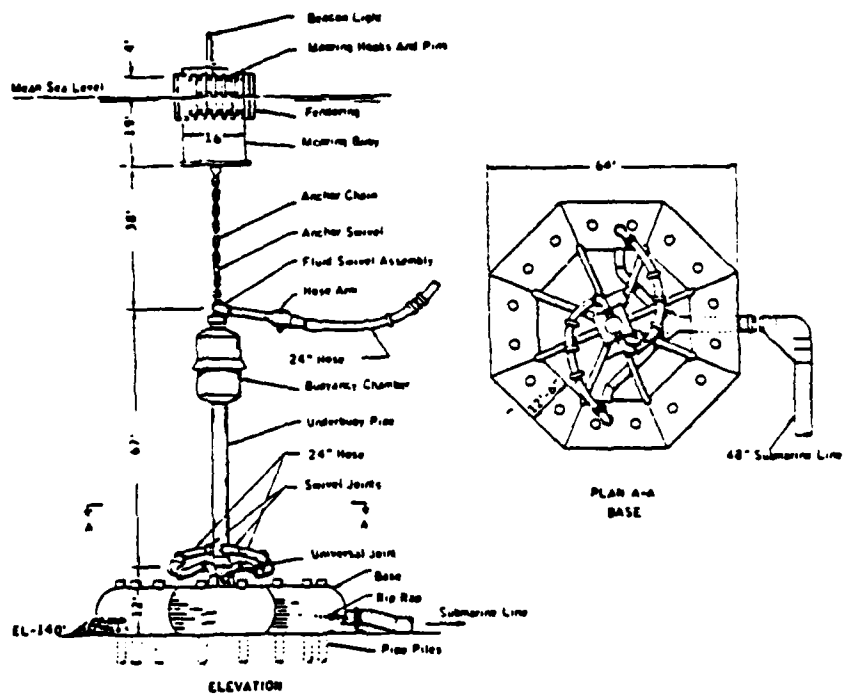


Figure I-1  
Diagram of the Brega, Libya Single Anchor Leg Mooring

cylinder is a 42 inch (106.68 cm.) diameter section of 1/2 inch (1.27 cm.) plate steel measuring 25 feet (7.62 m.) in length. The upper cylinder is also made of steel plate and has a maximum diameter of 36 inches (91.44 cm.) which gradually tapers to a minimum diameter of approximately 24 inches (60.96 cm.) at the upper end of its 40 feet (12.19 m.) length. A large subsurface cylindrical buoyancy chamber with dished ends serves to join these two sections. At the Port Hedland installation, the buoyancy chamber has a diameter of 9.5 feet (2.90 m.) and a maximum length of only 7.5 feet (2.29 m.). By compartmentalizing this buoyancy chamber into four sections, one section can become flooded without endangering the buoyancy of the entire structure.

Another group of articulated light beacons are those located at the entrance to Genoa harbor in Italy. At this location, the nearly one mile long entrance channel has been dredged to a depth of approximately 50 feet (15.24 m.) to accommodate large, deep draft tankers. (Dell'Aggio, 1972). However, the width of this entrance channel ranges from 850 feet (259.08 m.) at its seaward end to under 400 feet (121.92 m.) at the jettyhead. Consequently, conventional buoys with scopes of about 2:1 were found to be unsatisfactory for defining the edges of this narrow channel. To solve this problem a series of articulated light beacons were designed and built by the Resinex Company of Iseo, Italy. These beacons are some 56 feet (17.07 m.) in length and from photographs appear to be about 1 foot (0.30 m.) in diameter. They are composed of an anchor, a special spherical steel joint, a galvanized steel pipe and a steel frame platform which is mounted at the surface end of the structure and used for servicing purposes. Like similar structures, a series of subsurface floats fixed at mid-depth provide additional buoyancy and stability, thus reducing oscillation of the structure to a few

degrees. Being located in a relatively protected environment, these beacons were designed to withstand the combined forces of approximately 100 miles per hour (160.93 km./hr.) winds and 16 feet (4.88 m.) seas without excessive heeling.

In addition to being used as stable platforms and aids to navigation, an articulated spar has been successfully designed and constructed to measure oscillatory flow and wave direction. (Lowe et.al., 1974). Using an 8.9 cm diameter air filled, filament wound pipe attached through a universal joint to a bottom anchor, motion was measured by two orthogonally-mounted accelerometers located in the top portion of the spar. Moored in 33 feet (10.06 m.) of water, this spar behaved as a forced, damped oscillator. Spectral analysis of the accelerometer records showed that for wave periods less than 10 seconds, the tilting spar showed reasonable agreement with a computer simulation model of its behavior. At larger wave periods the model predicted tilt angles which were too low. It was conjectured that this was the result of the computer model's use of constant drag and inertia coefficients.

Excluding Lowe's tilting spar used for wave measurements, all of the aforementioned devices have been located in water depths of 40 feet (12.19 m.) or greater. To the author's knowledge, no proposed designs and/or constructions of articulated spars in the 15 to 30 feet (4.57 to 9.14 m.) water depths, typical of river channels, currently exist in the literature. Without exception, the greatest design force imposed upon any of these existing structures is the result of wave action. In the relatively confined area of a river or shipping channel where the proposed articulated spar device would be employed, however, current forces are expected to be the most important design consideration.

## CHAPTER II

### THE ANALYTICAL MODEL

#### II-1 INTRODUCTION

An analytical model which computes the total force, resultant moment and list angle of a spar device with either a circular or elliptical cross-section in the presence of wind, current and wave forces has been developed. In the sections that follow, a detailed derivation of this analytical model is presented.

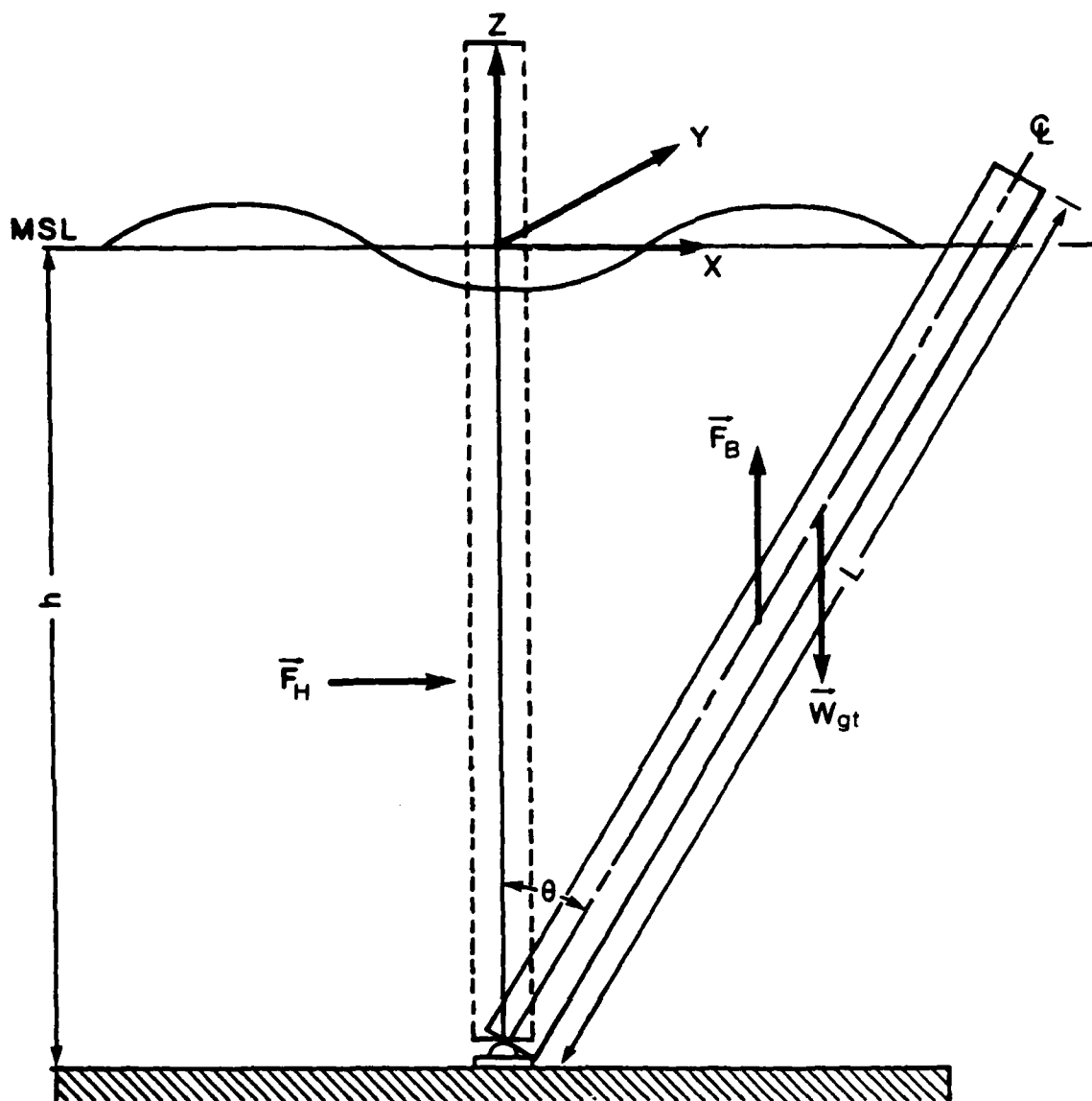
#### II-2 Overview

##### II-2.1 Theoretical Considerations

In dealing with the forces on a three-dimensional structure such as a spar, it is important to establish a coordinate system and fix its location in space. The origin of the coordinate system used in this analysis is the geometric center of the spar cross-section defined by the still water surface at zero angle of inclination,  $\theta$ , as shown in Figure II-1. The velocity components  $U, V$ , and  $W$  correspond to velocities, in the  $X, Y$ , and  $Z$  directions respectively with the  $Z$  axis being defined as positive upwards.

A combination of wind, current and wave forces are considered to be acting on the articulated spar in this analysis. Since the time responses of this spar system to changes in the current forces, the most critical for the proposed application, are shorter than the time rate of change of the current field, dynamic effects are assumed to be unimportant to this analysis. Consequently, this analysis assumes the articulated spar to be in a state of static or quasi-static equilibrium.

Fluid particles traveling past a fixed body exert both normal and tangential forces on it. Under conditions of static equilibrium, the



$\bar{F}_H$  - HYDRODYNAMIC FORCE

$\bar{F}_B$  - BUOYANT FORCE

$\bar{W}_{gt}$  - SPAR WEIGHT

$\theta$  - SPAR ANGLE OF INCLINATION

FIGURE II-1 DEFINITION SKETCH OF THE  
COORDINATE SYSTEM

body must remain stationary, requiring that the summation of forces and moments must be zero:

$$\Sigma \vec{F} = 0 \quad (1)$$

$$\Sigma M_o = 0 \quad (2)$$

where o may be any point on the body. The forces on the spar in Figure II-1 may be described in vector form by

$$\Sigma \vec{F} = 0 = \vec{F}_H + \vec{F}_B + \vec{W}_{gt} \quad (3)$$

where  $\vec{F}_H$  is the hydrodynamic force composed of a drag and inertia component following the approach of Morison, et. al. (1950),  $\vec{F}_B$  is the buoyant force and  $\vec{W}_{gt}$  is the spar weight. It should be noted that the hydrodynamic force,  $\vec{F}_H$  also includes the force of wind on the exposed portion of the spar. Similarly, the moments about any point o may be described by

$$M_o = 0 = M_H + M_B + M_{Wgt} \quad (4)$$

where the subscripts are the same as those used in Eq. (3). By applying these two fundamental principles of statics to this analysis, the list angle,  $\theta$ , of the articulated spar device may be resolved. A further term could be added to Eqs. (3) and (4) to represent a lumped mass such as might occur if light signal equipment and daymarks were added to the spar or to denote additional floatation.



In this analysis, the wind velocity is assumed to act on that portion of the spar which is above the still water surface to induce the wind force shown in Figure II-1. Similarly, a combination of current and wave particle velocities and accelerations are assumed to act on the submerged portion of the spar inducing the hydrodynamic force also shown in Figure II-1. By convention, these wind, current and wave particle velocities and accelerations are resolved into components normal and tangential to the spar. In addition to these two normal hydrodynamic forces, the buoyant force acts vertically upwards from the center of buoyancy and the weight acts vertically downward from the center of gravity as described in Equation (3). Once these forces are resolved, moments are taken about the anchor attachment point. In the convention adopted in this analysis, the overturning moment created by the wind and water particle forces acts clockwise while the righting moment resulting from the buoyant force acts counterclockwise as shown in Figure II-1.

The total hydrodynamic force on the spar may be described by the Morison equation as

$$\vec{F}_H = \frac{1}{2} \rho A_p |\vec{v}_n| \vec{v}_n C_D + \rho A_c L \frac{d\vec{v}}{dt} C_M \quad (5)$$

where the first term on the right hand side is the drag force and the second term the inertia force. In the drag force term of Equation (5),  $\rho$  is the fluid density,  $A_p$  is the projected area normal to the flow,  $\vec{v}_n$  is the velocity normal to the object and  $C_D$  is a dimensionless drag coefficient. The absolute signs are included to preserve the directionality of the resulting force term. The inertia portion of the total hydrodynamic force is composed of  $\rho$ , the density of the fluid,  $A_c$  the cross-sectional area of the body,  $L$ , the length of the body,  $\frac{d\vec{v}}{dt}$ , the

local fluid acceleration and  $C_M$  the hydrodynamic mass coefficient.

## II-2.2 Steady Flow Forces

Over a time period on the order of minutes, those forces induced by reasonably steady winds and currents may be considered steady while those induced by waves will be time dependent. Consequently, for these steady flow forces, the  $\frac{d\vec{v}}{dt}$  term is zero and, therefore, the total wind and current forces may be completely described by their drag component. Thus

$$\vec{F}_{\text{wind}} = \frac{1}{2} \rho A_p |\vec{v}_{\text{wind}_n}| \vec{v}_{\text{wind}_n} C_D \quad (6)$$

$$\vec{F}_{\text{current}} = \frac{1}{2} \rho A_p |\vec{v}_{c_n}| \vec{v}_{c_n} C_D \quad (7)$$

In this analysis, one may specify the fluid in which the spar is immersed as either fresh or salt water. Although the density of brackish river water is a function of salinity and temperature, the variation in these properties is small over the range of variation expected and as a result, this value is assumed to be constant. The density values of air and water selected for use in this model are defined at a temperature of 68°F (20°C).

It is well known that near a surface such as land or water the wind velocity profile over that surface is not uniform but varies with both time and altitude. Ignoring the time scale variations, the wind velocity profile in this model is assumed to follow the well known Prandtl-von Karman universal velocity distribution law:

$$\frac{\vec{U}_a}{\vec{U}_{10}} = \frac{\ln(z/z_0)}{\ln(10/z_0)} \quad (8)$$

where  $z$  is the height of measurement in meters and  $z_0$  is an effective roughness parameter. Since only large velocity winds are expected to significantly effect a spar's list angle, a  $z_0$  value of .003 m. as suggested by Myers, et.al. (1969) for strong winds is used in this model.

As a result of this assumed distribution, the wind speed used as input to this computer model must have an elevation associated with it. Based upon this one wind data point, an entire wind profile including the velocity at the 10 meter level is determined. Furthermore, this 10 meter wind velocity value is used as input to the Sverdrup, Munk and Bretschneider (S.M.B.) computations described below.

#### II-2.3 Wave Induced Forces

In order to determine the total water particle force on a structure using Equation (5), it is necessary that the horizontal and vertical particle velocities and accelerations be known. Unlike the wind and current velocities which are easily measured, the wave velocities and accelerations required for this analysis are often estimated using simple wave theory. The question as to which wave theory to apply to determine the appropriate values for use in the Morison equation has been studied extensively. Patton (1966) states that for a body that is small compared to the wavelength, the water wave may be adequately described by Airy wave theory. Dean (1967) has shown that higher order Stokes theories (3rd and 5th) as well as Cnoidal wave theory are not uniformly more applicable than Airy theory. Further, Dean points out that Airy wave theory satisfied the kinematic boundary conditions at the surface much better than these higher order theories for shallow water waves (Edge and Myer, 1969). In general, the literature seems to support the premise that for most applications, the well known Airy formulations for particle

velocity and acceleration are the most logical for substitution into the Morison equation. Using Airy theory, the horizontal and vertical components of the local fluid particle velocity,  $\vec{U}$  and  $\vec{W}$  respectively, are:

$$\vec{U} = \frac{agk}{\sigma} \frac{\cosh k (h + z)}{\cosh kh} \sin (kx - \sigma t) \quad (9)$$

$$\vec{W} = \frac{agk}{\sigma} \frac{\sinh k (h + z)}{\cosh kh} \cos (kx - \sigma t) \quad (10)$$

where  $g$  is the gravitational constant,  $k$  is the wave number, and  $\sigma$  is the wave frequency. The local fluid acceleration terms in the horizontal and vertical directions may be found by differentiating Eqs. (9) and (10) with respect to time,  $t$ , resulting in

$$\frac{\partial \vec{U}}{\partial t} = -agk \frac{\cosh k (h + z)}{\cosh kh} \cos (kx - \sigma t) \quad (11)$$

$$\frac{\partial \vec{W}}{\partial t} = -agk \frac{\sinh k (h + z)}{\cosh kh} \sin (kx - \sigma t) \quad (12)$$

Equations (9) to (12) have two parts: an amplitude term and a phase term. The phase term in each describes the oscillatory nature of the wave particle velocity and acceleration. The amplitude term in each equation is composed of a constant part and a hyperbolic part. This hyperbolic portion accounts for the exponential decay of the horizontal and vertical velocity and acceleration components with increasing water depth.  $h$  in these equations is the time dependent total depth which is defined as

$$h = d + \eta \quad (13)$$

where  $d$  is the still water depth and  $\eta$  is the corresponding wave height defined by

$$\eta = a \cos \frac{2\pi t}{T} \quad (14)$$

where  $a$  is the wave amplitude and  $T$  the wave period.

Because of the nonlinearity of the drag coefficient used in these drag force determinations, the total water particle force may not be determined by the superposition of the current and wave forces (Wu and Tung, 1975). Rather, this total water particle force must be determined by first vectorally summing the individual velocity components and then substituting this resultant water particle **velocity** into the drag force term of the Morison equation. Thus the water particle force may be defined by

$$\vec{F}_{wp} = \frac{1}{2} \rho A_p |\vec{v}_{wp}| \vec{v}_{wp} C_D + \rho A_c L \frac{d\vec{v}}{dt} C_M \quad (15)$$

where the water particle velocity,  $\vec{v}_{wp}$ , is defined as

$$\vec{v}_{wp} = \vec{v}_c + \vec{v}_{wa} \quad (16)$$

where  $\vec{v}_c$  is the current velocity and  $\vec{v}_{wa}$  is the water particle velocity.

In this analysis, however, no consideration is given to the possible interaction effects between wave induced and current velocities. Such

interaction effects have been examined in detail by Jonsson, et. al. (1970). When a current and waves are traveling in the same direction, for example, wave length tends to increase and height and period tend to decrease. These effects have been considered significant enough that they have been accounted for in the design of North Sea oil drilling platforms where waves are the dominant forces on the structures. (Mes, 1977). However, since the use of a wave correction factor to account for these interaction effects necessitates the use of an effective average current value, this formulation was not included in the analytical model.

The waves in this analysis are assumed to be wind generated and consequently act in the same direction as the wind. When considering wave forces, input data is either supplied in terms of wave height and period or can be calculated using the S.M.B. method.

#### II-2.4 Drag Coefficient Determination

A cylinder with a circular cross-section is the most common structural element in the ocean and as a result a great many experiments both in the laboratory and in the field have been performed in an effort to define precisely the drag and inertia coefficients of the Morison equation. The general procedure followed in these experiments has been to measure the forces on the structure as well as the wave and current conditions. Using a suitable wave theory, the water particle velocity is subsequently computed. The results of these experiments, however, differ widely. (Bretschneider (1957), Agerschou and Edens (1965), Wieselburger (1968), Keulegan and Carpenter (1956), etc.). Since it is necessary to employ a wave theory to calculate the water particle kinematics from the measured surface profile, the resulting range in these coefficient values reflects not only possible inaccuracies in the Morison formulation but in

the wave theory used as well. More significantly, it was discovered that even in a series of identical waves, scatter was found in the wave forces measured. Further analysis has shown that this wide scatter in the published data is related not only to the wave theory selected and the accuracy of the measurement system but also to the roughness of the pile, local currents, vibrations in the test piles, the proximity of neighboring piles and other effects. The U.S. Army Coastal Engineering Research Center has examined a great deal of this data in an attempt to simplify the problem of selecting the proper data set and have subsequently developed a recommended design curve. This curve, shown in Figure II-2, has been incorporated into this analytical model for application when dealing with circular cylinders. One should note for purposes of comparison, Figure II-2 also presents results of some laboratory and field measurements of drag coefficients.

In Equation (5), it was shown that the drag coefficient is not only a function of Reynolds number but roughness and length effects as well. Further it was pointed out that data regarding these effects is generally obtained in separate analyses to establish trends. In the case of the dimensionless spar length-to-diameter ratio ( $L/D$ ), it has been observed that the importance of this parameter increases as the spar length decreases. In such cases, the pressure at the end(s) of the spar is relieved since water is allowed to flow around the end of the spar rather than being forced to one side of it. Consequently, as the ( $L/D$ ) ratio decreases so does the drag coefficient. However, empirical data regarding this effect has only been documented for Reynolds numbers in the range  $10^4$  to  $10^5$ . Furthermore, this ratio has been shown to be most significant for small [ $<10$ ] ( $L/D$ ) ratios. By contrast the articulated spar considered in the analytical model is generally expected to have an

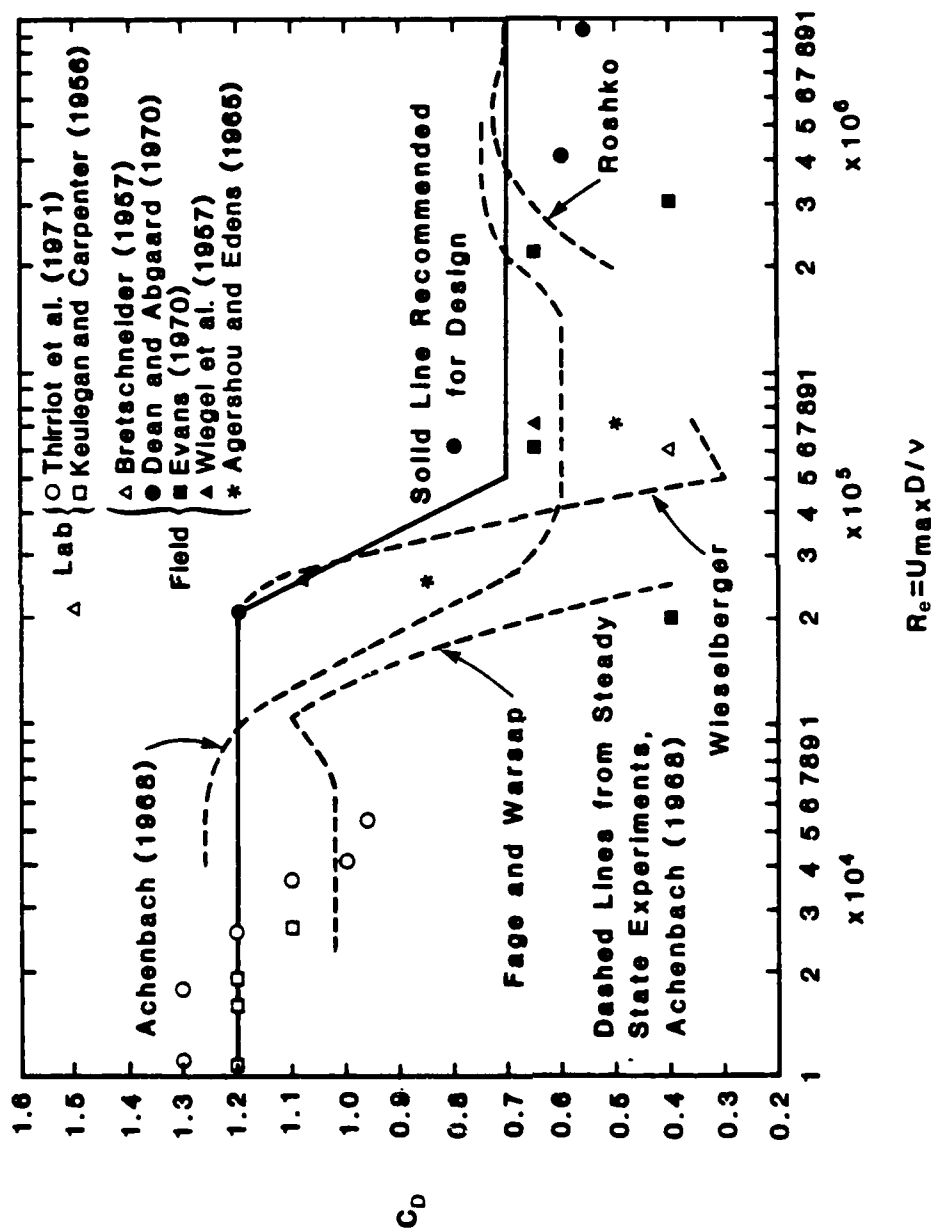


FIGURE II-2 THE SHORE PROTECTION MANUAL RECOMMENDED DESIGN CURVE FOR THE VARIATION IN DRAG COEFFICIENT WITH REYNOLDS NUMBER FOR CIRCULAR CYLINDERS (U.S. ARMY CORPS OF ENGINEERS, 1973)



(L/D) ratio larger than 10 thus minimizing this effect.

In general, roughness elements tend to increase the effective characteristic dimension of a body and thereby effectively increase its Reynolds number. In the circular cylinder case, decreased roughness tends to result in the transition from laminar to turbulent flow occurring at lower Reynolds numbers. In addition because of the effectively increased projected area, the total drag force on such a cylinder is larger than if the roughness elements were absent. While such effects have been measured experimentally, the present analysis assumes the spar to be smooth and thus ignores these effects.

Drag coefficient information on an elliptical shape is by contrast almost non-existent. Some of the earliest drag coefficient information on this shape was reported by Prandtl (Daugherty and Franzini, 1977). Unfortunately, however, this information only examined an ellipse whose major-to-minor axis ratio was 4:1. In addition, the drag coefficient was determined only over a small range of Reynolds numbers from about  $3 \times 10^4$  to  $3 \times 10^5$ . Hoerner (1965), after examining published data as well as performing his own experiments, developed a series of empirical relationships for the drag coefficient on an ellipse based upon Reynolds number considerations as well as the major-to-minor axis ratio of the ellipse. For flow parallel to the major axis these relationships were employed in the analytical model to compute an appropriate drag coefficient.

In regard to flow in the minor axis direction, no data could be found in the literature regarding the drag coefficient on such a section. However, it was noted that such a section generally resembles a flat plate and as a result a drag coefficient value of 2.0 was assigned arbitrarily for flows in this direction. While such a value may be rather large, in

a directionally uniform flow field, a spar would align itself with the current and thus not respond to these off-axis flows. However, if vertical shear were present in the water column, resolving the various velocities acting on the spar into components results in only a small portion of any off-axis flow being actually incorporated into the formulation of this potentially large drag coefficient value. Furthermore, since any off-axis flow would also generate some lift on the spar, the use of such a large drag coefficient value represents a poor attempt at including this effect. Generally the lift on a wing section for angles of attack below stall is proportional to the sine of the angle of attack. Unlike a wing section, however, the elliptical spar section is symmetric about its minor axis and has a blunt trailing edge which acts to reduce streamlining effects. Consequently, the coefficient of lift of such a section would be much smaller than that of an airfoil shape. Therefore, because of a lack of adequate lift and drag information as well as the comparatively small likelihood of large off-axis flows, a minor axis drag coefficient value of 2.0 was adopted.

Nearly all of the previous studies which define the drag coefficient on a circular cylinder attempt to quantify the inertia coefficient as well. Like the drag coefficient data, a great deal of scatter exists in this inertia coefficient information also. Unfortunately, no published data or empirical relationships could be found relating this coefficient to some measurable spar parameter. Consequently, the analytical model employed the potential flow formulation for the inertia coefficient of an ellipse:

$$C_M = (1 + B/A) \quad (17)$$

where A and B are the major and minor axis lengths of the ellipse, respectively. Since a circle represents a special case of an ellipse where the two axes are of equal length, this formulation reduces to the correct potential flow value of 2.0. Generally speaking, potential flow values of  $C_M$  tend to be somewhat higher than those measured in the field. Consequently, the forces and resulting list angles computed using these potential flow values will tend to result in a somewhat conservative design formulation.

### II-3 Computer Model Description

The forces, moments and list angle of an articulated spar device are calculated according to the procedure described above. Using Equations (6) and (15), this computer model consists of a main program, ASB1, and 19 internally called subroutines. Written in Fortran IV, this program has been run successfully on the University of Rhode Island's ITEL 5 digital computer. In developing this model, every effort has been made to keep this program as general as possible, and as a result the program accepts a wide variety of input. The large number of arrays which may be needed by this program require that 320k bytes of core be allocated for its execution.

A flowchart summarizing the major steps in the program is shown in Figure II-3. Initiation of this computer model starts by defining a series of fluid, physical and environmental parameters which are described in detail in the users manual (Appendix B). In summary, the first set of input variables serves to define the basic fluid properties of viscosity and density as well as the water depth in which the spar is located. The physical dimensions and material properties of the spar including the orienting vane, if present, are the next parameters to be

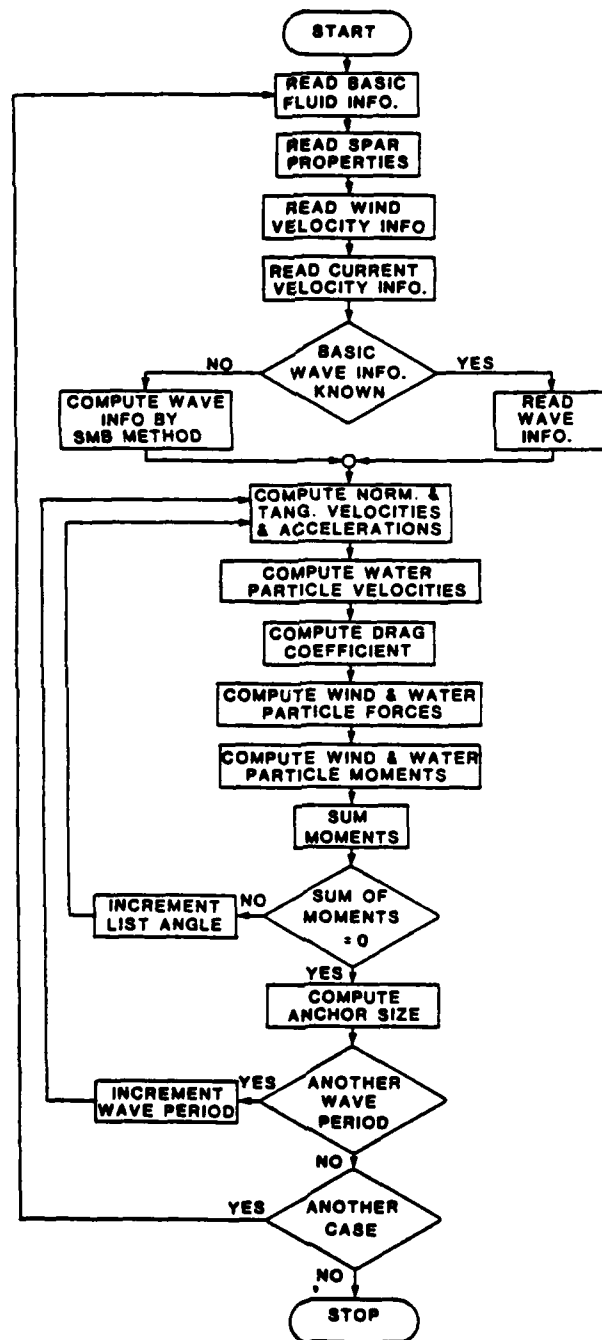


Figure II-3

Summary Flowchart of the Analytical Model

defined. This is followed by a description of the distribution of the velocities acting on the spar. Following the input of this environmental information a series of subroutines are called which compute information that remains unchanged by variations in the spar's list angle. From these subroutines, such information as the weight of the spar in air, a variety of wave information and the wind velocity profile are obtained.

Since the distribution of velocities on the spar may have large spatial variations in the vertical, the spar is divided into a number of elemental areas. By computing the total force of each of these areas and then summing over the entire length, the total force acting on the spar may be computed. Since the variation in one driving force profile may be much larger than that of another, three sets of areas, one for each force, are initially defined. However, because the wave and current velocities must be combined in order to determine the water particle force, this number of area sets is reduced to two; one for the wind forces and the other for water particle forces. In this reduction scheme, the maximum number of equal area elements describing the current and wave particle velocities is selected.

Having defined the driving force velocity profiles acting on the spar, its orientation relative to magnetic north is ascertained based upon a hierarchy structure. In this hierarchy, the force due to current is assumed to predominate over those caused by wind and waves. The coordinate system described above is fixed to the spar and as a result, the bearing of the buoy relative to magnetic north can be determined. The computer program assumes that the spar will orient itself such that its major axis is parallel to the direction of the flow. Further, an orienting vane present on the structure will always act as the trailing edge, thereby fixing the orientation of the spar relative to the forces

acting on it.

Once the orientation and number of elemental areas has been determined, the relative normal and tangential velocities, and in the case of waves, accelerations acting on each of these areas in the X and Y directions are determined. Using these normal velocities to first compute a series of elemental Reynolds numbers, an associated drag coefficient for each element is computed using one of the previously described empirical relationships. Subsequently, the force on each of these elemental areas is determined from Equations (6) and (15). By summing these elemental forces, the total wind and water particle force acting on the spar is computed.

These driving forces produce an overturning moment which is computed next. Buoyancy forces produce a righting moment which acts in opposition to this overturning moment. Once these two moments have been calculated, they are compared in the main program. Depending upon which of the two moments predominate, the list angle is altered and the computational process, starting with the determination of the normal and tangential velocities and accelerations, is repeated. When the two moments are equal or nearly so, depending upon the convergence criteria specified, the computation is complete. At this time the wave time step is incremented by one and the general computational process is repeated.

When the forces, moments and list angles have been determined for all of the wave time steps then one final subroutine is called. This subroutine selects an appropriate anchor for the spar based upon the maximum net buoyant force seen by the spar during one wave period. In addition a factor of safety for this anchor is determined. The program then checks the input data file to determine if there are additional cases to be computed. If appropriate, a check is made to determine if during the

next analysis only the environmental parameters will be altered or if the physical dimensions of the spar will also be changed. By returning to the appropriate location, the new data is input to the main program and the computational process is repeated. When no further data is supplied to the program, it terminates.

## II-4 Sensitivity Analysis

### II-4.1 Introduction

It is clear that the analytical model which has been developed is of a very general nature and consequently a sensitivity analysis to cover all contingencies could not be made. Therefore, in order to determine the relative importance of the various physical and environmental parameters present on a spar's list angle, one must make some assumptions about the nature of these possible conditions. The first step in the process was to determine the significant forces involved and then attempt to ascertain the relative importance of the physical and environmental parameters influencing these forces.

### II-4.2 Analysis of Forces

The analytical model previously developed allows for the action of wind, wave and current forces to act upon a spar. In the present analysis, it is envisioned that an articulated spar designed using this model would be placed in the relatively confined area of a river or shipping channel as described in Chapter I. In such a situation, current velocities could be on the order of 2 to 3 knots or greater. The significance of wind forces in such a situation is best illustrated by the following example. An exceptionally strong wind of 75 miles per hour (120.70 km./hr.) is equivalent to a velocity of 110 ft/sec. The force created by

such a wind velocity, however, is smaller than that created by a current velocity of 3 knots (5.1 ft./sec.), on an equal area basis. For example, on a one square foot area, with an assumed drag coefficient of 1.0, the wind would produce a force of 28 pounds (12.73 kg.) while that created by the 3-knot current would be 51 pounds (23.18 kg.). Aside from the large velocity differential, the difference in the magnitude of these two forces is the result of density differences: that of water being approximately 1000 times greater than that of air. More significantly, while such current velocities are expected to be common in the location where such a spar might be used, the wind speed used above is representative of hurricane force winds and thus represents an extreme case. Further, since much of an articulated spar is assumed to be submerged, the area on which the current force acts will be significantly larger than that exposed to wind forces. Consequently, under normal conditions, when small daymarks are used, it is reasonable to assume that in comparison with current forces, wind forces may be neglected.

In general, it is possible to omit from consideration, the action of wave forces on the spar as well. For example, consider the wave forces created by a large, but not excessive, wind velocity of 40 miles per hour (64.37 km./hr.). Such a velocity will, over a fetch of 10,000 feet (3.05 km.) in 30 feet (9.14 m.) of water, produce a wave with a significant height of 2.5 feet (0.76 m.) and significant period of 3.0 seconds as predicted by the S.M.B. method. Based upon Airy theory, such a wave would result in a maximum horizontal particle velocity of 2.6 feet per second (0.79 m./sec.). While this value is approximately 50% of the 3 knot (1.55 m./sec.) current velocity, several factors should be considered. First, such a wind velocity and fetch condition, while not rare, is still exceptional in the semi-enclosed areas in which this articulated



spar would be used. More importantly, this velocity represents a maximum surface condition and while such a force at this location would produce a sizable moment, this force is exponentially decreasing with both time and depth. Consequently, based upon the scenario developed in Chapter I, combined with the likelihood of forces of this magnitude occurring, wave forces on a spar in comparison with the expected current forces are generally small and may therefore be eliminated from further consideration. As a result of this discussion, current forces may be considered the dominant and only significant force acting on this articulated spar device.

A parametric sensitivity analysis was performed on many of the physical and environmental parameters which effect the overall list angle of the spar. As this analysis proceeded, it became apparent that because of the large number of variables involved, different spar configurations might result in very different sensitivity results. In general, by varying one parameter while keeping all others constant, trends would be established, but quantitative assessment of the various differences was limited to discussion of a single design. Consequently, the parameters effecting the overall list angle of a spar buoy are most meaningfully assessed in a qualitative rather than quantitative sense. Table II-1 is a list of a variety of physical and environmental parameters with a qualitative assessment of their influence on a spar buoy's overall list angle. These influences are rated as either significant, moderate or slight and are based upon numerous computer simulations under a multitude of conditions. Table II-1 serves further to demonstrate the value of this analytical model. For a given situation where many of these parameters are either limited or fixed due to certain constraints, the user may alter the remaining parameters within whatever physical and

TABLE II-1

## INFLUENCE OF VARIOUS PARAMETERS ON A SPAR'S LIST ANGLE

<u>Parameter</u>	<u>Influence</u>
current velocity	significant
spar weight per unit length/buoyant weight per unit length	significant
spar length/water depth ratio	moderate
cross-sectional area	moderate
major to minor axis ratio	moderate
wind velocity	slight
wave height	slight
anchor attachment offset	slight

environmental conditions dictate to obtain a better design for a given situation. Table II-1 may therefore be used as a guide as to the effect of varying those parameters which in a given situation may be altered.

Of the parameters presented in Table II-1, the current velocity and the WPL/BPL ratio where WPL is the spar weight per unit length and BPL is the buoyant force per unit length, were judged to effect significantly the spar's list angle. Figure II-4 shows the effect of changes in the WPL/BPL ratio for circular cylinders with an L/h ratio of 1.3, where L is the spar length and h is the local water depth. At low velocities, it can be seen that the spar is very sensitive to changes in the WPL/BPL ratio, while at large velocities this effect is less significant. Total spar submergence occurs at a list angle of  $39.7^{\circ}$ . Visibility considerations dictate an upper limit on WPL/BPL of approximately 0.65. Spars with ratios greater than this value will have such incrementally small amounts of reserve buoyancy per foot that their list angle in any current would be excessive. Material properties and structural considerations govern the lower limit of this ratio.

Figure II-5 shows the effect of various L/h ratios on the list angle of a circular spar in various uniform current fields. It can be seen in this figure that at small velocities the variation in L/h is most significant while at large velocities a spar's list angle is less dependent on this ratio. In a given water depth as the spar length is increased so is its overturning moment, due to the additional weight. To compensate for this increased overturning moment, the spar must submerge a greater portion of its length. Hence, for a given velocity, spars with large L/h ratios exhibit greater list angles than those with small L/h ratios. Therefore, to minimize its list angle, a spar should have as small an L/h ratio as possible. However, the use of excessively small L/h ratios

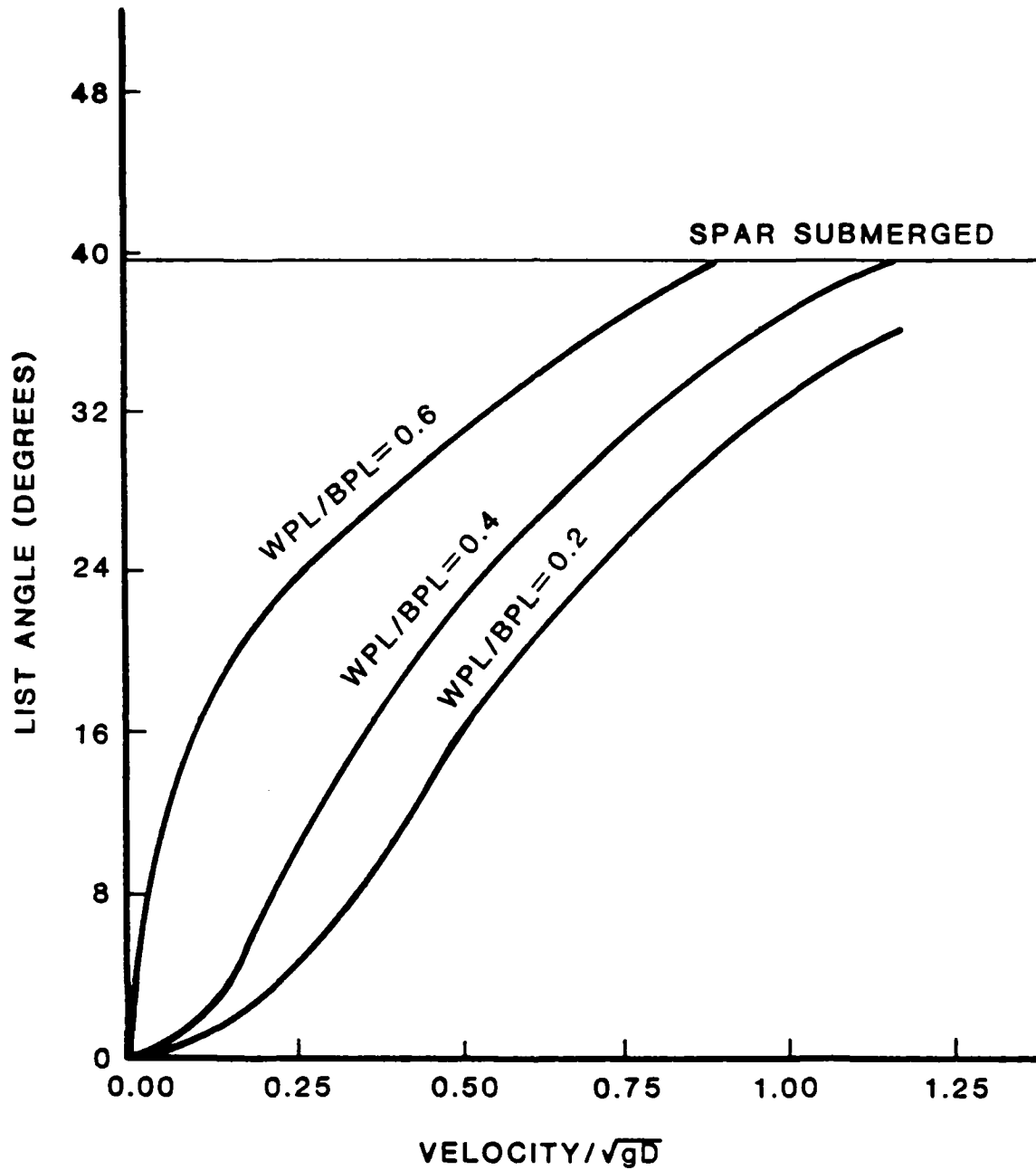


FIGURE II-4 INFLUENCE OF CURRENT ON CIRCULAR  
CYLINDERS OF VARIOUS WPL/BPL RATIOS  
 $L/h = 1.3$

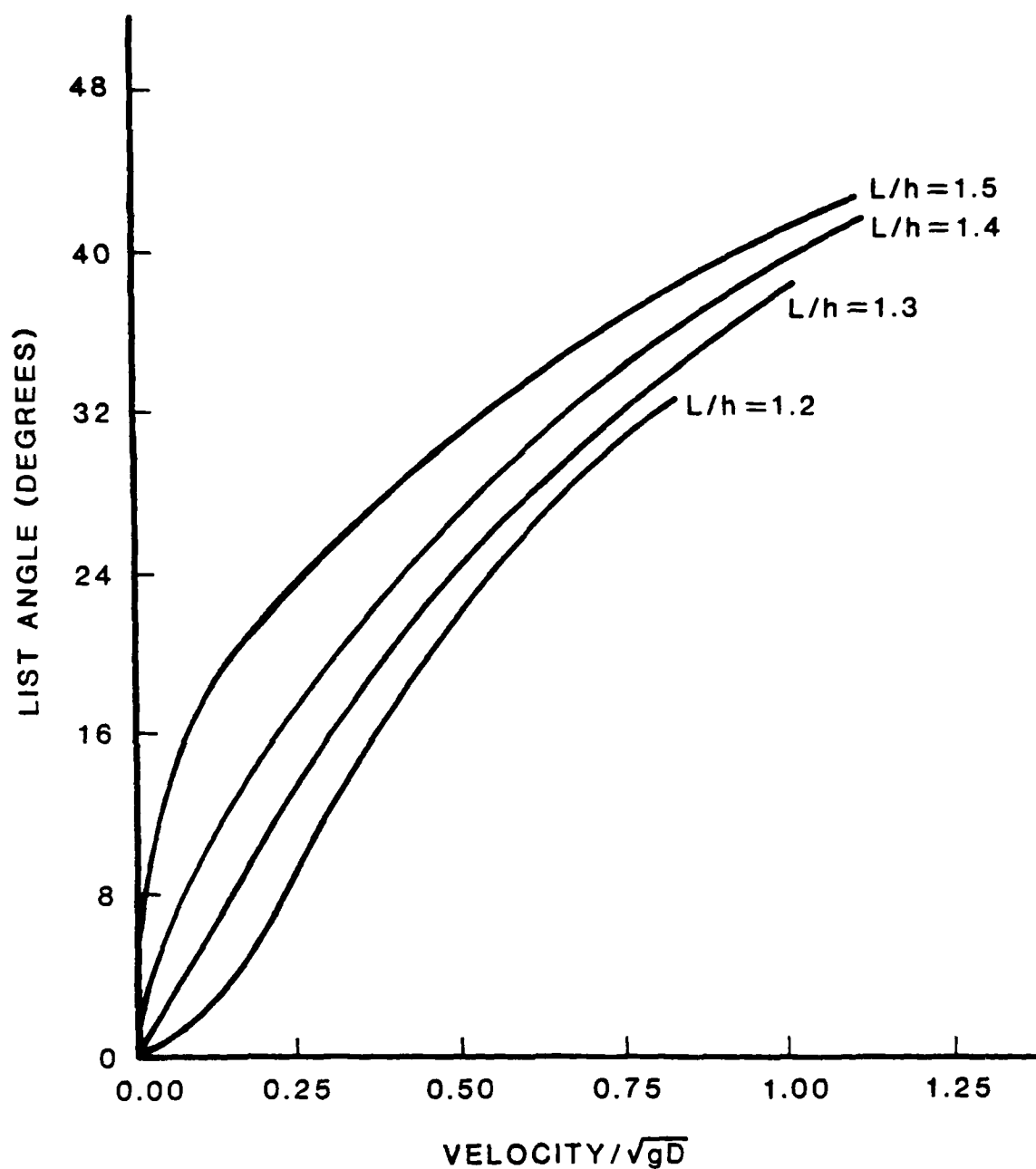


FIGURE II-5 INFLUENCE OF CURRENT VELOCITY ON  
CIRCULAR CYLINDERS OF VARIOUS L/h RATIOS  
WPL/BPL=0.446

(i.e., approaching 1.0) results in a spar becoming submerged sooner than spars with large values of  $L/h$ . For example, in Figure II-5, the  $L/h = 1.2$  line terminates at a dimensionless velocity value of 0.75 and the  $L/h = 1.3$  line terminates at a dimensionless value of 1.05, indicating the total submergence of the spar. By comparison, spars with  $L/h$  values of 1.4 and 1.5 become totally submerged at dimensionless velocities greater than those shown in this figure.

The effect of changes in the major-to-minor axis ratio,  $A/B$ , on spars of constant projected area with a fixed  $L/h$  ratio is shown in Figure II-6. It can be seen in this Figure that significant reductions in list angle can be achieved by changing the  $A/B$  ratio from 1:1 (a circular cross-section) to 2:1. Further streamlining of the elliptical shape from a 2:1 axis ratio to a 3:1 ratio results in less significant reductions in spar list angle. In addition, any off-axis flow condition would be subject to large projected areas at these large  $A/B$  ratios. As a result of this analysis, an ellipse with a 2:1  $A/B$  ratio was selected for prototype testing.

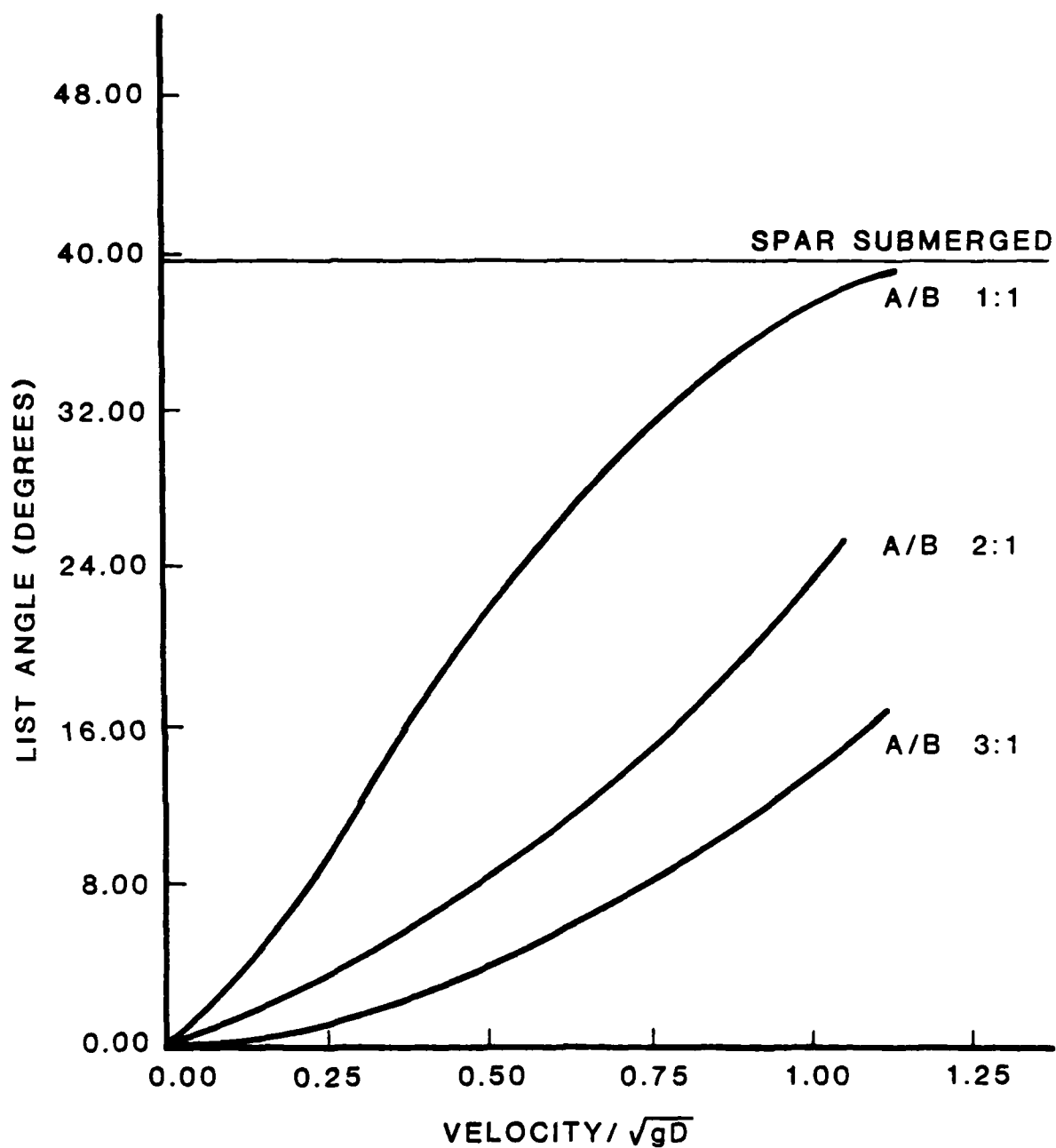


FIGURE II-6 INFLUENCE OF CURRENT VELOCITY ON  
VARIOUS A/B RATIOS CONSTANT PROJECTED AREA

WPL/BPL=0.446

L/h=1.3

## CHAPTER III

### PROTOTYPE TESTING

#### III-1 Introduction

The validity of any analytical model is governed by its ability to describe the actual situation being studied. For the purpose of obtaining validation data for this analytical model, a series of laboratory tests using several different spar shapes were performed in the circulating water channel at the U.S. Coast Guard Academy.

#### III-2 Description of Facilities

The circulating water channel used in these tests is a two-story high, primarily stainless steel structure located in MacAllister Hall on the grounds of the U.S. Coast Guard Academy in New London, Connecticut. Designed at the University of Michigan by Vern Phelps and Francis Ulgive, this system is powered by an axial flow propeller pump. By adjusting the propeller speed, velocities up to a maximum of 10 ft./ sec. (3.05 m./sec.) can be obtained in the channel. In addition to being able to select the current value, plexiglas viewing ports on the side and bottom of the circulating water channel's 10.0 x 4.0 x 2.0 feet (.305 x 1.22 x 0.61 m.) of usable work space allow the user to observe the object under study from many different angles. In addition, colored dye is available for use in observing general flow patterns around objects. To provide for the study of objects which must be anchored, such as this articulated spar, a series of screw holes are located in several places on the bottom of the work area. With more than one location available at a given time, for comparison purposes, two potential spar shapes could be observed together in the same flow. Because of these facilities several spar shapes and a variety of orienting devices could be tested quickly and



easily.

Current velocity measurements in the circulating water channel were made using a Teledyne-Gurley Model #625 6-cup pygmy current meter. When in use, this current meter is positioned on a steel rod which is also mounted on a cross-bar across the tank opening. A hand held revolution counter connected directly to this steel rod allows for the direct determination of the average flow rate over any known time interval.

### III-3 Model Descriptions

Initially, two prototype shapes, one with an elliptical cross-section and the other with a circular cross-section, were constructed for testing purposes. Later, a third spar with a more streamlined airfoil shaped cross-section was built. Figure III-1 is a photograph of the three spar shapes which were tested.

Each of the prototype spars was constructed from a styrofoam-type material. Initially a template of the desired cross-section was constructed and used as a pattern for tracing onto the foam board. Subsequently, thirty, approximately 1 inch (.54 cm.) thick foam pieces of a given cross-section were cut and then fiberglassed together to obtain the desired spar shape. Each of these shapes was then sanded to remove any discontinuities, and a bottom attachment plate of 1/4 inch (0.64 cm.) thick plywood was glued to the bottom of each spar. In this way, ball joints or other anchor attachment mechanisms could be easily secured at any desired location on this bottom plate. To reduce roughness effects and minimize drag, each model was then painted with several coats of varnish.

The analytical model had previously shown that an ellipse with a major-to-minor axis ratio of approximately 2:1 would have less drag than

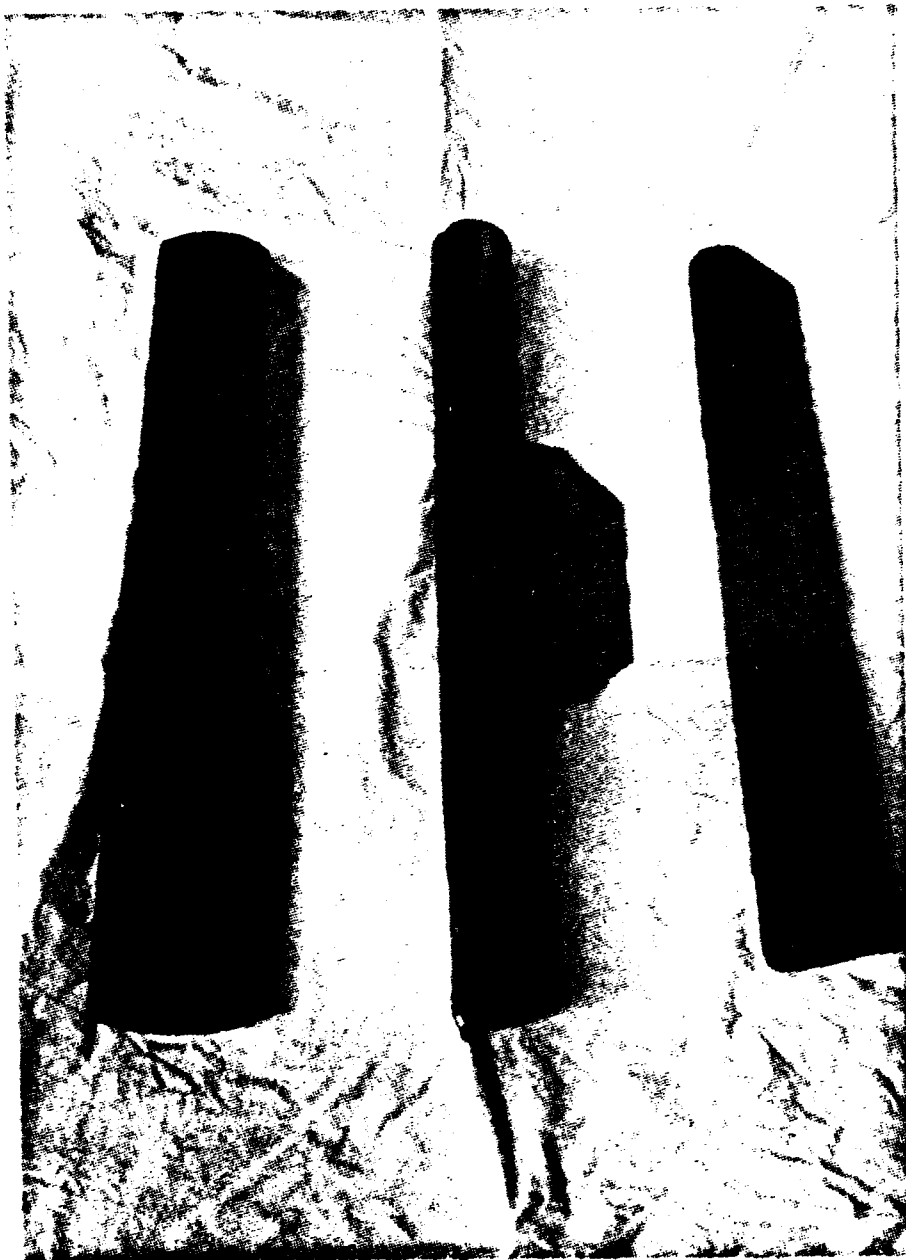
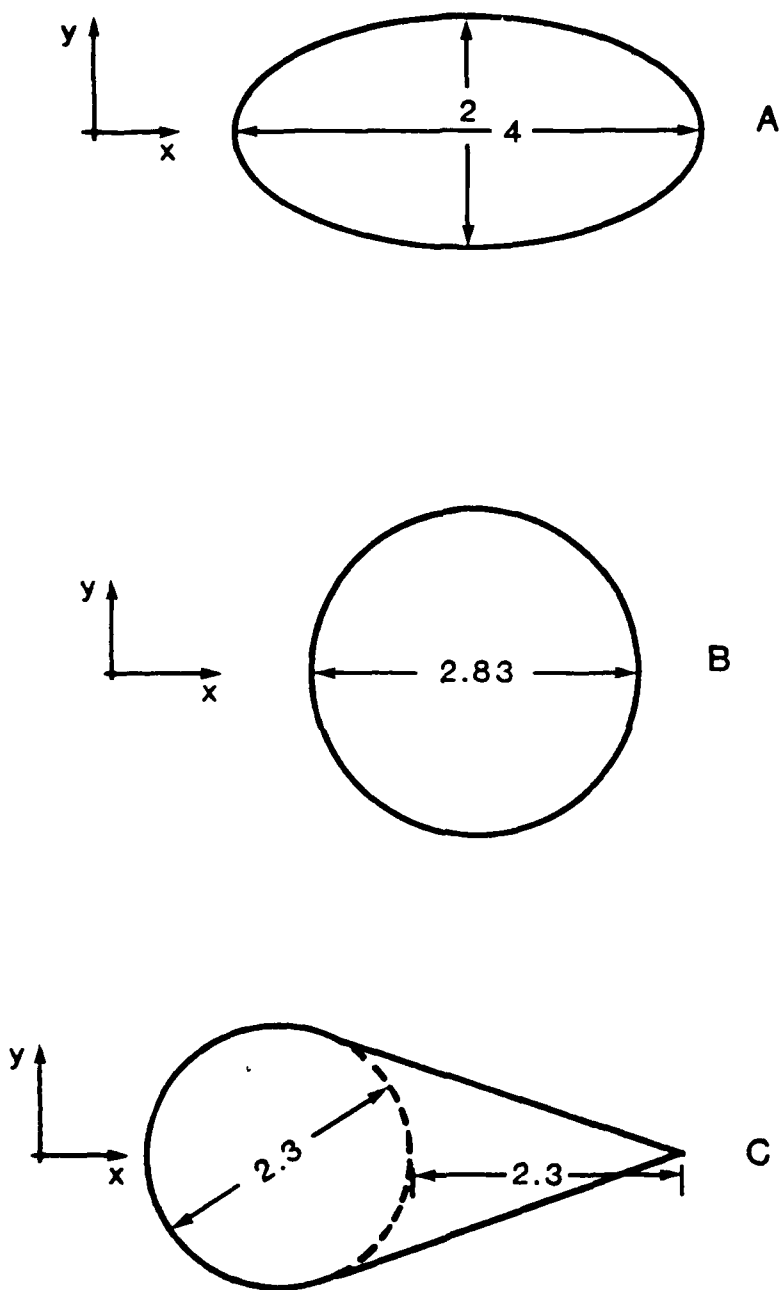


Figure III-1

The Three Buoy Shapes Used in the Circulating Water Channel Tests

a circular cylinder of the same cross-sectional area and yet be less affected by off-axis flows than ellipses with larger axis ratios. Consequently, the first model which was constructed had a major axis length of 4 inches (10.16 cm.) and a minor axis length of 2 inches (5.08 cm.) as shown in Figure III-2A. Such dimensions were selected to approximate a one-third scale model of the prototype articulated spar. In order that each shape have the same buoyancy per unit length, the subsequent prototype shapes were constructed so that their cross-sectional area was the same as that of the elliptical spar. By selecting a spar's dimensions in this manner, the shape with the smallest list angle in a given current would be the one with the least drag and consequently the most desirable for field test purposes. By comparison, the circular cross-sectioned spar had a diameter of 2.83 inches (7.19 cm.) as shown in Figure III-2B. After some initial testing, a third spar with a cone shaped cross-section was constructed and tested. This shape had a chord length of 4.60 inches (11.68 cm.) which was exactly twice its maximum width of 2.30 inches (5.84 cm.). This spar configuration is shown in Figure III-2C. To accommodate the 2 feet (0.61 m.) water depth of the channel, all of the spar shapes were built to a length of 2 1/2 feet (76.20 cm.). Since the full scale prototype was expected to be considerably greater than 3 times this length (7 1/2 feet) [2.29 m.], geometric similarity between these models and the field prototype was not fully maintained. This was not considered significant, however, because the models were constructed primarily to determine an optimized spar cross-section and as such their overall length was of secondary importance.

In comparison with the pressure drag forces acting on the spar, however, the wave-making forces created by the spar's piercing the surface were minimal and consequently all velocity scaling considerations were



**FIGURE III-2 SCALE DRAWINGS OF THE THREE  
PROTOTYPE SPAR CROSS-SECTIONS**

based upon the Reynolds number rather than the Froude and/or Weber numbers.

#### III-4 Results

The initial testing was done using only the elliptical and circular cross-sectioned spars. Initial tests with the circular spar showed that at any significant velocity it would oscillate in a direction transverse to the current flow. This type of motion is the result of vortex shedding and is well documented in the literature (Blevins, 1977). The period of this oscillation was measured and generally found to be in good agreement with that predicted by empirical formulations based on the Strouhal number. The Strouhal number is generally considered to be a function of the Reynold's number although for values between  $1.0 \times 10^5$  and  $3.0 \times 10^6$ , there is a large degree of spread in the data (Blevins, 1978). In the  $1.0 \times 10^4$  to  $8.8 \times 10^4$  Reynold's number range of these tests, however, the Strouhal number may be considered constant having a value of 0.19.

Some rather unexpected results were observed when the elliptical cylinder was placed in the circulating water channel. It was anticipated that this elliptical shape when anchored from a point near its leading edge would align itself such that its major axis was parallel to the direction of the current flow. In this orientation, an ellipse would present a very small projected area and consequently the drag force on the spar would be minimized. Unfortunately, however, using this elliptical prototype it was found that regardless of the location of the anchoring point on the bottom face of the spar, this shape would not align itself in the desired direction. Instead, when placed in a current the elliptical spar would immediately rotate so that its major axis was

perpendicular to the direction of flow. Once aligned in this position, the ellipse would then oscillate transverse to the flow because of vortex shedding. Milne-Thomson (1938) has shown that an ellipse free to pivot about its geometric center will rotate until the two stagnation points at either end of the major axis of the ellipse lie on a line passing through the center of the ellipse. Therefore, a spar mounted in this manner would be expected to orient itself broadside to the flow direction. However, this elliptical spar was attached to the bottom very near its leading edge, thereby greatly reducing the magnitude of the couple which would tend to rotate the buoy model.

Several possible causes for the lack of directional stability in this elliptical spar were considered. The anchor attachment mechanism used in these initial tests consisted of crudely fabricated pieces of aluminum which in principle allowed the buoy to list along its major axis and to rotate freely about its vertical axis. Since speculation as to the reason for this unusual behavior initially centered around this attachment device, a more precise mechanism; a small ball joint, was obtained and used in all future testing. Even with this device secured on the bottom face of the spar at its leading edge, the elliptical spar turned broadside to the current. Having eliminated the anchor attachment device from suspicion, other possible reasons were considered to explain the spar's unexpected behavior. It was hypothesized or deduced that compared with an airplane wing or other fixed airfoil shape, the additional degrees of freedom of this system were responsible for its lack of directional stability. Consequently, either a perturbation in the flow, a discontinuity in the actual shape of the spar, a slight offset in the anchor attachment point to either the left or right of the centerline or some combination of these possibilities caused the initial turning of the

spar in one direction. Once this turning began, there was a shift in the stagnation points and a differential pressure force which caused a net lift force to begin to act on the ellipse. This lift force would continue to increase until stall was reached. However, the spar would continue to rotate in opposition to the increasing drag force until such time as the stagnation points were on a line which passed through the point of rotation. This stable condition would thus occur when the spar was broadside to the current.

Having concluded that the spar alone would not orient itself in the desired manner, a vane made of sheet aluminum was attached to the trailing edge of the spar in an attempt to obtain directional stability. Because of the problem of attaching the aluminum to the foam material of the buoy, an exceedingly large vane, some 24 inches (60.96 cm.) in width and spanning the entire length of the spar was tried initially. In subsequent tests the vane was shortened by cutting from the trailing edge what was deemed to be excess. The results of this series of experiments, also performed with the anchor attachment point being located on the bottom face of the spar at its leading edge, showed that for vane widths greater than 8 inches (20.32 cm.) (i.e., twice the buoy's major axis) the desired effect of having the major axis of the ellipse align itself parallel to the direction of flow of the current was achieved. Even with these large vanes, however, the spar was found to be very sensitive to slight perturbations in the trailing edge of the vane. Any small change in this trailing edge would lead to the entire spar assuming a list angle which was transverse to the flow. However, such vane widths being at least twice the length of the major axis of the spar were considered to be excessive and thus this design was excluded from further consideration.

As the vane width was shortened to less than 8 inches (20.32 cm.), the overall shape of the spar with a blunt leading edge and a sharp trailing edge began to resemble that of a wing section. The consequence of this reduction was that the spar became increasingly sensitive to very slight perturbations in the flow. Once this perturbation occurred, greater lift would develop on one side of the spar and the entire spar, while maintaining its orientation to the flow, would assume a large transverse list angle (Y axis) resulting in the spar being completely submerged. While it was at times possible to adjust the orienting vane so that the lift forces on either side of the spar were nearly equal as shown in Fig. III-3, any slight deflection of either the flow in front of the spar or of the spar itself resulted in an unstable condition from which the spar never recovered.

Three possible mechanisms to reduce this lift force and consequently improve the stability of the spar vane system were tried using a vane 4 inches (10.16 cm.) in width. In the first, a hairy fairing was added to the trailing edge of the vane. With this device no notable improvement in system stability was observed. The second method consisted of making a series of horizontal cuts about  $3/4$  inches (1.91 cm.) deep at a spacing of approximately 1 inch (2.54 cm.) all along the trailing edge of the vane. By bending these resulting tabs in alternating directions, a flairing of the trailing edge was accomplished. This vane modification improved directional stability somewhat but not without greatly increasing the drag force and the resulting list angle as well. Furthermore, it was found that only slight changes in these tabs, especially those located near the water surface, could drastically change the buoy's stability. Since any vessel which struck such a spar would be likely to alter these trim tabs, especially those near the water surface, this idea



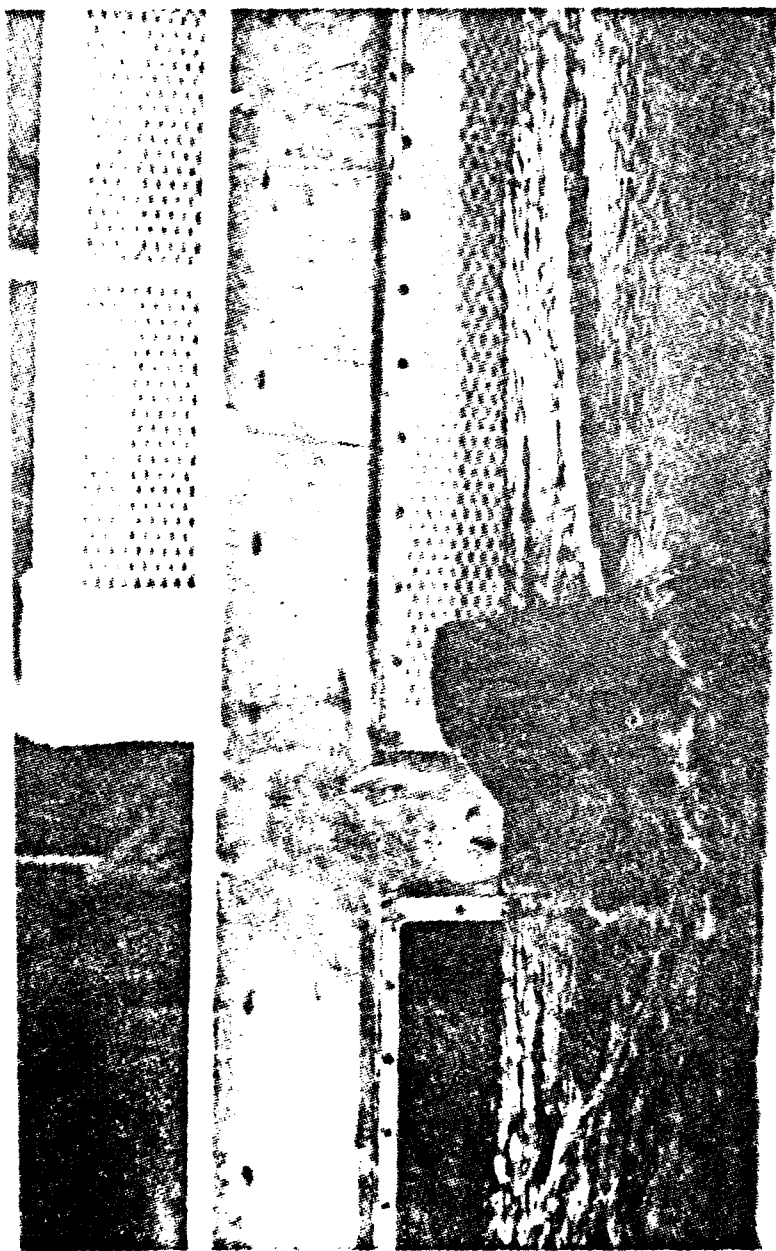


Figure III-3

The Elliptical Spar Being Tested in the Circulating Water  
Channel

was eliminated from further consideration. The placement of a series of holes drilled in the vane near its trailing edge did appear to reduce the magnitude of the lift force somewhat, and consequently increased the spar's stability. Unfortunately however, no way was found to either significantly reduce or stabilize the effect of this lift force.

Measurements of the list angle of this elliptical spar with a vane attached were taken when the system was in a stable mode. These measured values were found to be in good agreement with the previously developed analytical model. However, the analytical model (Chapter II) did not address directional stability criteria and, therefore, these circulating water channel tests were essential to demonstrate that while an elliptical spar does have a low drag shape, directional stability problems preclude its use without a more in depth study of appropriate orienting vanes.

Since the ellipse which had been under study had a major to minor axis ratio of 2:1 and ellipses of larger ratios would produce even greater amounts of lift efforts to determine a stable spar focused on the circular cross-sectioned spar. The oscillatory motion due to vortex shedding had been previously observed and its frequency found to correspond with that predicted by the Strouhal number;  $f = \frac{S\vec{v}}{D}$ .

It is well known that one of the most common ways to suppress this shedding motion is through the use of a splitter plate or vane which acts to inhibit the formation of an oscillating pressure field. Consequently, one of these plates was fashioned from a sheet of aluminum and attached to the circular cross-sectioned spar. When placed in the circulating water channel, this spar-splitter plate combination not only aligned with the flow very quickly but also proved to be very stable. Even when physically displaced from its equilibrium position, the spar quickly

returned to its original position.

Having met with this success, a number of different splitter plate sizes and shapes were investigated to determine the minimum size vane which would ensure the stability of the structure. This minimum size was found to be about 1.25 diameters, or 3.5 inches (8.89 cm.) in width, and approximately 10.5 inches (26.67 cm.) in length (or 45% of the still water submerged length of the spar). Figure III-4 is a photograph of this design being tested in the circulating water channel at a velocity of 2.5 ft./sec (0.76 m./sec.). This photograph shows the vane located near the center of the overall length of the spar. Later experimentation found greater directional stability, as determined by the rate at which the spar returned to an equilibrium position once deflected, could be achieved by locating the vane closer to the top of the spar. While the optimum location of this splitter plate relative to the water depth varies with the current velocity, the closer the top of the vane is to the water surface without protruding above it, the better. In this location, the splitter plate suppresses the oscillating lift force which would, if present, produce the largest overturning moment on the spar.

Having determined the minimum size splitter plate necessary to maintain the stability of the spar structure, numerous measurements of the current velocity and the corresponding list angle were made. This data presented in Table III-1 was then compared with that predicted by the analytical model. The results of this comparison are shown in Figure III-5. This figure shows generally good agreement between the observed and predicted results. At low current velocities, the theoretical model appears to overpredict the list angle, most likely because of the conservative nature of the 1.2 drag coefficient value used in the list angle determination. At these low velocities and correspondingly small list

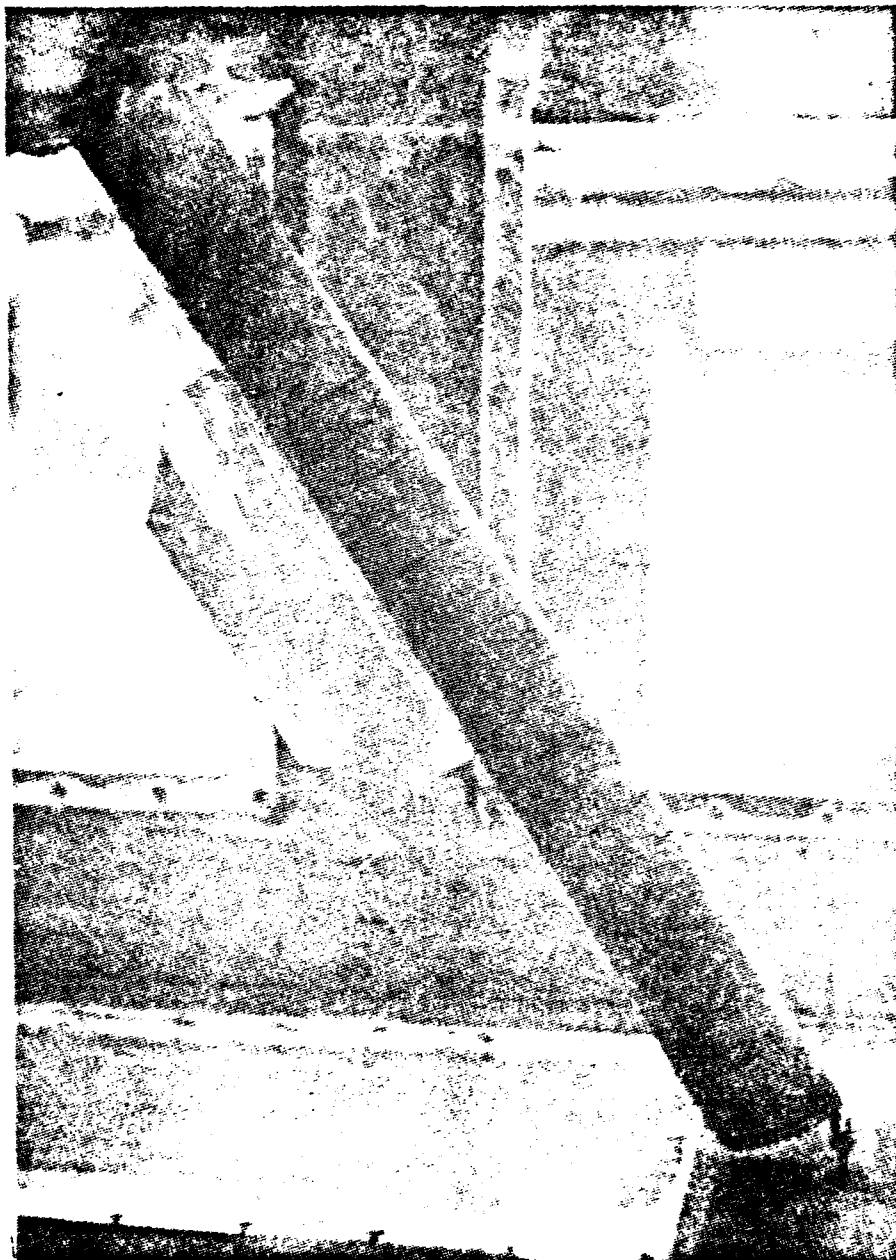


Figure III-4

The Circular Spar in the Circulating Water Channel with a  
Splitter Plate

TABLE III-1

LIST ANGLE DATA FOR A 2.83 INCH (7.19 cm.) DIAMETER SPAR, 30 INCHES  
(76.20 cm) IN LENGTH WITH A SPLITTER PLATE

Velocity (FT./SEC.)	[cm./sec.]	MEASURED LIST ANGLE (DEGREES)	ESTIMATED ERROR (DEGREES)
0.00	[ 0.00]	-3.5	$\pm 0.50$
0.50	[15.24]	-1.0	$\pm 0.50$
1.00	[30.48]	3.0	$\pm 1.00$
1.50	[45.72]	11.0	$\pm 1.50$
2.00	[60.96]	20.0	$\pm 1.50$
2.50	[76.20]	28.0	$\pm 2.00$
3.00	[91.44]	34.0	$\pm 2.50$
3.50	[106.68]	39.0	$\pm 3.00$

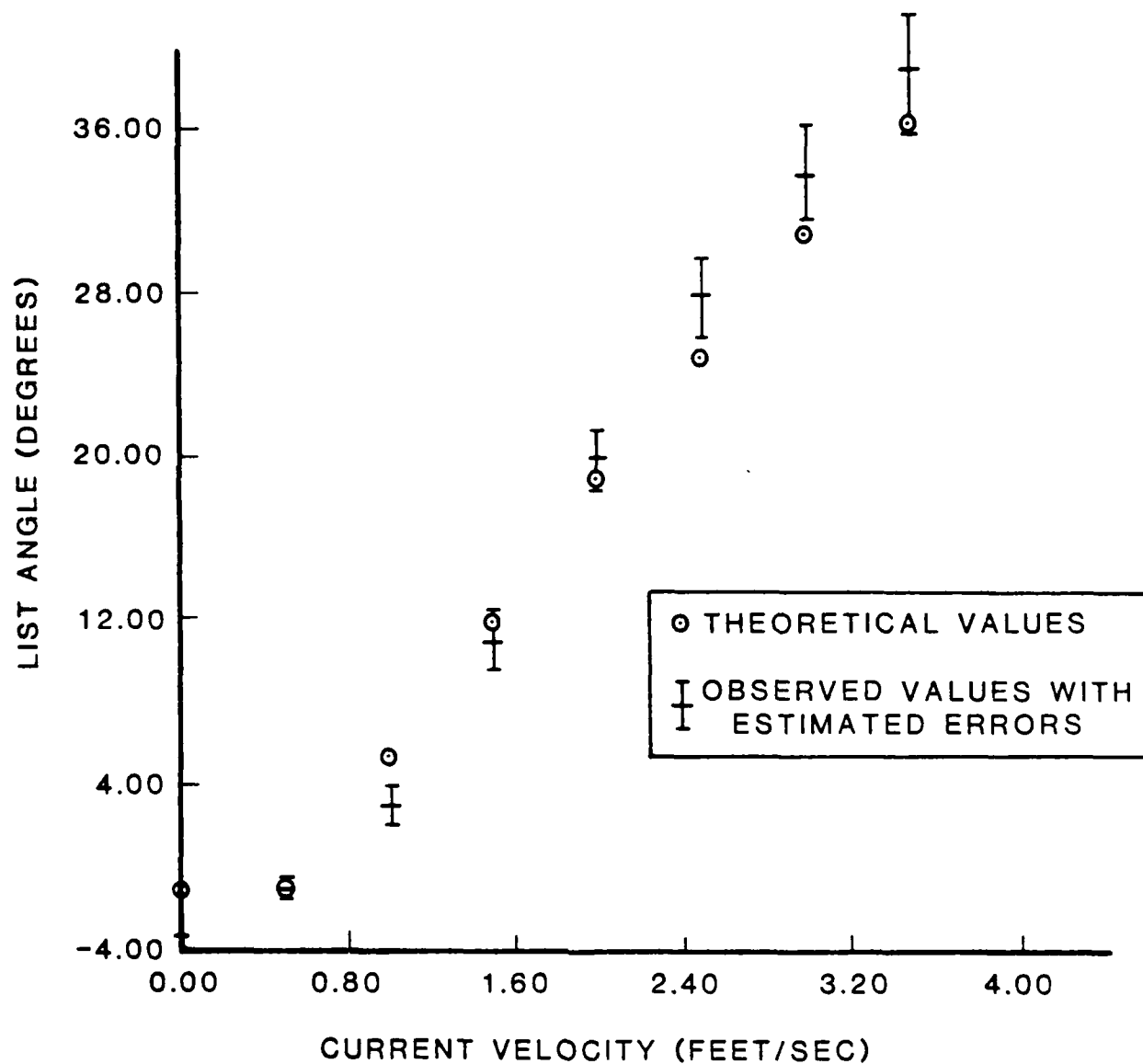


FIGURE III-5 CIRCULATING WATER CHANNEL. THEORETICAL AND OBSERVED LIST ANGLES FOR A CIRCULAR CYLINDER

$$WPL/BPL = 0.094$$

$$L/h = 1.25$$

angles, the length-to-diameter ratio of the spar may be of importance, thus indicating the use of a smaller drag coefficient as outlined in Chapter II. At higher velocities and consequently greater list angles, this L/D ratio is of doubtful importance. However, at these higher velocities, the surface roughness of the spar may become significant. The effect of such roughness elements is to increase the drag coefficient and consequently the resulting list angle would be greater than that predicted by theory.

### III-5 Additional Testing Results

In an effort to find another design which had the stability characteristics of the circular cylinder with a small splitter plate attached yet having a smaller drag coefficient, a third buoy shape was constructed and tested. When a fluid moves past a cylinder with a splitter plate, two identical Foppl vortices form on either side of the plate in the region near where it joins the cylinder. The location of these vortices is shown in Figure III-6. Once formed, these vortices remain stationary and, therefore, by filling in these areas with some material and thus eliminating them altogether, it was postulated that another stable buoy configuration would result. The resulting buoy had a conical shaped cross-section as shown in Figure III-2C. While this streamlined shape does have a smaller drag coefficient than a cylinder of the same projected area, tests performed on this shape showed that it was unstable as it sailed back and forth transverse to the flow. Efforts at suppressing this sailing motion met with only limited success. A hairy fairing attached to the trailing edge of this conical shaped device proved to be the most successful, but was only able to reduce the frequency of the sailing motion by approximately 50%.

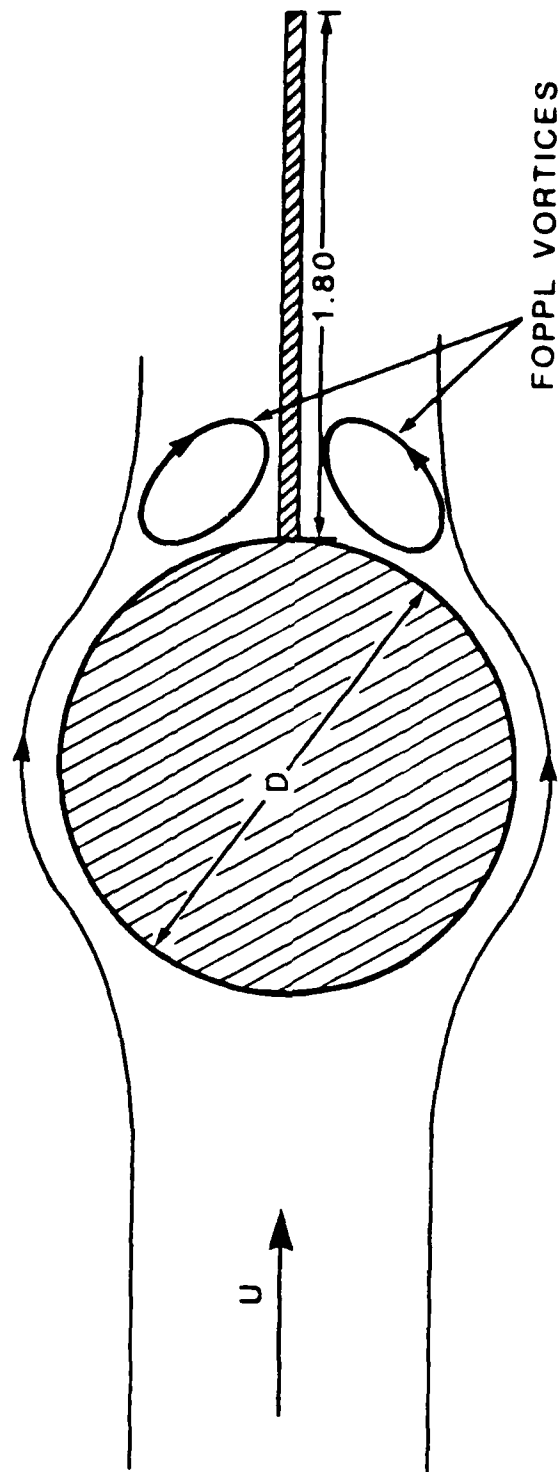


FIGURE III-6 FOPPL VORTICES FORMED BEHIND A CIRCULAR CYLINDER WITH A SPLITTER PLATE



### III-6 Field Model Selection

The results of this series of laboratory tank tests demonstrated that only a cylinder with a circular cross-section and a splitter plate was directionally stable and would return to an equilibrium position when temporarily displaced. In addition, generally good agreement was found between the measured list angle of this spar section and that predicted by the analytical model. Consequently this shape was chosen for the field testing phase of this validation study.

## CHAPTER IV

### THE FIELD TEST

#### IV-1 Spar Description

A full scale spar prototype was constructed for the purpose of validating the analytical model under actual field conditions. The actual spar was constructed from 18 feet (5.49 m.) of 6 inch (15.95 cm.) diameter schedule 40, T6061 aluminum pipe. In addition to this pipe, two end caps, a mooring attachment device and a vane attachment guide were fabricated and then welded to the spar section. Drawings used in the construction of this field prototype are presented in Appendix III. While it is recognized that a spar of these dimensions is quite small in comparison with standard government aids, weighing about 130 pounds (59.1 kg.), this spar represented the most practical design which could be easily transported and deployed without mechanical assistance. Fabrication of this articulated spar was performed by the Durant Machine Company of Noank, Connecticut.

Once fabricated, a vane constructed from 1/2 inch (1.27 cm.) plywood was bolted to the vane attachment guide. This vane measured 11.72 feet (3.57 m.) in length and 10.5 inches (26.67 cm.) in width and was situated so that the bottom edge of the vane was 4 feet above the mooring attachment point. The ratio of the width of this vane to the diameter of the spar was about 1.58, which was slightly larger than the minimum 1.25 value determined in the circulating water channel tests. The reason for this slight increase was to provide some margin of safety in assuring that the spar would perform as expected.

Once the vane was attached, the spar was painted with 8 inch (20.32 cm.) alternating orange and white bands. Figure IV-1 is a photograph of

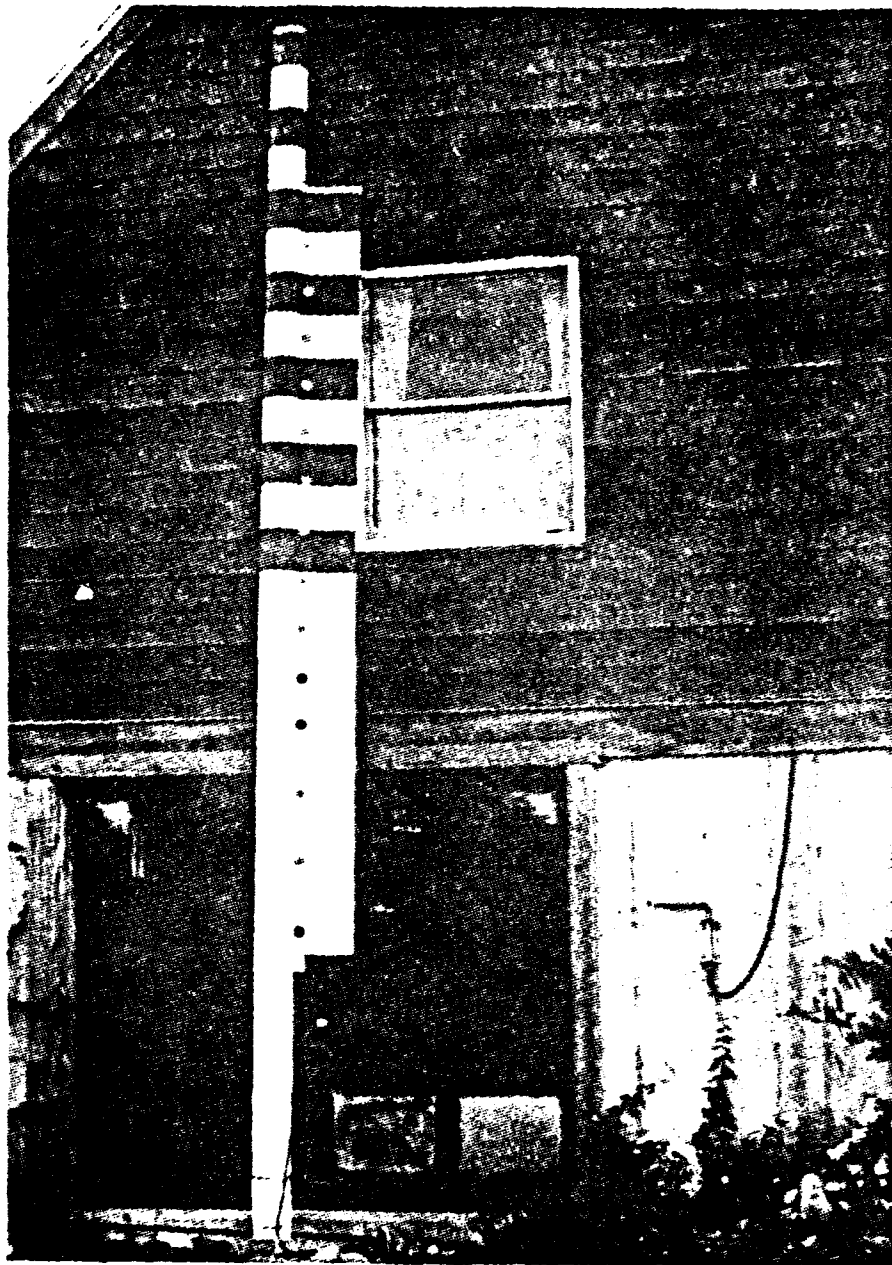


Figure IV-1

The Field Prototype Articulated Spar Buoy

the completed spar device. During the actual deployment a quick flashing white light was mounted on top of the spar as an additional safety precaution.

A swivel joint served to connect the spar to its mooring. This swivel could be attached in any one of three locations along the bottom of the spar depending upon the desired angle of list at slack current. this attachment swivel and the three possible holes are shown in Figure IV-2.

The anchor used in these tests consisted of four 100 pound (45.45 kg.) lead blocks placed in a box as shown in Figure IV-3. When initially deployed, each of these four blocks was individually placed in the box, after which the spar was attached to the iron eye at the center of the box.

#### IV-2 Siting Considerations

In order to test this spar, an area with a relatively high current and shallow water near the University of Rhode Island was required. Point Judith Pond, a large coastal pond located along the southern shoreline of Rhode Island was selected for the field test. It has predominately shallow water and in the vicinity of its narrow opening to the ocean, high currents. Figure IV-4 is a map of the pond showing the test site location. While currents in this pond are strongest in the entrance, safety considerations with regard to the large amount of boat traffic here precluded placing the spar in this area. The entrance channel coming into the pond separates into two sections just north of the narrow entrance. The banks of the much less traveled right hand fork of the channel is occupied by numerous waterfront cottages and the Department of Environmental Management's Marine Experiment Station. At

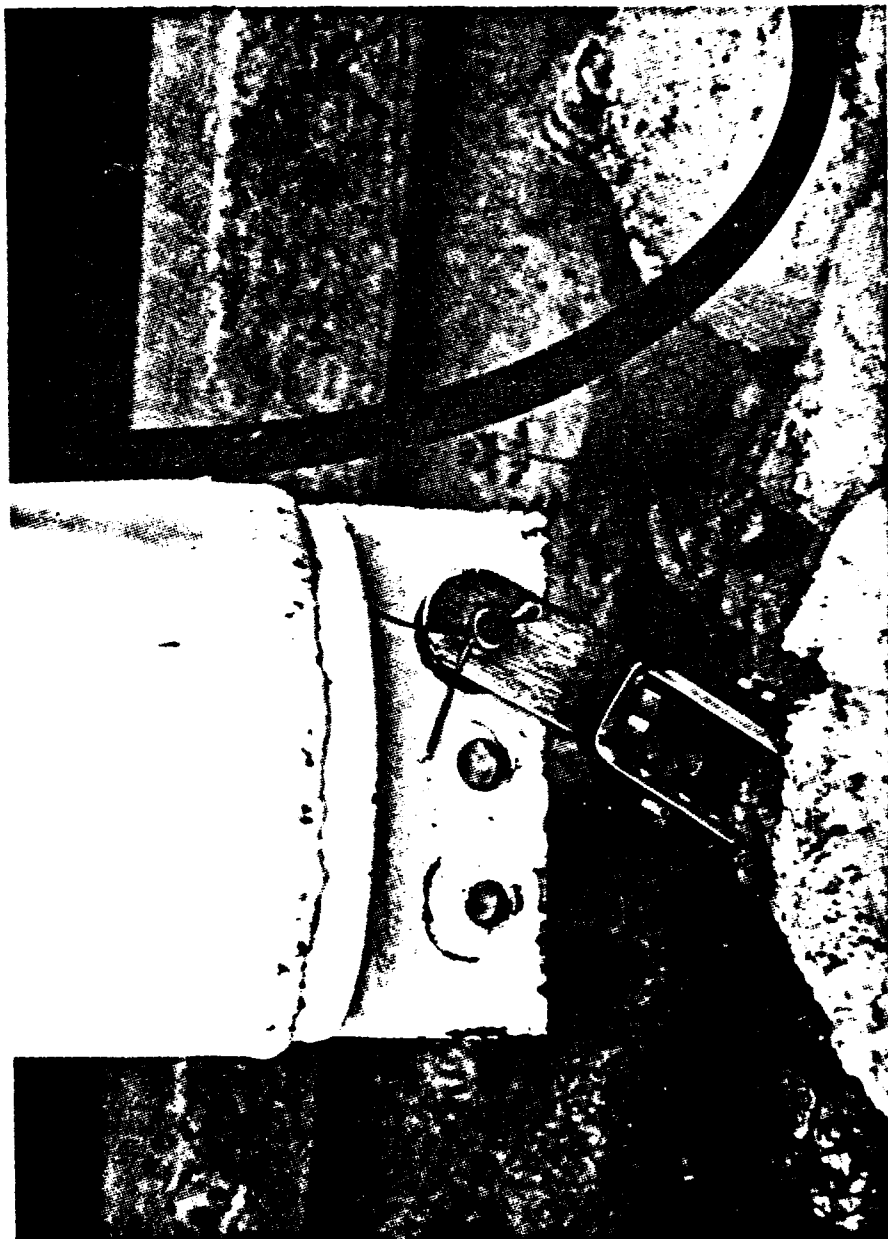


Figure IV-2  
The Field Prototype Anchor Attachment Point



Figure IV-3

The Anchor Used for Testing the Field Prototype

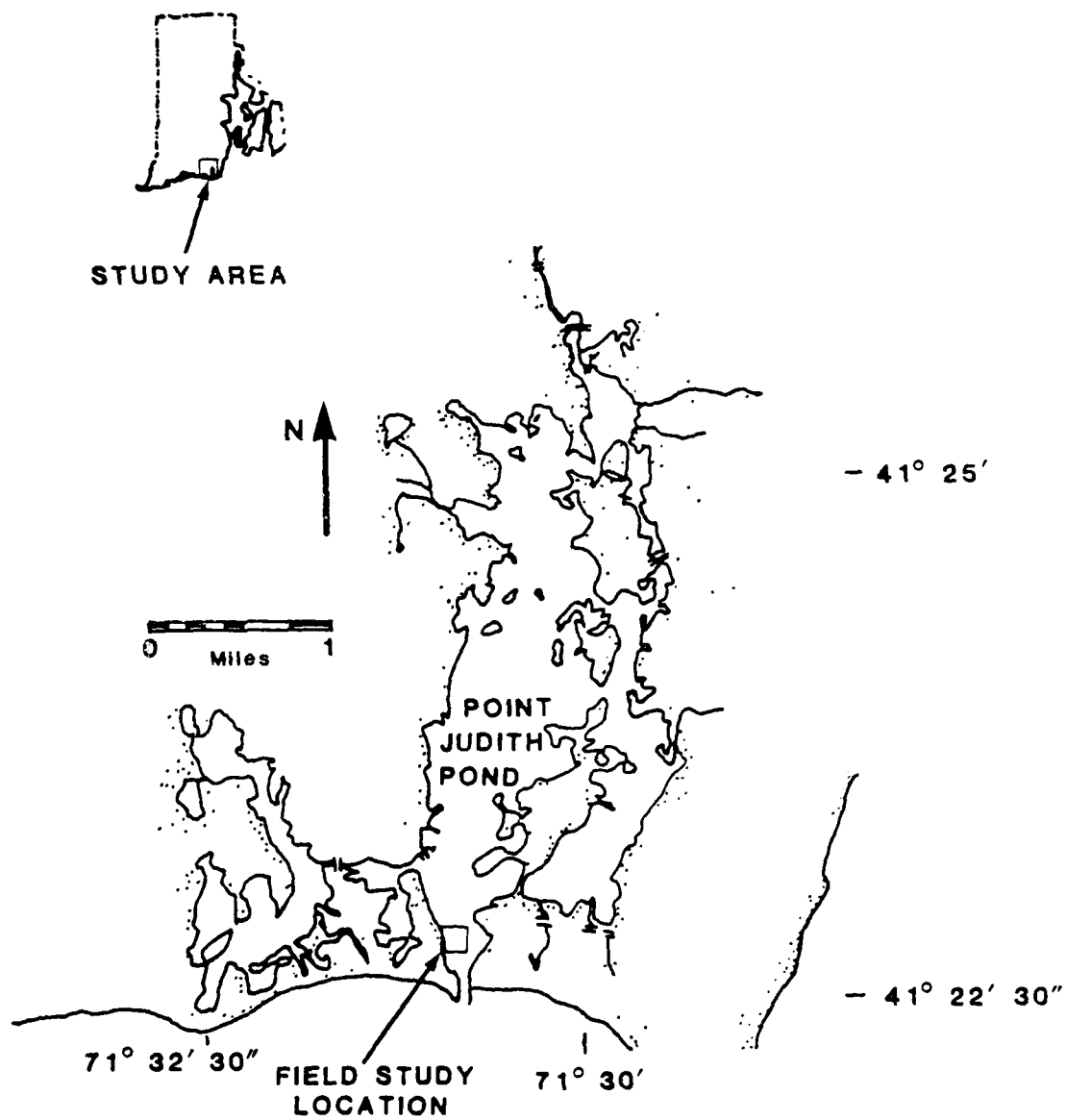


FIGURE IV-4 MAP OF POINT JUDITH POND AND VICINITY

this station, two piers protrude from the shore to the edge of the channel, making an excellent observation and work platform. Further, the availability of working space for locating the instrumentation recorders, ample shore power and the cooperation and assistance of the employees of the Department of Environmental Management made this site a most logical selection from which to perform the field test. The width of the channel at this location is very narrow being only about 200 ft. (60.96 m.) wide, and consequently, the current velocities here, while not as strong as those at the pond's opening are still as large as 2.0 ft./sec. (60.96 cm./sec.).

#### IV-3 Data Collection

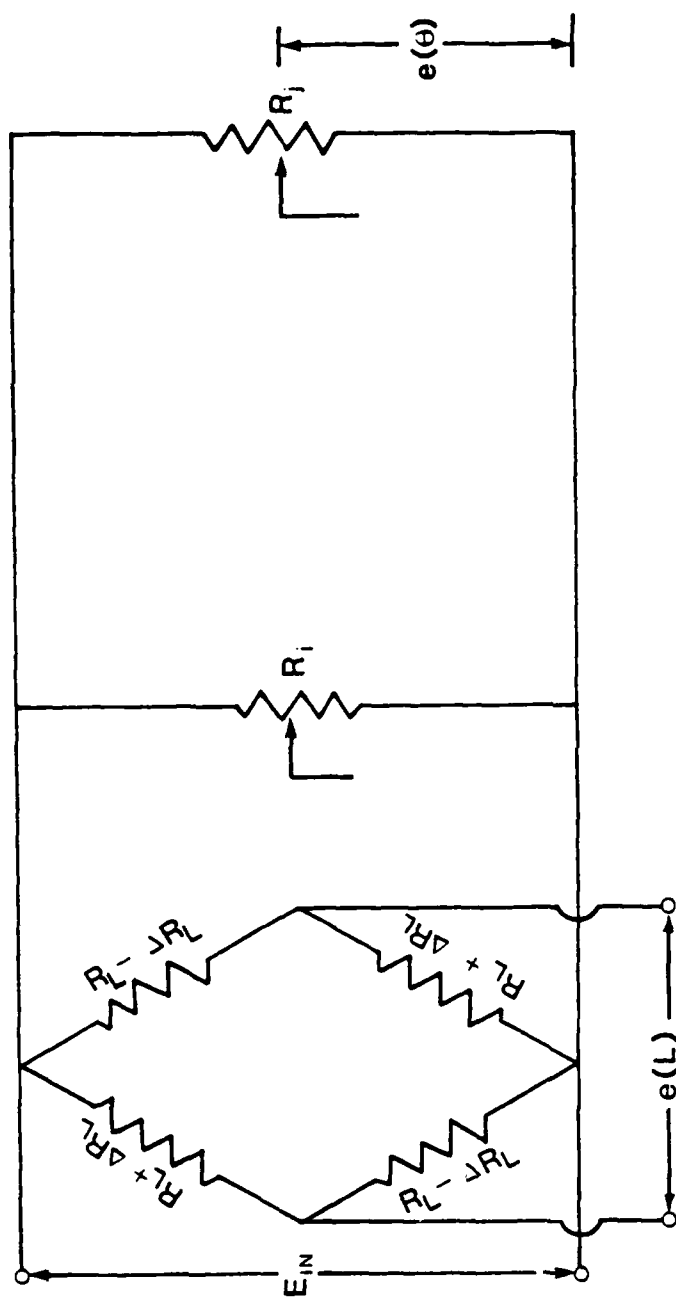
The spar was instrumented with two Humphrey's Model CP17-0601-1 inclinometers mounted orthogonally to one another on the inside portion of the upper end cap. These inclinometers shown with the end cap in Figure IV-5 were secured to the spar in such a way that the list angles parallel and perpendicular to the orienting vane and consequently the expected flow, were measured. A multi-conductor cable passing through a water-tight seal in the end cap supplied the necessary input voltage and also carried the output signal to the shore based recorders.

The inclinometers used in this field test consisted of a series of wire wound potentiometers whose resistance was controlled by the motion of a pendulum type slider. Thus by supplying a constant current at a known voltage to this inclinometer and recording the output voltage, the angle of inclination could be computed. A schematic drawing of this inclinometer system is shown in Figure IV-6. The output signal from both of these inclinometers was continuously recorded on a Hewlett-Packard





Figure IV-5  
Inclinometers Used in the Field Prototype Spar Buoy



$$e(L) = \Delta R_L / R_L \quad E_{IN} \quad (\text{Load Cell})$$

$$e(\theta) = r / R_L \quad E_{IN} \quad (\text{Inclinometers})$$

FIGURE IV-6 INCLINOMETER AND LOAD CELL WIRING DIAGRAM

Model 7100B two-pen strip chart recorder using different colored recording pens to distinguish the two output signals. The input signal was periodically monitored to ensure its consistency with a digital voltmeter.

In an effort to measure the total tangential force which the spar exerts on the mooring system, a load cell was connected between the mooring eye and the swivel at the lower end of the spar. By measuring this force and by knowing the list angles in both the X and Y directions, the total force acting on the spar could be readily computed. Furthermore, by measuring the local current velocity and knowing the resultant force, an estimation of the average drag coefficient of the spar could be made. Operating in much the same manner as the inclinometers, changes in load were detected by a pressure transmitter, changes in load were detected by a pressure transmitter which converted these signals to changes in resistance. By supplying a known voltage to this load cell and measuring its output, the force being applied could be computed as schematically shown in Figure IV-6. A separate cable was used to connect this piece of instrumentation with the necessary shore power and recording device. Output data from this load cell was recorded on a single channel Linear Instruments strip chart recorder. Like the inclinometers, the output signal from this load cell was recorded continuously and the input signal was periodically checked with the voltmeter to ensure its consistency.

Current velocity measurements in the vicinity of the articulated spar were made using a Savonius rotor-type current meter. As this current meter was equipped only with a rotor, only speed measurements were made. Current direction was recorded based upon visual observation as being either ebb or flood. These current speed measurements, taken from a small boat moored immediately adjacent to the spar, were made at three different locations in the water column, near the surface, at mid-depth.

and at the bottom, to detect any vertical variation which might be present. Because of the rather large tidal range of approximately 39 inches (99.06 cm.) at this location, no attempt was made to determine the exact depths at which these current measurements were taken. Further, except for small periods of time near slack water, little or no vertical variation was found in these current profiles. Because of the time involved in making these current measurements, as well as the relative rate of change of the current speed, these readings were taken at approximately 30 minute intervals. Like many coastal ponds, a large amount of seaweed and other debris was present in the water column. Consequently the problem of fouling of the rotor precluded the use of a moored current meter.

The water depth at the spar was another parameter which was measured as part of this field test. Using a stilling well mounted on the Marine Experiment Station dock nearest the spar, relative tidal height changes were obtained. By measuring the depth at the spar and simultaneously recording the stilling well reading, a correlation between other stilling well observations and the water depth at the spar could be made. Because of the large tidal range at this location, stilling well observations were made approximately every 20 minutes to ensure accuracy.

#### IV-4 Results

##### IV-4.1 Configuration #1

Data from this field test was accumulated over the period 21 May to 24 May 1979. Initially the spar configuration and data collection procedure described above were used and those results are presented below as Table IV-1. The time recorded in this table has as its origin 00:00 on the 21st of May. cursory examination of this data indicates that the

TABLE IV-1

## CONFIGURATION # 1 FIELD DATA

TIME (HOURS)	VELOCITY (FT./SEC.)	DEPTH (FEET)	MEASURED * LIST ANGLE (DEGREES)
16.50	0.34	11.68	32.6
17.00	0.10	11.91	31.7
17.50	0.56	11.90	32.6
18.00	0.39	11.77	33.5
18.62	0.39	11.48	37.1
23.50	0.81	8.39	50
24.20	0.25	8.35	---
24.83	0.03	8.50	---
25.50	0.79	8.78	50
26.12	0.64	9.46	48
26.75	0.57	9.75	43
27.33	0.17	10.25	42
27.75	0.56	10.57	40
28.42	0.03	11.04	35
29.00	0.32	11.33	31
29.52	0.01	11.48	30
30.00	0.34	11.42	33
30.67	0.68	11.16	33
31.17	0.81	10.89	35
31.58	1.00	10.58	35
32.17	1.52	10.07	42
33.00	1.69	9.38	47
33.58	1.69	8.85	50
34.17	1.40	8.46	50
34.83	1.42	8.25	52
36.05	0.32	8.13	50
36.50	0.64	8.21	55

\* Whole number values from hand inclinometer

magnitude of the list angle of the spar in this configuration was quite large with values ranging in size from  $31.7^{\circ}$  to  $55^{\circ}$ . Since the inclinometers mounted in the spar were only capable of resolving angles up to  $45^{\circ}$ , much of the inclination data presented in this table was obtained from hand inclinometer/protractor measurement. To differentiate between those inclinometer values obtained from the internal inclinometers and those measured with the hand held inclinometer/protractor, values fitting into the latter category are listed as whole numbers in Table IV-1. Figure IV-7 is a photograph of the spar in this first configuration. It is apparent from this figure that a great deal of the spar's 18 feet (5.49 m.) of length is above the water surface thereby explaining the large list angle values. In addition, this photograph shows the spar oriented with the splitter plate directed into the current. Observations of this unexpected behavior revealed that it only occurred at very low velocities, generally less than 0.25 ft./sec. (7.62 cm./sec.). At velocities greater than this threshold value, the vane would turn so that it was no longer oriented into the current but at some angle. As the velocity continued to increase, the spar would continue to rotate until the vane was situated downstream and parallel to the flow at velocities of 0.4 ft./sec. (12.19 cm./sec.) or greater. It was initially suspected that this unusual orientation at low velocities was the result of the buoyancy of the vane material. However, subsequent analysis of this behavior revealed that the off-center mooring attachment point was the cause. In this first configuration, the spar was anchored by the forward most of the three anchor attachment holes (i.e., the hole furthest from the vane).

After observing the behavior of the spar in this configuration for approximately two tidal cycles, several facts became evident. Because of

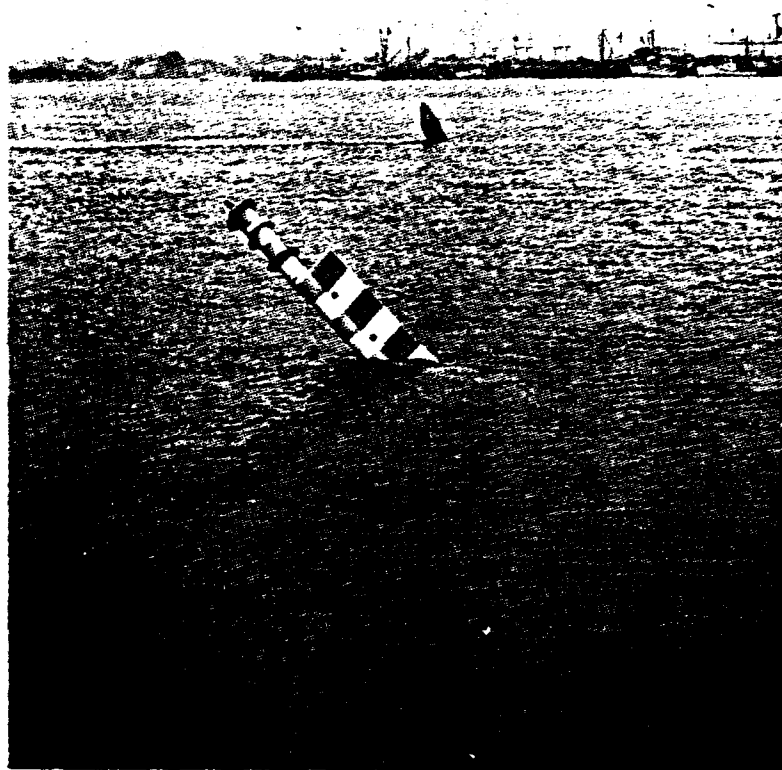


Figure IV-7

The Field Articulated Spar Anchored in Configuration #1

the shallow water depth there were periods of time in which the water depth was less than half of the total spar length. Consequently, with so much weight in the air, large list angles were encountered.

This experiment was extremely useful in that the effects of spar submergence compared to spar length became readily apparent. It was concluded that in any future tests the total spar should be shortened. Since the load cell, which is 27 inches (68.58 cm.) in length, had not provided useful data during this test, it was decided to remove it in future field tests.

#### IV-4.2 Configuration #2

In the second configuration, the load cell was removed, effectively decreasing the spar length-to-water depth ratio, and the mooring attachment point was shifted to the aftermost of the three attachment holes (i.e., the hole nearest the vane) to prevent any reverse orientation of the spar at low velocities. A photograph of the spar in this new configuration is shown in Figure IV-8. Data obtained from the spar in this configuration is presented in Table IV-2. In addition to the list angle values measured by the inclinometer, this table also included corresponding output from the analytical model. Comparison of these two sets of values, however, can only be made following an analysis of the errors inherent in these field data measurements as summarized in Table IV-3.

Slight variations in the actual wind and current profiles as well as vibrations in the spar contributed to the uncertainty in the inclinometer measurements which were estimated to be  $\pm 1.3^{\circ}$ . Current and water depth measurements were taken during this field test for use as input data to the analytical model.



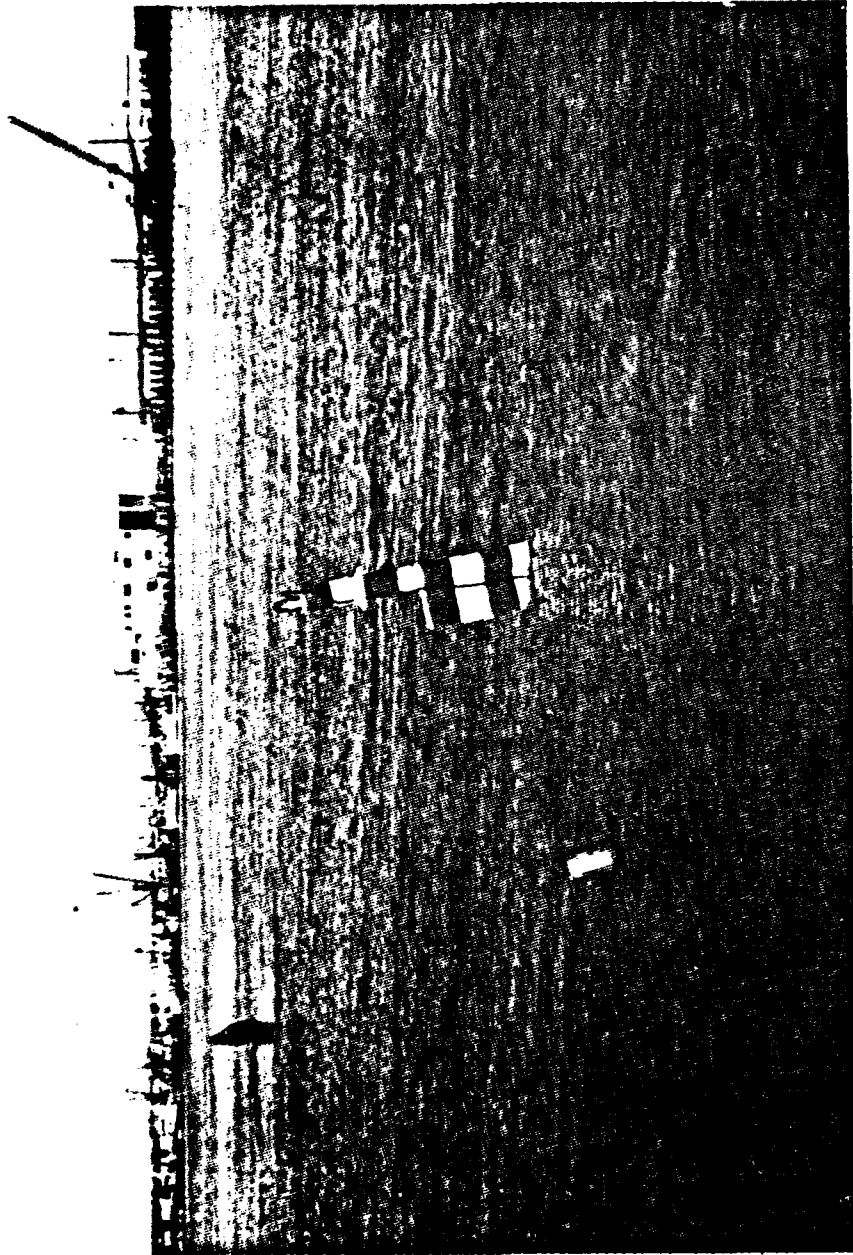


Figure IV-8

The Field Articulated Spar Anchored in Configuration #2

TABLE IV-2  
CONFIGURATION # 2 FIELD DATA

VELOCITY (FT./SEC.)	DEPTH (FEET)	LIST ANGLE (DEGREES)	COMPUTED LIST ANGLE (DEGREES)
0.78	10.46	32.4	34.2
0.25	11.43	22.9	25.8
0.34	12.37	13.6	2.0
0.32	12.17	5.9	1.6
0.10	13.40	3.4	1.0
0.34	13.17	7.7	1.6
0.85	12.60	17.0	15.2
1.32	12.25	19.6	24.2
1.49	11.94	23.8	27.2
1.76	10.40	36.6	38.1
1.55	9.83	38.4	39.8
1.18	9.62	38.8	40.4
0.76	9.58	39.2	40.2
0.34	9.59	38.5	39.9
0.34	9.76	37.7	38.9
0.81	9.94	37.3	38.6
1.00	10.34	34.1	35.8
0.68	10.78	31.2	32.3
0.51	11.20	27.5	27.3
0.34	11.74	22.8	20.5
0.01	12.20	16.8	1.3
0.34	12.62	11.5	1.8
0.08	12.82	7.3	1.1
0.34	12.85	9.0	1.7
0.30	12.87	8.1	1.7
0.68	12.57	11.1	14.3
0.51	12.34	13.3	14.3
0.85	12.09	18.0	20.9
1.13	11.77	21.5	26.4
1.35	11.32	27.2	31.2
1.52	10.88	30.6	33.7
1.77	10.21	35.8	38.9
1.64	9.77	37.5	40.2
1.27	9.54	38.2	41.0
1.27	9.54	38.2	41.0
0.08	9.47	37.9	40.5
0.47	9.67	37.1	39.5
0.41	9.91	35.0	38.5
0.20	10.57	30.7	32.9

TABLE IV-3

FIELD TEST MEASUREMENT ERRORS

Variable	Estimated Error
List Angle	$\pm 1.3^\circ$
Current $> 10.76$ cm./sec. (Threshold = $10.76$ cm./sec.)	$\pm 10\%$
Water Depth	$\pm 7.62$ cm.

A Savonius rotor, which is well known in the literature for its non-linearity, was used to determine current profiles in the vicinity of the spar. Typically these current meters have a non-zero threshold, a tendency to stall at very high speeds, and exhibit more rapid acceleration than deceleration (Beardsley, et. al., 1967). In addition tilt effects have been shown to significantly effect the accuracy of measurements made with these devices although their exact impact varies from one instrument to another as well as over various speed ranges. During the field test, however, it was observed that at low velocities (less than 0.35 ft./sec. (10.67 cm./sec.)) the current meter readings were subject to large fluctuations resulting from the inability of the magnetic reed switches in the current meter to function properly. Consequently, the errors associated with these low velocity measurements were extremely large and, therefore, such values were omitted from further study. Current values greater than 0.35 ft./sec. (10.67 cm./sec.) were estimated to be accurate to within  $\pm 10\%$ .

The water depth measurement used as an input variable to the analytical model is the distance from mean sea level to the bottom of the spar. These water depth values were estimated from stilling well observations and a single correlation measurement of the total water depth. Although the stilling well observations were virtually error-free, the total depth determination was subject to an error estimated to be  $\pm 2$  inches ( $\pm 5.08$  cm.). In addition, the distance from the base of the spar to the pond bottom was measured to an accuracy of  $\pm 1$  inch ( $\pm 2.54$  cm.). Consequently, the total error associated with these water depth measurements was  $\pm 3$  inches ( $\pm 7.62$  cm.).

A sensitivity analysis was performed to determine the significance of these current velocity and water depth uncertainties on predicting the

list angle of the spar. Assuming a  $\pm 10\%$  error in current values greater than 0.35 ft./sec. (10.67 cm./sec.), the change in the spar's list angle was found to be on the order of  $0.1^\circ$  to  $0.2^\circ$ . Consequently, for this buoy configuration, potentially large errors in the current velocity measurements did not significantly effect the spar's list angle.

Figure IV-9 shows the results of a sensitivity analysis of the effect of changes in the water depth over the range experienced in this field test on the spar's list angle assuming three separate current velocities. The relative steepness of the slope of these lines indicates that this field test spar buoy was very sensitive to slight changes in the water depth especially at low velocity values. Therefore, of the two parameters measured for use as input data to the analytical model, only errors in the water depth were found to significantly affect the spar's predicted list angle.

Figure IV-10 is a parity plot of the measured vs. computed list angle data with error bars indicating the uncertainties associated with individual water depth and inclinometer determinations. The relative variation in the width of these error bars results from absolute variations in the current velocity and water depth measurements from which these list angle values were computed. Comparison of model predictions and field measurements as noted in Figure IV-10 shows excellent agreement with a correlation coefficient of 0.986.

#### IV-4.3 Splitter Plate Removal

As the final phase of this field test the splitter plate was removed from the spar to determine the effect such a change would have on the performance of the spar. It was expected that in stronger current situations ( $>0.5$  knots) [ $>25.76$  cm./sec.] that some vortex shedding motion

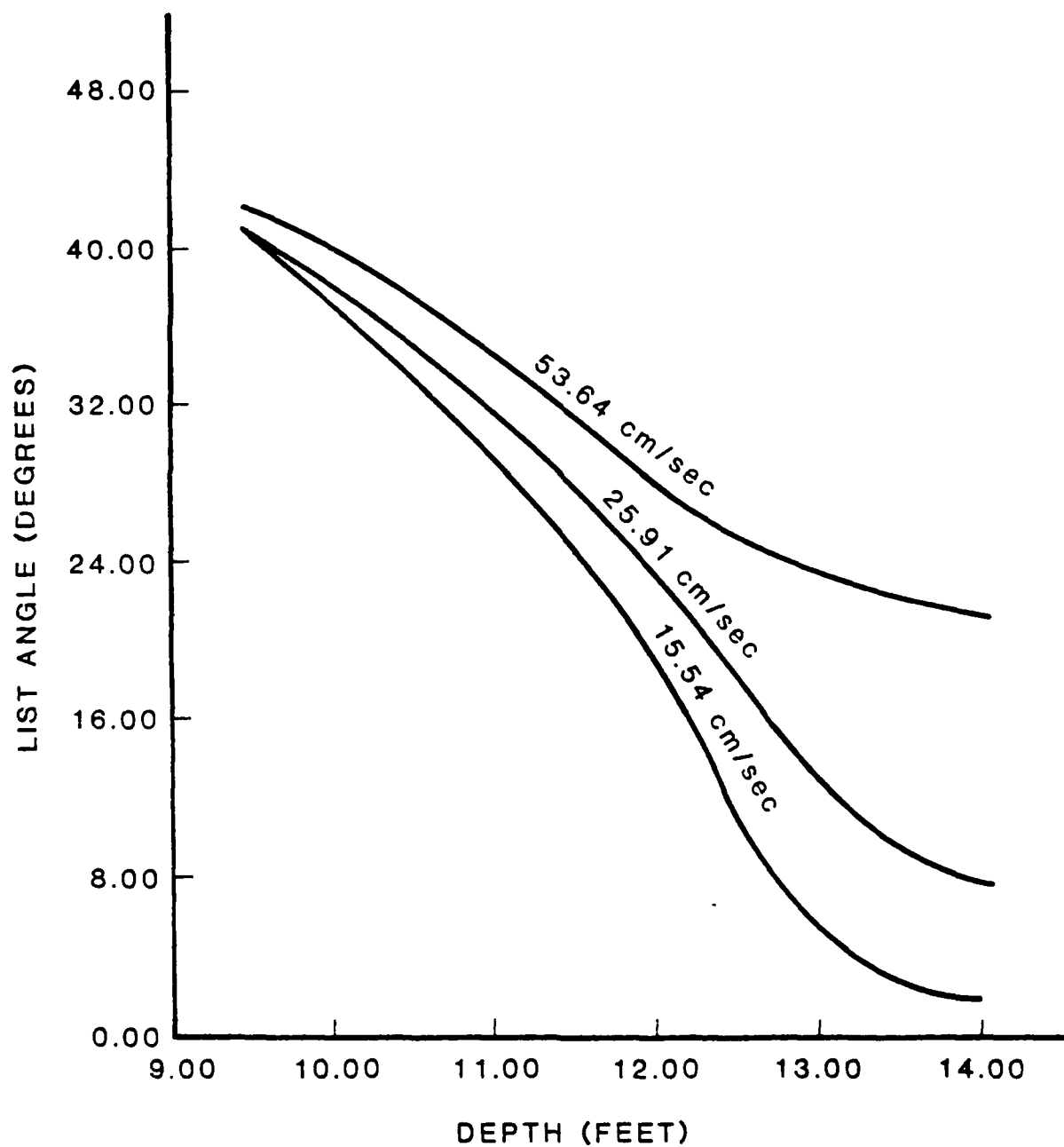


FIGURE IV-9 LIST ANGLE VS DEPTH CURVES OF THE FIELD PROTOTYPE SPAR AT VARIOUS CURRENT VELOCITIES

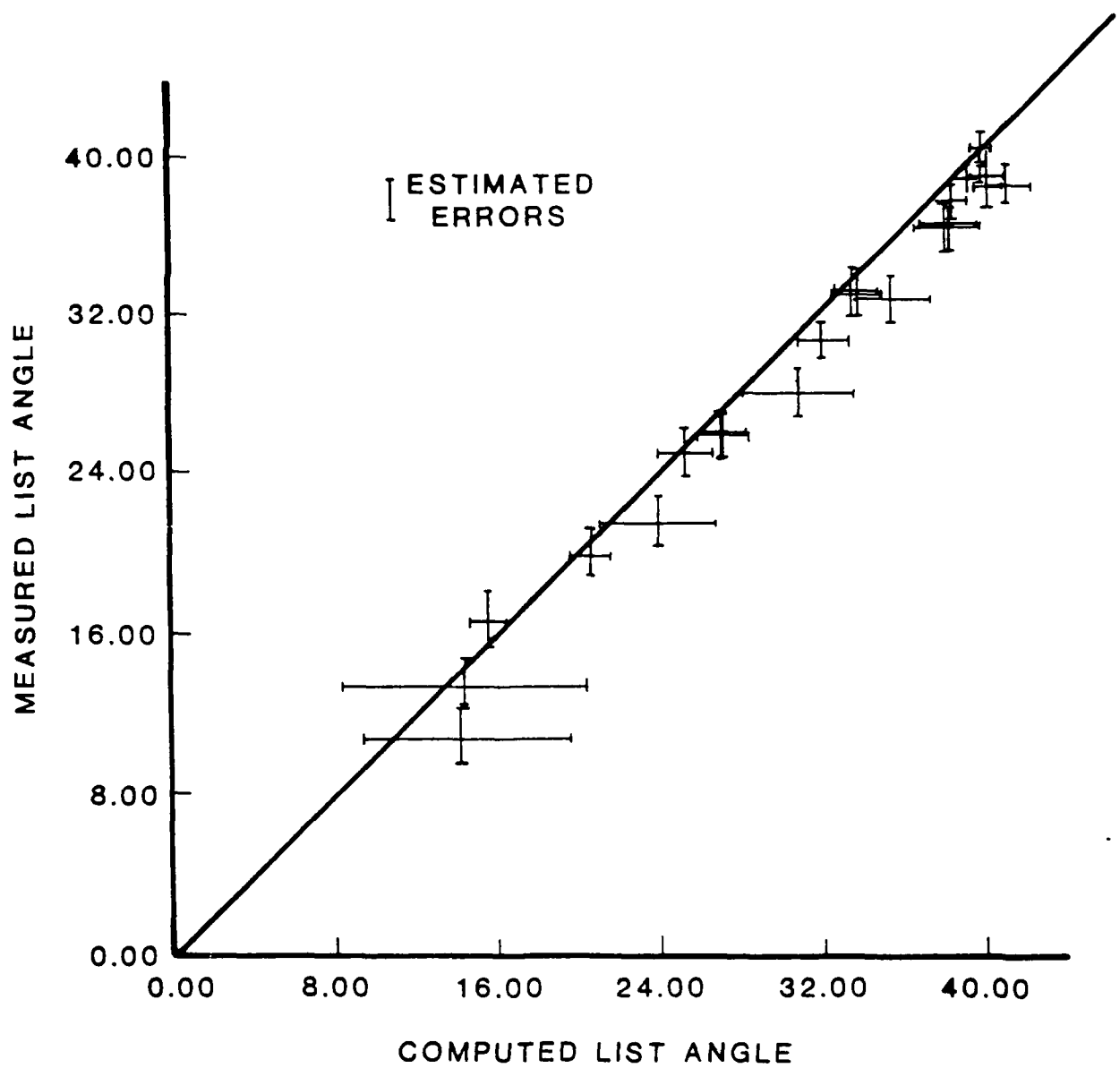


FIGURE IV-10 PARITY PLOT OF MEASURED VS  
COMPUTED LIST ANGLE DATA

would be observed. Equipment problems prevented the accurate determination of the spar list angle, but no unusual list angles were observed when the splitter plate was removed. However, the expected vortex shedding motion did not occur.

As was true in configuration #2, the spar was moored at the aftermost of the three mooring attachment points. It was observed that turning the spar about its vertical axis did not result in an arbitrary reorientation of the spar. Rather, the spar always tended to return to a position where the mooring attachment plate was parallel to the current. Initially, it was speculated that the welded, vane attachment point was acting as a splitter plate and thus preventing any vortex shedding motion. The hypothesis was rejected because subsequent analysis revealed that the uncentered mooring attachment resulted in a torque being placed on the spar. This torque combined with the asymmetry of the spar resulting from the vane attachment plate resulted not only in the spar orienting itself into the current, but prevented vortex shedding from occurring at these velocities by inhibiting transverse motion.



## CHAPTER V

### SUMMARY

#### V-1 Review of Results

An articulated spar as described in this study might serve as a functional alternative to buoys and fixed aids to navigation which are presently used in rivers and other high current areas. When struck, fixed structures are frequently destroyed, whereas an articulated spar, being free to rotate about its attachment point, would either move out of the way or be forced underwater until the object passed over.

To investigate such a structure, an analytical model capable of resolving the forces, moments and list angle of an articulated spar being acted upon by the forces of wind, current and waves was developed. An analysis of the major physical and environmental parameters influencing these forces and moments was made subsequently. In the relatively confined areas of a river or shipping channel, only current forces were found to contribute significantly to the motion of the spar. Further analysis revealed that in addition to current, only one other parameter, the spar weight-per-unit-length/buoyant-force-per-unit-length ratio, affected significantly a spar's list angle. An investigation of several shape related parameters, including the spar length-to-diameter ratio and the effect of varying cross-sectional areas, demonstrated that these variables affect moderately the determination of a spar's list angle.

To validate this analytical model a series of tests were performed in a circulating water channel. An elliptically cross-sectioned spar with a major-to-minor axis ratio of 2:1, moored near its leading edge, was found to be unstable in a current flow. Since the analytical model did not address directional stability, this result was not predicted. Rather than align itself with its major axis parallel to the current, the spar

would rotate so that this axis was perpendicular to the flow. Careful study revealed that this behavior was the result of an asymmetric lift force being generated either by slight perturbations in the flow or slight asymmetries in the spar shape. Subsequent attempts at improving the directional stability of this elliptical spar met with only very limited success. As a result, the scope of the testing program was expanded to include identifying a spar cross-section which was directionally stable. Numerous tests of both circular and tear-drop cross-sectioned spars revealed that of those tested only a circular cross-sectioned spar with a splitter plate had the desired directional stability characteristics over a broad range of flow conditions. A study of different splitter plates found that the minimum size necessary to ensure stability was 1.25 spar diameters in width and approximately 45% of the water depth in length. Comparison of the performance of this design shape with that predicted by the analytical model showed generally good agreement.

Based upon the results obtained in the circulating water channel tests, a field prototype spar was fabricated from nominal 6 inch (16.83 cm.) diameter schedule 40 aluminum pipe. Like the circulating water channel prototype, this spar was equipped with a splitter plate as well as two orthogonally-mounted inclinometers to measure list angles. Testing of this prototype spar took place over a four-day period during which current velocity, water depth, list angle and axial load data were recorded. After one day of testing the initial buoy configuration was altered. Shallower than expected water depths at the test site resulted in spar list angles which were frequently larger than the  $45^{\circ}$  limit of range of the inclinometers. Since it was not possible to move the spar, the original configuration was modified. By removing the load cell, from

which no meaningful data had been obtained, the water depth at the spar was effectively increased by 27 inches (0.61 m.).

In the first configuration, it was observed that the spar would orient itself so that the splitter plate was upstream of the spar at low current velocities ( $< 0.25$  ft./sec.) [7.62 cm./sec.]. To prevent this undesirable orientation from reoccurring, the mooring attachment point was shifted from the forwardmost to the aftermost location (i.e., to the hole nearest the splitter plate). Before comparing the results obtained from the spar in this second configuration with those predicted by the analytical model an analysis of the errors inherent in these field measurements was made. This analysis revealed that the error associated with the inclinometers was on the order of  $\pm 1.3^\circ$ . Current velocity and water depth measurements taken during this field test were used as input data to the analytical model. An estimated error of  $\pm 10\%$  in the measured current velocity was found to alter a spar's predicted list angle by only  $0.1^\circ$  to  $0.2^\circ$ . Depth measurements were estimated to have an accuracy of  $\pm 3$  inches ( $\pm 7.62$  cm.). Over the range of water depths experienced in this field test, uncertainties of this magnitude were found to significantly affect the list angle predicted by the analytical model. Despite these inherent errors, comparison of the analytical model predictions with the field test measurements showed excellent agreement, having a correlation coefficient of 0.986.

#### V-2 Conclusions

The general conclusion of this study is that the development of an analytical model of the forces, moments and resulting list angle on an articulated spar of circular cross-section was successful. Validation of

this model for the test spar over a broad range of environmental conditions showed generally good agreement between predicted and measured list angles. In the field test where there were several sources of error, the results obtained showed excellent agreement. Therefore, this analytical model would serve as one component of a design tool to predict the performance of a variety of articulated spars of circular cross-section under a range of current velocities. The use of this analytical model for predicting the list angle of elliptically cross-sectioned spars is not recommended without additional consideration of directional stability.

### V-3 Suggestions for Future Study

During the course of this work, it became evident that research in several areas could yield additional information which would improve the design of the articulated spar.

#### V-3.1 A Better Shape

The use of the circulating water channel in this experiment was invaluable in facilitating the testing of numerous spar/vane shapes under a variety of conditions. Of the sections examined, the circular shape used as the basis for this study, was unquestionably the most stable. However, for a portion of this project which was not scheduled, the testing with these facilities was constrained by time and consequently was by no means exhaustive. Therefore, one potential area of future research would be the examination of additional low-drag but directionally stable shapes. Despite the problems with spar length, it is felt that because the computer analysis of this spar incorporates the use of elemental areas, Reynolds scaling of any shape could, with some slight modifications to the drag coefficient subroutines, be accomplished for any spar

shape. Unless such a shape is commercially available, the field testing of such a design could require a special extrusion and thus prove to be costly.

One possible suggestion for such a shape would be a hybrid system involving a wing-shaped device which is clamped over a circular spar. By being free to rotate about the spar axis, these airfoil shapes should reduce the overall drag on the system and be free to align themselves with the prevailing currents. Presently, similar-in-design but much more massive clamshell structures are being successfully used on oil drill risers to reduce the drag due to current forces (Chadakoff, 1978).

#### V-3.2 Field Test Modifications

It was clear from the field test that for the conditions and equipment available some very useful information was gathered. However, several important improvements could be made in future field tests.

Since the current velocity profile and water depth are critical input parameters to the analytical model, a more accurate determination of these values would lead to more precise predictions of the list angle. Unfortunately most areas with strong currents generally tend to have large amounts of bulky material such as seaweed suspended in the water column. Consequently, a permanently mounted current meter is likely to soon become fouled and thus its use is not suggested. However, a permanent anchor with a wire attached might be deployed in such a way that a current meter could be easily clamped to it and then lowered in a near vertical mode through the water column. If a ship with lifting capabilities were available, near-vertical orientation of a current meter could be obtained by attaching a large weight to its base.

As an alternative to the Savonius rotor, current measurements might be obtained through other means. In this regard, one device which has been recently explored and shows promise for measuring flows in estuaries is an acoustic current meter. Because such a device has no exposed moving parts, the problem of short-term fouling is eliminated.

If additional tests were to be performed with the present spar, it is suggested that they be made in deeper water. Since the portion of the spar which is above the water surface serves only as a daymark, or platform from which to mount one, the present spar might be modified so that a small daymark shape could be attached to the top using small diameter aluminum tubing such as that used for airplane struts. In this way nearly all of the spar's length would be submerged and provide a large buoyant moment. As a result much of the large degree of sensitivity that this spar showed to small depth changes would be eliminated.

## REFERENCES

- Abbot, Ira H. and VanDoenhoff, Albert E. Theory of Wing Sections, New York: Dover Publications, Inc., 1959.
- Acnenbach, E., "Distribution of Local Pressure and Skin Friction Around a Circular Cylinder in Cross-Flow Up to  $Re = 5 \times 10^6$ ." Journal of Fluid Mechanics 34, Part 4, 1968.
- Beardsley, R.C.; Boicourt, W.; Huff, L.C.; and Scott, J.; "CMICE 76: A Current Meter Intercomparison Experiment Conducted Off Long Island in February-March, 1976," Woods Hole, Massachusetts: Woods Hole Oceanographic Institution, October 1977. (Unpublished Manuscript).
- Berteaux, Henri O., Buoy Engineering, New York: John Wiley and Sons, 1976.
- Bitting, K.R., "A Preliminary Economic Analysis of the Use of Synthetic Mooring Materials on Aids to Navigation Buoys," 1976 (Mineographed).
- Blevins, Robert D., Flow Induced Vibrations, New York: VanNostrand Rienhold Co., 1977.
- Borgman, L.E., "Wave Forces on Piling for Narrow-Band Spectra," Journal of Waterways and Harbors Division, A.S.C.E. 91 No. WW3, Proc. Paper 4443, August 1965, :65-90.
- Bretschneider, C.L., "Evaluation of Drag and Inertia Coefficients from Maximum Range of Total Wave Force." Technical Report No. 55-5, College Station, Texas: Texas A&M University, Department of Oceanography, 1957.
- "Probability Distribution of Wave Force."  
Journal of Waterways and Harbors Division, A.S.C.E. 93 No. WW2, Proc. Paper 5217, May 1967, :5-26.
- Chadakoff, Rouchelle, "Plastic Clamshells," Popular Science, November 1978, p. 60.
- Chen, H.S. and Mei, C.C. "Wave Forces on a Stationary Platform of Elliptical Shape." Journal of Ship Research 17 (June 1973) : 61-71.
- Comstock, John P., ed. Principles of Naval Architecture, New York: The Society of Naval Architects and Marine Engineers, 1967.
- Crooke, R.C. "A Re-Analysis of Existing Wave Force Data on Model Piles," Technical Memorandum No. 71 Washington, D.C., U.S. Army Corps of Engineers, Coastal Engineering Research Center, April 1955.
- Cross, R.H. "Water Wave Teaching Aids." Hydrodynamics Laboratory Technical Note No. 13 Cambridge, Massachusetts: School of Engineering, Massachusetts Institute of Technology, September 1968.
- Dean, R.G. "Relative Validities of Water Wave Theories." Civil Engineering in the Oceans, Proceedings of A.S.C.E. Conference, San Francisco, 1967.

Daugherty, Robert L. and Franzini, Joseph B. Fluid Mechanics with Engineering Applications. New York: McGraw-Hill Book Co., 1977.

Dell'Aggio, Bruno Vittorio, "Beacon for Multedo (Genoa)" Porto e Aeroporto di Genova, 8 August 1972.

Edge, Billy L. and Mayer, Paul G. "A Stochastic Model for the Response of Permanent Offshore Structures Subject to Soil Restraints and Wave Forces." Atlanta, Georgia: Georgia Institute of Technology, April 1969 (available N.T.I.S. PB-232-178).

Evans, J. Harvey and Adamchak, John C. Ocean Engineering Structures, Cambridge, Mass.: The M.I.T. Press, 1972.

Greene, Michael L., Carriker, A. Wendell, and Dewan, Rajinder, N., "Comparison of Calibration Equations for Reducing Savonius Rotor Data." Marine Technology Society Journal 10 (September 1976) : 25-31.

Gruy, R.H. and Kiely, W.L. "The World's Largest Single Point Mooring Terminals: Design and Construction of the SALM System for 750,000 DWT Tankers," Proceedings of the 9th Annual Offshore Technology Conference (May 1977) : 159-169.

Herbich, John B. and Brahme, Shashikant, B., "Estimation and Analysis of Horizontal Bottom Velocities Due to Waves," College Station, Texas: Texas A&M University, 1977. TAMU-SG-77-208, COE Report No. 202.

Hoerner, Sighard, F., Fluid-Dynamic Drag, Brick Town, N.J.: Hoerner Fluid Dynamics, P.O. Box 342, 1965.

Hurlbut, Stephen E. and Spaulding, Malcolm L. "A Numerical Model of Fluid-Structure Interaction for Circular Cylinders," Kingston, R.I.: University of Rhode Island, Department of Ocean Engineering, 1978.

Ippen, Arthur T., ed., Estuary and Coastline Hydrodynamics. New York: McGraw-Hill Book Co., 1965.

Jonsson, I.G., Skougaard, C., and Wang, J.D. "Interaction Between Waves and Currents." Proceedings of the 12th Coastal Engineering Conference A.S.C.E., Washington, D.C.: September 1970.

Keulegan, G.H. and Carpenter, L.H., "Forces on Cylinders and Plates in an Oscillating Fluid." Journal of Research, Washington, D.C.: National Bureau of Standards 60 (May 1958) :423-400.

Kinsman, Blair, Wind Waves, Englewood Cliffs, N.J.: Prentice-Hall, Inc., 1965.

Komar, Paul D., Beach Processes and Sedimentation, Englewood Cliffs, N.J.: Prentice-Hall, Inc., 1976.

Lentner, Marvin, Elementary Applied Statistics, Tarrytown-on-Hudson, N.Y.: Bogden & Quigley, Inc., 1972.



Lowe, R.L., Inman, D.L., and Winant, C.D., "Current Measurements Using a Tilting Spar," Proceedings of the 14th Coastal Engineering Conference, American Society of Civil Engineers, (1974) 225-239.

MacCamy, R.C. and Fuchs, R.A., "Wave Forces on Piles: A Diffraction Theory." Technical Memorandum No. 69, Washington, D.C." U.S. Army Corps of Engineers, Beach Erosion Board, December 1954.

Masubuchi, Koichi, Materials for Ocean Engineering. Cambridge, Mass.: The M.I.T. Press, 1970.

Milne-Thomson, L.M., Theoretical Hydrodynamics, London: MacMillan and Co., Ltd., 1938.

Morison, J.R., "Design of Piling." Proceedings of the First Conference on Coastal Engineering (October, 1950) :254-258.

Muga, Bruce J. and Wilson, James F., Dynamic Analysis of Ocean Structures, New York: Plenum Press, 1970.

Myers, John J.: Holm, Carl H., and McAllister, Raymond F., eds. Handbook of Ocean and Underwater Engineering. New York: McGraw-Hill Book Co., 1969.

Nath, John H., "Laboratory Validation of Numerical Model Drifting Buoy-Tether-Drogue System," Corvallis, Oregon: Oregon State University, 1977.

Newman, J.N., Marine Hydrodynamics. Cambridge, Mass. The M.I.T. Press, 1977.

Paape, A. "Wave Forces on Piles in Relation to Wave Energy Spectra," Proceedings of the Eleventh Conference on Coastal Engineering A.S.C.E., London: September 1968.

Prandtl, L. and Tietjens, O.G. Fundamentals of Hydro and Aerodynamics. New York: Dover Publications, Inc. 1934.

Sarpkaya, T. and Garrison, O.J., "Vortex Formation and Resistance in Unsteady Flow." Journal of Applied Mechanics A. S.M.E., 30 March 1963 :16-24.

Saville, T., Jr., "The Effect of fetch width on wave Generation," TM-70, U.S. Army Corps of Engineers, Beach Erosion Board (Washington, D.C., 1954).

Shames, Irving, H., Mechanics of Fluids. New York: McGraw-Hill Book Co., 1962.

Silvester, Richard.. Coastal Engineering. New York: Elsevier Scientific Publishing Co., 1974.

Synodis, Steve T. and Flory, John F. "Six Years Experience with the Barge Single Anchor Leg Mooring," Proceedings of the 9th Annual Offshore Technology Conference. O.T.C. 2824 (May 1977) :135-140.

Thirriot, A.L., Wohlt, P.E., and Hrrison, A.S. "Sur la Perte de Charge due on Obstacle en Mouvement Periodique." Proceedings of the 14th Congress of International Association of Hydraulic Research, 1971.

U.S. Army Coastal Engineering Research Center, Shore Protection Manual, Washington, D.C., U.S. Government Printing Office, 1973.

U.S. Coast Guard, "Aids to Navigation Manual, CG-222-1." Washington, D.C.: U.S. Coast Guard, 1972.

Vilain, R. "Plateforme Oscillante Experimentale Elf-Ocean," Bulletin de l'A.I.S.M.-I.A.L.A. 44 (April 1970) :11-20.

White, Frank M. Viscous Fluid Flow. New York: McGraw-Hill Book Co., 1977.

Wiegel, Robert L. Oceanographical Engineering, Englewood Cliffs, N.J.: Prentice-Hall, Inc., 1964.

Wu, S.C. and Tung, C.C. "Random Response of Offshore Structures to Wave and Current Forces," (Raleigh, North Carolina: University of North Carolina, Sea Grnt Program, 1975). UNC-SG-75-22.

AD-A110 561

RHODE ISLAND UNIV KINGSTON DEPT OF OCEAN ENGINEERING  
DESIGN OF AN ARTICULATED SPAR BUOY.(U)  
FEB 80 J W CUTLER

F/O 13/10

DOT-C8-81-78-1882

UNCLASSIFIED

USCG-0-71-81

NL

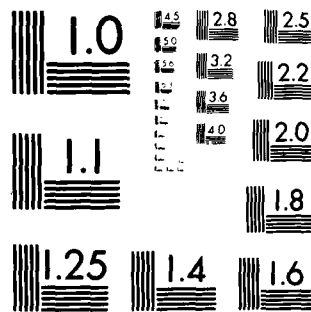
2-2  
2-18-80

END

DATE

FILED

DTIC



MICROCOPY RESOLUTION TEST CHART  
NATIONAL BUREAU OF STANDARDS 1963-A

APPENDIX A

Listing of the Computer Model, ASB1

```

// JOB (PJF100,320,5,7,,,,), 'JACK CUTLER'
// EXEC MONITOR, REGION=320K
//SYSIN DD *
/FTC
CHARACTER XX*7, YY*7, ZZ*7, SH*10, VM*10, PM*10
C
C DIMENSION NECESSARY ARRAYS
C
DIMENSION WA(100)
DIMENSION WSP(100), ELEV(100), Z(100), SPEED(100)
DIMENSION VEL(501), DIR(501), DEP(501), DEPC(500), CAA(501),
1DEPHP(500)
DIMENSION WVELX(100), WVELY(100), WVELNX(100), WVELNY(100)
DIMENSION CVX(500), CVY(500), CVNX(500), CVNY(500)
DIMENSION HWAUX(500), HWAUY(500), VWAUX(500), VWAUY(500)
DIMENSION XREL(500), YREL(500), AX(500), AY(500), BX(500), BY(500)
DIMENSION WAVNX(500), WAVNY(500), WAVX(500), WAVY(500)
DIMENSION WAANX(500), WAANY(500)
DIMENSION WPNX(500), WPNY(500)
DIMENSION RENX(100), RENY(100), RENPX(500), RENPY(500)
DIMENSION CHDX(100), CHDY(100), CHDPX(500), CHDPY(500)
DIMENSION WFX(100), WFY(100)
DIMENSION WPDFX(500), WPIFX(500), WPFY(500), WPDFY(500),
1WPIFY(500), WPFY(500)
DIMENSION AOL(100), TSBF(100), SBWGT(100)
COMMON PI, G, DEPTH, RAIR, RWAT, UAIR, UWAT, ICOUNT, AOLX, AOLY
COMMON NWDP, NCDP, NWADP, NWDPD
DATA XX/' WIND ', YY/'CURRENT', ZZ/' WAVE ' /
REAL LENGTI, M, NEWL
C
C INITIALIZE CASE NUMBER
NCASE=1
C
C DEFINE CONSTANTS
C
PI=3.141592654

```

```

ASB10001
ASB10002
ASB10003
ASB10004
ASB10005
ASB10006
ASB10007
ASB10008
ASB10009
ASB10010
ASB10011
ASB10012
ASB10013
ASB10014
ASB10015
ASB10016
ASB10017
ASB10018
ASB10019
ASB10020
ASB10021
ASB10022
ASB10023
ASB10024
ASB10025
ASB10026
ASB10027
ASB10028
ASB10029
ASB10030
ASB10031
ASB10032
ASB10033
ASB10034
ASB10035
ASB10036

```

ASB10037  
ASB10038  
ASB10039  
ASB10040  
ASB10041  
ASB10042  
ASB10043  
ASB10044  
ASB10045  
ASB10046  
ASB10047  
ASB10048  
ASB10049  
ASB10050  
ASB10051  
ASB10052  
ASB10053  
ASB10054  
ASB10055  
ASB10056  
ASB10057  
ASB10058  
ASB10059  
ASB10060  
ASB10061  
ASB10062  
ASB10063  
ASB10064  
ASB10065  
ASB10066  
ASB10067  
ASB10068  
ASB10069  
ASB10070  
ASB10071  
ASB10072

G=32.174  
INDP1=100  
INDP2=501  
NEWPD=0

C  
C DEFINE FLUID DENSITIES  
RAIR=0.00234  
RFW=1.93632  
RSW=1.98918

C  
C DEFINE FLUID VISCOSITIES  
C VISCOSITY OF WATER AT 68.4 F AND ATMOSPHERIC PRESSURE  
UPW=2.083E-05  
USW=2.067E-05  
UAIR=3.80E-07

C  
C READ IN THE MAXIMUM NUMBER OF CASES TO BE COMPUTED  
READ(5,20) NMAX  
WRITE(6,43) NCASE

C  
C DETERMINE THE WATER DENSITY (1 = SALT; ELSE FRESH)  
1 READ(5,10) IWAT  
IF(IWAT.NE.1) GOTO 2  
RWAT=RSW  
UWAT=USW  
GOTO 4  
2 RWAT=RFW  
UWAT=UPW

C  
C READ IN STILL WATER DEPTH  
4 READ(5,30) DEPTH  
WRITE(6,5) DEPTH,RWAT,UWAT  
5 FORMAT('1',/,/,/,52X,'ENVIRONMENTAL PROPERTIES',/,/,/,  
1/,56X,'GENERAL INFORMATION',/,/,/,40X,  
2,'WATER DEPTH',27X,F7.3,' FEET',/,/,40X,  
3,'MASS DENSITY OF WATER',19X,F6.4,' SLUGS/FT \* 3',/,/,40X,

```

C *****4. VISCOSITY OF WATER',17X,E11.5,' SLUGS/FT - SEC.'*****
C *
C *      INPUT SPAR BUOY STRUCTURAL INFORMATION
C *
C *****
C
C READ IN SPAR BUOY DIMENSIONS
C   READ(5,50) SPL,SPW,SPD
C
C
C FORCE SPAR BUOY DEPTH TO BE THE SMALLEST DIMENSION
C   IF(SPD.LE.SPW) GOTO 6
C     DUM=SPW
C     SPW=SPD
C     SPD=DUM
C
C COMPUTE A OVER B RATIO
C   6 AOB=SPW/SPD
C
C READ IN BUOY'S MATERIAL PROPERTIES
C   READ(5,60) SM,SMD,SWT
C
C ORIENTING VANE PRESENT ?
C   READ(5,10) IVANE
C   IF(IVANE.EQ.1) GOTO 8
C
C IF NO ORIENTING VANE PRESENT, INITIALIZE VANE DIMENSIONS TO ZERO
C   VW=0.0
C   VL=0.0
C   VT=0.0
C   VHGT=0.0
C   VMD=0.0
C   GOTO 16
C
C READ IN ORIENTING VANE DIMENSIONS
C   8 READ(5,50) VL,VH,VT

```

```

ASB10073
ASB10074
ASB10075
ASB10076
ASB10077
ASB10078
ASB10079
ASB10080
ASB10081
ASB10082
ASB10083
ASB10084
ASB10085
ASB10086
ASB10087
ASB10088
ASB10089
ASB10090
ASB10091
ASB10092
ASB10093
ASB10094
ASB10095
ASB10096
ASB10097
ASB10098
ASB10099
ASB10100
ASB10101
ASB10102
ASB10103
ASB10104
ASB10105
ASB10106
ASB10107
ASB10108

```



```

C      C READ IN ORIENTING VANE'S MATERIAL PROPERTIES
C      READ(5,70) VM,VMD
C
C      C READ IN HEIGHT ABOVE THE BOTTOM OF THE LOWER EDGE OF THE
C      ORIENTING VANE AT ZERO ANGLE OF LIST
C      READ(5,30) VHGT
C
C      C BUOY ARTICULATED OR FIXED ?
C      C (1 = ARTICULATED; ELSE FIXED)
C      16 READ(5,10) IART
C      IF(IART.NE.1) GOTO 17
C
C      C READ IN THE COORDINATES OF THE ANCHOR ATTACHMENT POINT
C      C ON THE BOTTOM FACE OF THE BUOY
C      READ(5,40) ANCHX,ANCHY
C      GOTO 18
C      17 ANCHX=0.0
C      ANCHY=0.0
C
C      C CALCULATE THE TOTAL WEIGHT OF THE SPAR BUOY AND IF ARTICULATED
C      CHECK TO SEE IF IT HAS SUFFICIENT BUOYANCY TO FLOAT
C      18 CALL WEIGHT(SPL,SPH,SPD,SWT,SMD,VL,VW,VT,VMD,
C      1IART,CIRCUM,SWGT,VHGT,TSWGT,CAREA,VHWD)
C
C      C ECHO CHECK INPUT OF PHYSICAL DIMENSIONS OF SPAR BUOY
C      IF(SWT.EQ.0.0) GOTO 22
C      WRITE(6,15) SPL,SPW,SPD,CIRCUM,CAREA,AOB,SN,SN,SHD,SWT,SWGT
C      15 FORMAT('1',48X,
C      1'PHYSICAL PROPERTIES OF THE SPAR BUOY',/,/,/,/,55X,
C      2'PROPERTIES OF THE SPAR',/,/,/,40X,
C      3'SPAR LENGTH',27X,F7.3,' FEET',/,/,40X,
C      4'SPAR WIDTH',28X,F7.3,' FEET',/,/,40X,
C      5'SPAR DEPTH',28X,F7.3,' FEET',/,/,40X,
C      6'SPAR CIRCUMFERENCE',21X,F6.3,' FEET',/,/,40X,
C      7'SPAR CROSS-SECTIONAL AREA',14X,F6.3,' FEET ** 2',/,/,40X,

```

```

ASB10109
ASB10110
ASB10111
ASB10112
ASB10113
ASB10114
ASB10115
ASB10116
ASB10117
ASB10118
ASB10119
ASB10120
ASB10121
ASB10122
ASB10123
ASB10124
ASB10125
ASB10126
ASB10127
ASB10128
ASB10129
ASB10130
ASB10131
ASB10132
ASB10133
ASB10134
ASB10135
ASB10136
ASB10137
ASB10138
ASB10139
ASB10140
ASB10141
ASB10142
ASB10143
ASB10144

```

ASB10145  
 ASB10146  
 ASB10147  
 ASB10148  
 ASB10149  
 ASB10150  
 ASB10151  
 ASB10152  
 ASB10153  
 ASB10154  
 ASB10155  
 ASB10156  
 ASB10157  
 ASB10158  
 ASB10159  
 ASB10160  
 ASB10161  
 ASB10162  
 ASB10163  
 ASB10164  
 ASB10165  
 ASB10166  
 ASB10167  
 ASB10168  
 ASB10169  
 ASB10170  
 ASB10171  
 ASB10172  
 ASB10173  
 ASB10174  
 ASB10175  
 ASB10176  
 ASB10177  
 ASB10178  
 ASB10179  
 ASB10180

```

8'SPAR WIDTH TO DEPTH RATIO',14X,F6.3,/,/,40X,
9'SPAR MATERIAL',26X,A10,/,/,40X,
X'MASS DENSITY OF ',A10,12X,F7.3,' SLUGS/FT * 3',/,/,40X,
1'SPAR WALL THICKNESS',21X,F6.4,' FEET',/,/,40X,
2'WEIGHT OF SPAR IN AIR',16X,F8.3,' POUNDS')
  GOTO 24
22 WRITE(6,25) SPL,SPW,SPD,CIRCUM,CAREA,AOB,SH,SM,SMD,SWGT
25 FORMAT('1',48X,
1'PHYSICAL PROPERTIES OF THE SPAR BUOY',/,/,/,55X,
2'PROPERTIES OF THE SPAR',/,/,40X,
3'SPAR LENGTH',27X,F7.3,' FEET',/,/,40X,
4'SPAR WIDTH',28X,F7.3,' FEET',/,/,40X,
5'SPAR DEPTH',28X,F7.3,' FEET',/,/,40X,
6'SPAR CIRCUMFERENCE',21X,F6.3,' FEET',/,/,40X,
7'SPAR CROSS-SECTIONAL AREA',14X,F6.3,' FEET ** 2',/,/,40X,
8'SPAR WIDTH TO DEPTH RATIO',14X,F6.3,/,/,40X,
9'SPAR MATERIAL',26X,A10,/,/,40X,
X'MASS DENSITY OF ',A10,12X,F7.3,' SLUGS/FT * 3',/,/,40X,
1'WEIGHT OF SPAR IN AIR',16X,F8.3,' POUNDS',/,/,47X,
2'SPAR IS A SOLID (NON HOLLOW) STRUCTURE')
24 IF(IART.EQ.1) GOTO 26
  WRITE(6,35)
35 FORMAT(' ',/,/,/,47X,
1'SPAR BUOY IS FIXED AT THE OCEAN BOTTOM')
  GOTO 28
26 WRITE(6,45) ANCHX,ANCHY
45 FORMAT(' ',/,/,/,44X,
1'SPAR BUOY IS ARTICULATED AT THE OCEAN BOTTOM',/,/,40X,
2'ANCHOR ATTACHMENT HAS COORDINATES (' ,F7.4,1X,F7.4,')',/,43X,
3'(IN FEET) RELATIVE TO THE CENTER OF THE BUOY')
28 IF(IVANE.EQ.1) GOTO 32
  WRITE(6,55)
55 FORMAT('1',42X,
1'PHYSICAL PROPERTIES OF THE SPAR BUOY (CONTINUED)',/,/,49X,
2'NO ORIENTING VANE IN THIS ANALYSIS')
  GOTO 42

```

```

C 32 WRITE(6,65) VL,VW,VT,VM,VN,VMD,VHGT,VWGT
C 65 FORMAT('1',42X,
1'PHYSICAL PROPERTIES OF THE SPAR BUOY (CONTINUED)',/,/,/,49X,
2'PROPERTIES OF THE ORIENTING VANE',/,/,40X,
3'VANE LENGTH',28X,F6.3,' FEET',/,/,40X,
4'VANE WIDTH',29X,F6.3,' FEET',/,/,40X,
5'VANE THICKNESS = ',23X,F6.4,' FEET',/,/,40X,
6'VANE MATERIAL = ',24X,A10,/,/,40X,
7'MATERIAL DENSITY OF ',A10,' =',6X,F7.3,' SLUGS/FT**3',/,/,
840X,
9'VANE HEIGHT ABOVE THE BOTTOM',11X,F6.3,' FEET',/,/,40X,
X'VANE WEIGHT = ',24X,F7.3,' POUNDS')
*****
C * INPUT FORCES ACTING ON THE SPAR BUOY *
C * *****
C * INPUT WIND FORCE INFORMATION *
C * *****
C IF NO NEW PHYSICAL DATA, WRITE OUT NEW CASE NUMBER
C
C 42 IP(NEWPD.NE.1) WRITE(6,43) NCASE
C READ IN THE NUMBER OF WIND DATA POINTS
READ(5,20) NWDP
IF(NWDP.EQ.0) GOTO 44
IF(NWDP.LT.100) GOTO 46
IF(NWDP.EQ.999) GOTO 1000
WRITE(6,105) XX,NWDP,INDP1,XX
STOP
C 46 READ(5,60) WSPD,WDIR,WELEV,PETCH
C CONVERT NILES PER HOUR TO FEET PER SECOND
WSPD=WSPD*.5280./3600.

```

ASB10217  
ASB10218  
ASB10219  
ASB10220  
ASB10221  
ASB10222  
ASB10223  
ASB10224  
ASB10225  
ASB10226  
ASB10227  
ASB10228  
ASB10229  
ASB10230  
ASB10231  
ASB10232  
ASB10233  
ASB10234  
ASB10235  
ASB10236  
ASB10237  
ASB10238  
ASB10239  
ASB10240  
ASB10241  
ASB10242  
ASB10243  
ASB10244  
ASB10245  
ASB10246  
ASB10247  
ASB10248  
ASB10249  
ASB10250  
ASB10251  
ASB10252

```

C
C  CONVERT WIND SPEED REFERENCE ELEVATION FROM FEET TO METERS
      WELEV=WELEV*0.3048
C
C  COMPUTE WIND SPEED AT THE 10 METER REFERENCE ELEVATION
      ZO=3.0E-03
      WSPD=WSPD/(ALOG(WELEV/ZO)/ALOG(10./ZO))
C
C  ECHO CHECK WIND FORCE INFORMATION
      DO 48 I=1,10
      48  ELEV(I)=FLOAT(I)
      CALL WNDSPD(WSPD,ELEV,10,SPEED)
      WRITE(6,115)
      115  FORMAT('1',/,/,55X,'WIND FORCE INFORMATION',/,/,55X,
      1'NEAR SURFACE WIND PROFILE',/,/,28X,'ELEVATION',25X,
      2'WIND SPEED',25X,'WIND DIRECTION',/,28X,
      3'(METERS)',27X,'(FT/SEC)',25X,
      4'(DEG. MAGNETIC)')
      DO 52 I=1,10
      52  WRITE(6,125) ELEV(I),SPEED(I),WDIR
      125  FORMAT('0',30X,F3.0,30X,F5.2,32X,F5.1)
      WRITE(6,135) FETCH
      135  FORMAT(' ',/,/,51X,'FETCH LENGTH = ',F10.0,' FEET')
      GOTO 62
      44  WRITE(6,145)
      145  FORMAT('1',/,/,55X,'WIND FORCE INFORMATION',/,/,48X,
      1'NO WIND FORCE PRESENT IN THIS ANALYSIS')
C
C      INPUT CURRENT FORCE INFORMATION
C
C
C  READ IN THE NUMBER OF CURRENT DATA POINTS
      62  READ(5,20) NCDP
      IF(NCDP.EQ.0) GOTO 64

```

```

IF(NCDP.LE.500) GOTO 66
WRITE(6,105) YY,NCDP,INDP2,YY
STOP
        66 NCDPT=NCDP+1
C
C CURRENT SPEED AND DIRECTION UNIFORM ???
      C   (1 = YES; 0 = NO)
      READ(5,10) ICUR
      IF(ICUR.NE.1) GOTO 68
C
C READ IN UNIFORM CURRENT SPEED AND DIRECTION
      READ(5,40) UCVEL,UCDIR
      DO 72 I=1,NCDPT
        VEL(I)=UCVEL
        DIR(I)=UCDIR
        J=I-1
          72 DEP(I)=DEPTH/FLOAT(NCDP)*J
            GOTO 74
C
C READ IN CURRENT VELOCITY AND DIRECTION AT EACH DEPTH OF INTEREST
      68 DO 76 I=1,NCDPT
        76 READ(5,50) VEL(I),DIR(I),DEP(I)
          DELTD=DEP(2)-DEP(1)
          DO 78 I=3,NCDPT
            DELTX=DEP(I)-DEP(I-1)
            IF(DELTX.NE.DELTD) GOTO 82
              78 CONTINUE
                GOTO 74
                  82 WRITE(6,205)
                    205 FORMAT('1' ,/,/,/,/,/,/,/,/,/,/,/,/.56X,
                      /,'*** CHECK DATA ***',/,/,/,/,/,/,/.35X,
                        /,'CURRENT VELOCITY VALUES NOT AT EQUALLY SPACED INTERVALS',
                          /,,/,/,/.56X,
                            /,'CORRECT AND RESUBMIT')
                              STOP
```

```

C COMPUTE AVERAGE CURRENT VELOCITY
74 TOTALX=0.0
TOTALY=0.0
DO 73 I=1, NCDPT
  CVX(I)=VEL(I)*COS(DIR(I)*PI/180.)
  CVY(I)=VEL(I)*SIN(DIR(I)*PI/180.)
  TOTALX=TOTALX+CVX(I)
73 TOTALY=TOTALY+CVY(I)
  AVGX=TOTALX/FLOAT(NCDPT)
  AVGY=TOTALY/FLOAT(NCDPT)
  AVCVEL=SQRT(AVGX**2+AVGY**2)
  AVCDIR=ATAN(AVGX/AVGY)*180./PI
  IF(AVGX.LT.0.00) AVCDIR=AVCDIR+180.
  IF(AVCDIR.LT.0.00) AVCDIR=AVCDIR+360.

C ECHO CHECK CURRENT FORCE INFORMATION
WRITE(6,215)
215 FORMAT('1',53X,'CURRENT FORCE INFORMATION',/,/,/,58X,
1'CURRENT PROFILE',/,/,24X,'DEPTH',25X,'CURRENT SPEED',25X,
2'CURRENT DIRECTION',/,23X,'(FEET)',28X,'(FT/SEC)',28X,
3'(DEG. MAGNETIC)')
DO 84 I=1,NCDPT
84 WRITE(6,225) DEP(I),VEL(I),DIR(I)
225 FORMAT('0',23X,F5.2,30X,F5.2,33X,F5.1)
GOTO 92
64 WRITE(6,235)
235 FORMAT('1',/,/,/,53X,'CURRENT FORCE INFORMATION',/,/,/,45X,
1'NO CURRENT FORCE PRESENT IN THIS ANALYSIS')

C
C INPUT WAVE FORCE INFORMATION
C
C READ IN THE NUMBER OF WAVE DATA POINTS
92 READ(5,20) NWADP
IF(NWADP.EQ.0) GOTO 94

```

```

ASB10289
ASB10290
ASB10291
ASB10292
ASB10293
ASB10294
ASB10295
ASB10296
ASB10297
ASB10298
ASB10299
ASB10300
ASB10301
ASB10302
ASB10303
ASB10304
ASB10305
ASB10306
ASB10307
ASB10308
ASB10309
ASB10310
ASB10311
ASB10312
ASB10313
ASB10314
ASB10315
ASB10316
ASB10317
ASB10318
ASB10319
ASB10320
ASB10321
ASB10322
ASB10323
ASB10324

```

[illegible]

```

ASB10361
ASB10362
ASB10363
ASB10364
ASB10365
ASB10366
ASB10367
ASB10368
ASB10369
ASB10370
ASB10371
ASB10372
ASB10373
ASB10374
ASB10375
ASB10376
ASB10377
ASB10378
ASB10379
ASB10380
ASB10381
ASB10382
ASB10383
ASE10384
ASB10385
ASB10386
ASB10387
ASB10388
ASB10389
ASB10390
ASB10391
ASB10392
ASB10393
ASB10394
ASB10395
ASB10396

IF(IWAVE.EQ.1) GOTO 104
CALL WAVSMB(WSPD,FETCH,TSIG,TAVG,HGTSIG,HGTAVG)
    GOTO 106
104 READ(5,80) TSIG,TAVG,HGTSIG,HGTAVG

C
C READ IN THE NUMBER OF TIME INCREMENTS THE WAVE PERIOD IS
C TO BE DIVIDED INTO
C
106 READ(5,20) ITIME
    IF(ITIME.LE.99) GOTO 108
    WRITE(6,320) ITIME
320 FORMAT('1',/,/,/,/,/,/,54X,
1'ITIME DECLARED AS = ',I3,/,/,/,45X,
2'THIS NUMBER MUST BE REDUCED TO 99 OR LESS',/,48X,
3'ELSE THE WAVE HEIGHT, ANGLE OF LIST',/,48X,
4'TOTAL SPAR BUOY FORCE AND TOTAL SPAR',/,46X,
5'WEIGHT ARRAYS MUST BE REDIMENSIONED')
    STOP
108 NHP1S=ITIME+1

C
C LINEAR (AIRY) OR STOKES SECOND ORDER WAVE THEORY ?
    READ(5,10) ITHERY
    IF((ITHERY.EQ.1).OR.(ITHERY.EQ.2)) GOTO 112
    WRITE(6,325)
325 FORMAT('1',/,/,/,/,/,/,/,/,39X,
1'CHOICE OF APPROPRIATE WAVE THEORY SPECIFIED INCORRECTLY',
2',/,/,/,41X,
3'ACCEPTABLE WAVE THEORY INPUT VALUES ARE : 1 - LINEAR (AIRY)',
4',78X,
5'WAVE THEORY',/,/,/,73X,
6'2 - STOKES SECOND',/,78X,
7'ORDER WAVE THEORY')
    STOP

C
C ECHO CHECK AND CALCULATE ADDITIONAL WAVE INFORMATION
112 CALL WAVE(TSIG,TAVG,HGTSIG,HGTAVG,NWHPTS,ITHERY,WVNO,SIG,
1WAMP,C-DELTAT,WA)

```



```

      GOTO 122
    94 WRITE(6,335)
    335 FORMAT('1',/,/,55X,'WAVE FORCE INFORMATION',/,/,/,48X,
      1'NO WAVE FORCE PRESENT IN THIS ANALYSIS')
C
C OUTPUT OF INTERMEDIATE VALUES DESIRED ?
C (1 = YES; 0 = NO)
    122 READ(5,10) ION
C
C IF WAVES ARE PRESENT DETERMINE THE PRESENT WAVE AMPLITUDE
    IF(NWADP.NE.0) GOTO 124
    NWHPTS=1
    WA(1)=0.0
    124 DO 126 N=1,NWHPTS
      PWAMP=WA(N)
C
C INITIALIZE ANGLES OF LIST AND OTHER COUNTERS
    AOLX=00.00
    AOLY=00.00
    ICOUNT=0
    KCOUNT=0
    LCOUNT=0
    XFAC=10.0
    YFAC=10.0
    100 CONTINUE
    ICOUNT=ICOUNT+1
C
C CHECK TO MAKE SURE THAT THE TOP OF THE SPAR BUOY
C IS ABOVE WATER
    PSPL=SPL*COS(AOLX*PI/180.)*COS(AOLY*PI/180.)
    TD=DEPTH+WA(N)
    IF(PSPL.LT.TD) GOTO 200
    PSPLAW=PSPL-TD
    CALL AREAS(SPL,SPD,SPW,EWAX,EWAY,
      1ECAX,ECAY,EWAAX,EWAAY)
C

```

```

ASB10397
ASB10398
ASB10399
ASB10400
ASB10401
ASB10402
ASB10403
ASB10404
ASB10405
ASB10406
ASB10407
ASB10408
ASB10409
ASB10410
ASB10411
ASB10412
ASB10413
ASB10414
ASB10415
ASB10416
ASB10417
ASB10418
ASB10419
ASB10420
ASB10421
ASB10422
ASB10423
ASB10424
ASB10425
ASB10426
ASB10427
ASB10428
ASB10429
ASB10430
ASB10431
ASB10432

```

```

C DETERMINE BUOY ORIENTATION
C
  IF (NCDP.EQ.0) GOTO 202
  IF (IVANE.NE.1) GOTO 203
  CALL CBEAR(VEL,DIR,DEP,VL,VN,VHGT,DIRV,BEAR)
  GOTO 204
  203 BEAR=AVCDIR+180.
  IF (BEAR.GT.360) BEAR=BEAR-360.
  204 IWIND=1
  GOTO 206
  202 IF (NHDP.EQ.0) GOTO 208
C
C IF NO CURRENT PRESENT THEN BUOY ORIENTS ITSELF TOWARDS THE WIND
  BEAR=WDIR
  WAA=000.00
  IWIND=2
  GOTO 206
C
C IF NO CURRENT OR WIND PRESENT THEN BEARING SET EQUAL TO ZERO
  208 BEAR=000.00
  WAA=000.00
  IWIND=3
C
C DETERMINE THE RELATIVE WIND, CURRENT AND WAVE PARTICLE VELOCITIES
C
  206 IF (NHDP.NE.0) CALL RWVEL(BEAR,PSPLAW,WSPD,WDIR,
    1ELEV,WAA,WSP,WVELX,WVELNX,WVELY,WVELNY)
  IF (NCDP.NE.0) CALL RCVEL(BEAR,DIR,VEL,CAA,DEPC,CVX,CVY,
    1CVNX,CVNY)
  IF (NHADP.NE.0) CALL RWAVA(NWADPT,ITHERY,DELTAT,WAMP,
    1SIG,N,WVNO,WAA,C,HWAVX,HWAVY,VHAVX,VHAVY,WAVNX,
    2WAVNY,WAANX,WAANY)
C
C COMPUTE AVERAGE ANGLE OF ATTACK
  IF (NCDP.EQ.0) GOTO 209
  TOTALX=0.0

```

```

ASB10433
ASB10434
ASB10435
ASB10436
ASB10437
ASB10438
ASB10439
ASB10440
ASB10441
ASB10442
ASB10443
ASB10444
ASB10445
ASB10446
ASB10447
ASB10448
ASB10449
ASB10450
ASB10451
ASB10452
ASB10453
ASB10454
ASB10455
ASB10456
ASB10457
ASB10458
ASB10459
ASB10460
ASB10461
ASB10462
ASB10463
ASB10464
ASB10465
ASB10466
ASB10467
ASB10468

```

```

TOTALY=0.0
DO 212 I=1,NCDP
    TOTALX=TOTALX+CVX(I)
    TOTALY=TOTALY+CVY(I)
212 CONTINUE
AVGX=TOTALX/FLOAT(NCDP)
AVGY=TOTALY/FLOAT(NCDP)
AVCAA=ATAN(AVGX/AVGY)*180./PI
GO TO 214

220 AVCVEL=0.0
AVCDIR=0.0
AVCAA=0.0

      C
      C DETERMINE WATER PARTICLE VELOCITIES BY COMBINING CURRENT
      C AND WAVE PARTICLE VELOCITIES
      C
224 IF((NCDP.EQ.0).AND.(NWADP.EQ.0)) GO TO 222
IF((NCDP.NE.0).AND.(NWADP.EQ.0)) GO TO 224
IF((NCDP.EQ.0).AND.(NWADP.NE.0)) GO TO 226
IF((NCDP.EQ.NWADP) GO TO 216
WRITE(6,345) NCDP,NWADP
FORMAT('1',/,/,/,/,/,/,/,46X,
1,NUMBER OF CURRENT DATA POINTS NOT EQUAL',/,49X,
2,TO THE NUMBER OF WAVE DATA POINTS',/,/,/,/,/,48X,
3,NUMBER OF CURRENT DATA POINTS = ',I3,/,/,50X,
4,NUMBER OF WAVE DATA POINTS = ',I3)
STOP
210 NWDPD=NCDP
EWPAW=ECAX
EWPAW=ECAY
DO 218 I=1,NWPDP
    WVNX(I)=CVNX(I)+WAVNX(I)
    WVNY(I)=CVNY(I)+WAVNY(I)
218 CONTINUE
222 NWPPD=0
GO TO 232
224 NWFPD=NCDP
EWPAW=ECAX

```

ASB10505  
ASB10506  
ASB10507  
ASB10508  
ASB10509  
ASB10510  
ASB10511  
ASB10512  
ASB10513  
ASB10514  
ASB10515  
ASB10516  
ASB10517  
ASB10518  
ASB10519  
ASB10520  
ASB10521  
ASB10522  
ASB10523  
ASB10524  
ASB10525  
ASB10526  
ASB10527  
ASB10528  
ASB10529  
ASB10530  
ASB10531  
ASB10532  
ASB10533  
ASB10534  
ASB10535  
ASB10536  
ASB10537  
ASB10538  
ASB10539  
ASB10540

```

      EWPAY=ECAY
      DO 228 I=1,NWPDP
        WAANY(I)=0.0
        WAANY(I)=0.0
        WPNX(I)=CVNX(I)
        WPNY(I)=CVNY(I)
      GOTO 232
226 NWPDP=NWADP
      EWPAX=EWAAX
      EWPAY=EWAAY
      DO 229 I=1,NWPDP
        WPNX(I)=WAVNX(I)
        WPNY(I)=WAVNY(I)
229 WPNY(I)=WAVNY(I)

C CHECK FOR THE DEGENERATE CASE OF ELLIPTICAL CROSS-SECTION OF
C THE SPAR BUOY BEING A CIRCLE.
232 IF (SPW.SP) GOTO 234
      CALL DRAGC(WVELNX,WPNX,SPD,PSPLAW,DEPWP,RENX,
1REWPX,CWDY,CWPDY)
      CALL DRAGC(WVELNY,WPNY,SPD,PSPLAW,DEPWP,RENY,
1REWPY,CWDY,CWPDY)
      GOTO 236
234 CALL DRAGX(WVELNX,WPNX,SPD,SPW,PSPLAW,DEPWP,
1RENX,REWPX,CWDY,CWPDY)
      CALL DRAGY(WVELNY,WPNY,SPD,SPW,PSPLAW,RENY,
1REWPY,CWDY,CWPDY)
236 CALL FORCE(N,NHPTS,SPD,SPW,CAREA,EWAY,EWAY,
1EWPAX,EWPAY,WVELNX,WVELNY,WPNX,WPNY,WAVNX,WAVNY,
2CWDX,CWDY,CWPDY,CWPDY,CHX,CHY,WFX,WFY,TWFX,TWFY,
3WPDFX,WPDFY,WPIFX,WPIFY,WPFY,WPFY,TWPDFX,TWPDFY,
4TWPIFX,TWPIFY,TWPFY,TWPFY,TFX,TFY,TSBF)

C
C SET END CAP FLAG
      IEND=1
C
C COMPUTE OVERTURNING MOMENTS

```

```

ASB10541
ASB10542
ASB10543
ASB10544
ASB10545
ASB10546
ASB10547
ASB10548
ASB10549
ASB10550
ASB10551
ASB10552
ASB10553
ASB10554
ASB10555
ASB10556
ASB10557
ASB10558
ASB10559
ASB10560
ASB10561
ASB10562
ASB10563
ASB10564
ASB10565
ASB10566
ASB10567
ASB10568
ASB10569
ASB10570
ASB10571
ASB10572
ASB10573
ASB10574
ASB10575
ASB10576

CALL OTHOM(WFX,WFY,WPFY,PSPLAW,PWAMP,CAREA,SPL,
1SWWD,VL,VHGT,VMMWD,IVSUB,VNWD,TBMGT,TSWGT,ANCHX,ANCHY,IEND,
2WOTMX,WOTHY,WPOTX,WPOTY,OTMONX,OTMOMY)
IF(IART.NE.1) GOTO 460

C
C COMPUTE RIGHTING MOMENTS
CALL RMOM(SPL,SPW,VN,VL,VHGT,SWGTV,VMGT,PFAHP,SMWD,VNWD,IVSUB,
1WMOMX,WNOMY,BMOMX,BMOMY,RMOMX,RMOMY)

C
C ITERATE THE LIST ANGLE UNTIL THE OVERTURNING MOMENT IS
C EQUAL TO THE RIGHTING MOMENT
DIFFX=OTMONX-RMOMX
DIFFY=OTMOMY-RMOMY
IF(ABS(DIFFY).GT.ABS(DIFFX)) GOTO 395
IP(DIFFY.GT.0.02) GOTO 300
IF(DIFFX.LT.-0.02) GOTO 350
395 IP(DIFFY.GT.0.02) GOTO 400
IP(DIFFY.LT.-0.02) GOTO 450
GOTO 460
300 KCOUNT=KCOUNT+1
IF(KCOUNT.EQ.1) XFAC=XFAC/10.0
AOLX=AOLX+XFAC
GOTO 100
350 AOLX=AOLX-XFAC/10.0
KCOUNT=0
GOTO 100
400 LCOUNT=LCOUNT+1
IF(LCOUNT.EQ.1) YFAC=YFAC/10.0
AOLY=AOLY+YFAC
GOTO 100
450 AOLY=AOLY-YFAC/10.0
LCOUNT=0
GOTO 100

C *****
C *
C * FINAL OUTPUT

```

**FINAL OUTPUT**

```

C *
C *****
C WRITE OUT BUOY ORIENTATION
460 IF (ININD.EQ.1) WRITE(6,505) BEAR
    IF (ININD.EQ.2) WRITE(6,515) BEAR
    IF (ININD.EQ.3) WRITE(6,525) BEAR
C
C WRITE OUT INTERMEDIATE VALUES IF DESIRED
    IF (ION.EQ.1) CALL INOUT1(ELEV,
1WAA,WSP,WVELX,WVELY,WVELNX,WVELNY,DEPC,DEPWP,VEL,DIR,CAA,CVX,
2CVY,CVNXX,CVNY,DEP,PWAMP,HWAAX,HWAAY,HWAAX,HWAAY,HWAAX,HWAAY,
3WAVTX,WAVTY,XREL,YREL,AX,AY,BX,BY,WPNXX,WPNY,SPW,SPD,
4REWX,REWY,REWPX,REWPY,CWDY,CWPDY,CWPDY)
    IF (ION.EQ.1) CALL INOUT2(EWAX,EWAY,CAREA,CMX,CMY,
1ELEV,WFX,WFY,TWFX,TWFY,EWPAY,DEPWP,WPDPX,WPDPY,WPIFX,
2WPIFY,WPFY,WPFY,TWDPFX,TWDPFY,TWPIFY,TWPIFY,TWPIFY,TWPIFY,
3WOTMX,WOTMY,WOTMX,WOTMY,OTMOMX,OTMOMY,IART,WOTMX,WOTMY,
4BOMOX,BOMY,RNOMX,RNOMY)
    IF (IART.EQ.1) GOTO 470
    IF (N.EQ.1) WRITE(6,475)
    WRITE(6,485) N,TFX,TFY,TSBF(N),OTMOMX,OTMOMY
    GOTO 126
C
C COMPUTE THE WATCH CIRCLE RADIUS AND THE TOTAL LIST ANGLE
470 XSPL=DEPTH*TAN(AOLX*PI/180.)
    YSPL=DEPTH*TAN(AOLY*PI/180.)
    WCA=SQRT(XSPL**2+YSPL**2)
    AOL(N)=ATAN(WCR/DEPTH)*180./PI
    IF (AOLX.LT.0.00) AOL(N)=-AOL(N)
    SBWGT(N)=TBWGT
C
C WRITE OUT FINAL RESULTS
    WRITE(6,605) AVCVEL,AVCDIR,AVCAA,PWAMP,ICOUNT,
1AOLX,OTMOMX,RNOMX,AOLY,OTMOMY,RNOMY,WCR,AOL(N)
    GOTO 126
200 WRITE(6,615) AVCVEL,AVCDIR,AVCAA,PWAMP,ICOUNT,SPL,AOLX,

```

```

ASB10577
ASB10578
ASB10579
ASB10580
ASB10581
ASB10582
ASB10583
ASB10584
ASB10585
ASB10586
ASB10587
ASB10588
ASB10589
ASB10590
ASB10591
ASB10592
ASB10593
ASB10594
ASB10595
ASB10596
ASB10597
ASB10598
ASB10599
ASB10600
ASB10601
ASB10602
ASB10603
ASB10604
ASB10605
ASB10606
ASB10607
ASB10608
ASB10609
ASB10610
ASB10611
ASB10612

```

ASB10613  
 ASB10614  
 ASB10615  
 ASB10616  
 ASB10617  
 ASB10618  
 ASB10619  
 ASB10620  
 ASB10621  
 ASB10622  
 ASB10623  
 ASB10624  
 ASB10625  
 ASB10626  
 ASB10627  
 ASB10628  
 ASB10629  
 ASB10630  
 ASB10631  
 ASB10632  
 ASB10633  
 ASB10634  
 ASB10635  
 ASB10636  
 ASB10637  
 ASB10638  
 ASB10639  
 ASB10640  
 ASB10641  
 ASB10642  
 ASB10643  
 ASB10644  
 ASB10645  
 ASB10646  
 ASB10647  
 ASB10648

```

1AOLY,PSPL,DEPTH,TD
TSBF(N)=00.00
AOL(N)=00.00
SBWGT(N)=00.00
126 CONTINUE
      WRITE(6,705) NCASE
705 FORMAT('1',58X,'CASE NUMBER ',I3,/,/,57X,
1'SUMMARY OF RESULTS',/,/,33X,
2'STEP',22X,'TOTAL FORCE',22X,'RESULTANT',/,33X,
3'NUMBER',24X,'(LBS.)',23X,'LIST ANGLE')
      DO 710 N=1,NWHPTS
710 WRITE(6,715) N,TSBF(N),AOL(N)
715 FORMAT('0',33X,I3,20X,F11.3,27X,F6.3)
      IF ((NWADP.EQ.0).AND.(SBWGT(1).EQ.0.00)) GOTO 716
      CALL ANCHOR(NWHPTS,TSWGT,SBWGT)
C
C INCREMENT CASE NUMBER
C IF CASE NUMBER EXCEEDS NMAX THEN STOP
C OTHERWISE CHECK TO SEE IF NEW PHYSICAL DATA IS TO BE READ IN
C
716 NCASE=NCASE+1
      IF (NCASE.GT.NMAX) GOTO 1000
      READ(5,10) NEWPD
      IF (NEWPD.NE.1) GOTO 42
      WRITE(6,43) NCASE
      GOTO 1
1000 CONTINUE
C *****
C * MAIN PROGRAM FORMAT STATEMENTS (INPUT FIRST OUTPUT SECOND) *
C *****
10 FORMAT(I1)
20 FORMAT(I3)
30 FORMAT(F10.0)
40 FORMAT(F10.0,F10.0)
50 FORMAT(F10.0,F10.0,F10.0)
60 FORMAT(A10,F10.0,F10.0)

```

[illegible]



```

C THIS SUBROUTINE CALCULATES THE WEIGHT OF THE SPAR BUOY IN AIR AND
C ITS BUOYANT WEIGHT IN WATER. IF THE SPAR BUOY IS ARTICULATED THEN
C A CHECK IS MADE TO DETERMINE IF AS A FREE FLOATING BODY IT HAS
C SUFFICIENT BUOYANCY TO FLOAT
C      COMMON PI,G,DEPTH,RAIR,RWAT,UAIR,UWAT,ICOUNT,AOLX,AOLY
C      COMMON NWDP,NCDP,NWADP,NWPPD
C
C CALCULATE THE WEIGHT OF THE SPAR BUOY AND ORIENTING VANE
C IN AIR

```

[illegible]

```

C IN METERS FOR WHICH THE WIND VELOCITY IS DESIRED.  A WIND SPEED
C ARRAY, WSPD(NPTS) CONTAINING THE WIND VELOCITY VALUES BASED UPON
C A LOGRITHMIC DISTRIBUTION IS RETURNED
C
    DIMENSION ELEV(NPTS), WSPD(NPTS)
    COMMON PI,G,DEPTH,RAIR,RWAT,UAIR,UWAT,ICOUNT,AOLX,AOLY
    COMMON NWDP,NCDP,NWADP,NWPD
    ZO=3.0E-03
    DO 100 I=1,NPTS
    WSPD(I)=(ALOG(ELEV(I)/ZO)/ALOG(10./ZO))*W10
    RETURN
    END
C *****
C * SUBROUTINE WAVSMB
C *****
C SUBROUTINE WAVSMB(WSPD,FETCH,TSIG,TAVG,HGTSIG,HGTAVG)
C
C SUBROUTINE WAVSMB CALCULATES THE SIGNIFICANT WAVE HEIGHT AND
C SIGNIFICANT PERIOD OF A WAVE FIELD AS WELL AS THE AVERAGE WAVE
C HEIGHT AND AVERAGE WAVE PERIOD UNDER SPECIFIED WIND, FETCH
C AND DEPTH CONDITIONS USING THE SMB METHOD.
C
    COMMON PI,G,DEPTH,RAIR,RWAT,UAIR,UWAT,ICOUNT,AOLX,AOLY
    COMMON NWDP,NCDP,NWADP,NWPD
    A=G*FETCH/(WSPD**2)
    B=G*DEPTH/(WSPD**2)
C
C COMPUTE SIGNIFICANT AND AVERAGE WAVE HEIGHTS
    HGTSIG=0.283*TANH(0.530*B**0.75)*TANH((0.0125*A**0.42)/(TANH
    1(0.530*B**0.75)))*WSPD**2/G
    HGTAVG=0.6257*HGTSIG
C
C COMPUTE SIGNIFICANT AND AVERAGE WAVE PERIODS
    TSIG=1.20*TANH(0.833*B**0.375)*TANH((0.077*A**0.25)/
    1(TANE(0.833*B**0.375)))*2*PI*WSPD/G
    TAVG=SQRT(HGTSIG/0.45)

```

ASB10757  
 ASB10758  
 ASB10759  
 ASB10760  
 ASB10761  
 ASB10762  
 ASB10763  
 ASB10764  
 ASB10765  
 ASB10766  
 ASB10767  
 ASB10768  
 ASB10769  
 ASB10770  
 ASB10771  
 ASB10772  
 ASB10773  
 ASB10774  
 ASB10775  
 ASB10776  
 ASB10777  
 ASB10778  
 ASB10779  
 ASB10780  
 ASB10781  
 ASB10782  
 ASB10783  
 ASB10784  
 ASB10785  
 ASB10786  
 ASB10787  
 ASB10788  
 ASB10789  
 ASB10790  
 ASB10791  
 ASB10792

ASB10793  
 ASB10794  
 ASB10795  
 ASB10796  
 ASB10797  
 ASB10798  
 ASB10799  
 ASB10800  
 ASB10801  
 ASB10802  
 ASB10803  
 ASB10804  
 ASB10805  
 ASB10806  
 ASB10807  
 ASB10808  
 ASB10809  
 ASB10810  
 ASB10811  
 ASB10812  
 ASB10813  
 ASB10814  
 ASB10815  
 ASB10816  
 ASB10817  
 ASB10818  
 ASB10819  
 ASB10820  
 ASB10821  
 ASB10822  
 ASB10823  
 ASB10824  
 ASB10825  
 ASB10826  
 ASB10827  
 ASB10828

```

RETURN
END
*****
C * SUBROUTINE WAVE *****
C * SUBROUTINE WAVE(TSIG,TAVG,HGTSIG,HGTAVG,NWHPTS,ITHERY,WVNO,
C * XSIG,WAMP,C,DELTAT,WA)
C
C SUBROUTINE WAVE COMPUTES INFORMATION ABOUT A WAVE USING EITHER
C LINEAR (AIRY) OR STOKES SECOND ORDER WAVE THEORY.
C
C DIMENSION WA(100)
C COMMON PI,G,DEPTH,RAIR,RWAT,UAIR,UWAT,ICOUNT,AOLX,AOLY
C COMMON NWDP,NCDP,NWADF,NWPDF
C REAL LENGTI,M,NEWL
C
C COMPUTE THE DEEP WATER WAVELENGTH, DLO
DLO=G*TAVG**2./(2*PI)
HOLO=DEPTH/DLO
C
C DETERMINE THE RANGE OF H OVER L AND CALCULATE H/L
IF (HOLO.LT.0.04) GOTO 10
IF (HOLO.LT.0.15) GOTO 20
IF (HOLO.LT.0.39) GOTO 30
HL=HOLO
GOTO 100
10 A=0.43
M=0.511
GOTO 40
20 A=0.54
M=0.580
GOTO 40
30 A=0.83
M=0.806
40 HL=A*HOLO**M
100 NEWL=DEPTH/HL

```

```

C ITERATE TO IMPROVE ESTIMATE
  WL=DLO*TANH(2*PI*DEPTH/NEWL)
  DO 200 K=1,500
    LENGTI=WL
    WL=DLO*TANH(2*PI*DEPTH/LENGTI)
    IF(0.001*LENGTI.GE.ABS(LENGTI-WL)) GOTO 300
  200 CONTINUE
C COMPLETION OF THE ABOVE DO LOOP INDICATES AN ERROR IN
C THE WAVELENGTH CALCULATION. CHECK RESULTS
  WRITE(6,250) NEWL,WL,LENGTI,TAVG,DEPTH
  GOTO 1000
C CHECK THE RATIO OF WAVE HEIGHT TO WAVE LENGTH FOR
C EXCESSIVE STEEPNESS
  300 R1=HGTAVG/WL
  IF(0.142*WL/DLO.LE.R1) GOTO 400
C COMPUTE WAVE CELERITY, WAVE FREQUENCY, WAVE NUMBER AND
C MAXIMUM WAVE AMPLITUDE
  WVNO=2.0*PI/WL
  SIG=2.0*PI/TAVG
  C=G/SIG*TANH(2.*PI*DEPTH/WL)
  WAMP=HGTAVG/2.0
  DELTAT=TAVG/(NWHPTS-1)
C COMPUTE THE WAVE AMPLITUDE ARRAY
  DO 500 I=1,NWHPTS
    500 WA(I)=HGTAVG/2.0*COS(SIG*DELTAT*(I-1))
    IF(ITHRY.EQ.2) WA(I)=WA(I)+(WAMP**2.*WVNO/2.*
      1COSH(2.*PI*DEPTH/WL)/SINH(2.*PI*DEPTH/WL)**3.*COS(-2.*SIGMAT))
    WRITE(6,550) HGT SIG,HGTAVG,TSIG,TAVG,WL,C,WVNO,SIG,DELTAT
    DO 600 I=1,NWHPTS
      600 WRITE(6,650) I,WA(I)
    650 FORMAT('0',40X,I3,31X,F5.2)

```

ASB10829  
 ASB10830  
 ASB10831  
 ASB10832  
 ASB10833  
 ASB10834  
 ASB10835  
 ASB10836  
 ASB10837  
 ASB10838  
 ASB10839  
 ASB10840  
 ASB10841  
 ASB10842  
 ASB10843  
 ASB10844  
 ASB10845  
 ASB10846  
 ASB10847  
 ASB10848  
 ASB10849  
 ASB10850  
 ASB10851  
 ASB10852  
 ASB10853  
 ASB10854  
 ASB10855  
 ASB10856  
 ASB10857  
 ASB10858  
 ASB10859  
 ASB10860  
 ASB10861  
 ASB10862  
 ASB10863  
 ASB10864

ASB10865  
 ASB10866  
 ASB10867  
 ASB10868  
 ASB10869  
 ASB10870  
 ASB10871  
 ASB10872  
 ASB10873  
 ASB10874  
 ASB10875  
 ASB10876  
 ASB10877  
 ASB10878  
 ASB10879  
 ASB10880  
 ASB10881  
 ASB10882  
 ASB10883  
 ASB10884  
 ASB10885  
 ASB10886  
 ASB10887  
 ASB10888  
 ASB10889  
 ASB10890  
 ASB10891  
 ASB10892  
 ASB10893  
 ASB10894  
 ASB10895  
 ASB10896  
 ASB10897  
 ASB10898  
 ASB10899  
 ASB10900

```

GOTO 1000
400 WRITE(6,450) HGTA VG,WL,R1
GOTO 1000
C *****
C SUBROUTINE WAVE FORMAT STATEMENTS
C *****
250 FORMAT('1',/,/,/,/,/,52X,
1'ERROR IN SUBROUTINE WAVE',/,/,/,55X,
2'NEWL = ',6X,P9.3,/,/,55X,
3'WAVELENGTH = ',9X,P9.3,/,/,55X,
4'LENGTHI = ',4X,P9.3,/,/,55X,
5'TAVG = ',6X,P9.3,/,/,55X,
6'DEPTH = ',5X,P9.3)
450 FORMAT('1',/,/,/,/,/,/,/,/,/,59X,
1'WAVE TOO STEEP',/,/,/,54X,
2'WAVE HEIGHT = ',F6.2,' FEET',/,/,54X,
3'WAVE LENGTH = ',F6.2,' FEET',/,/,53X,
4'H OVER L = ',F5.4)
550 FORMAT('1',/,/,58X,'WAVE INFORMATION',/,/,40X,
1'SIGNIFICANT WAVE HEIGHT',16X,P6.3,' FEET',/,/,40X,
2'AVERAGE WAVE HEIGHT',20X,P6.3,' FEET',/,/,40X,
3'SIGNIFICANT WAVE PERIOD',16X,P6.3,' SECONDS',/,/,40X,
4'AVERAGE WAVE PERIOD',20X,P6.3,' SECONDS',/,/,40X,
5'WAVELENGTH (AFTER WEIGAL)',13X,P7.3,' FEET',/,/,40X,
6'WAVE CELERITY',26X,P6.3,' FEET',/,/,40X,
7'WAVE NUMBER',28X,P6.3,' 1/FEET',/,/,40X,
8'ANGULAR WAVE FREQUENCY',17X,P6.3,' RADIAN/SEC.',/,/,40X,
9'TIME STEP INCREMENT',20X,P6.3,' SECONDS',/,/,54X,
X' WAVE HEIGHT INFORMATION',/,/,38X,
1'TIME STEP',25X,'WAVE HEIGHT',/,74X,' (FEET)')
1000 RETURN
END
C *****
C SUBROUTINE AREAS
C *****
C SUBROUTINE AREAS(SPL,SPD,SPW,EWAX,EWAY,

```

```

1ECAX,ECAY,EWAAX,EWAAY)
C
C THIS SUBROUTINE DETERMINES THE SIZE OF THE ELEMENTAL
C AREAS UPON WHICH THE WIND, CURRENT AND WAVE FORCES ACT.
C NOTE THAT THE WAVE AREA IS DETERMINED SOLELY FROM THE WATER
C DEPTH AND NOT FROM THE WATER DEPTH PLUS THE WAVE HEIGHT.
C THIS WAS DONE TO SIMPLIFY THE WAVE FORCE CALCULATION
C WITHOUT INTRODUCING ANY SIGNIFICANT ERROR.
C
COMMON PI,G,DEPTH,RAIR,RWAT,UAIR,UHAT,ICOUNT,AOLX,AOLY
COMMON NWDP,NCDP,NWADE,NWDPD
C
C CALCULATE PROJECTED CURRENT AND WAVE SPAR LENGTHS
PSPLX=DEPTH/COS(AOLY*PI/180.)
PSPLY=DEPTH/COS(AOLX*PI/180.)
C
C CALCULATE PROJECTED WIND SPAR LENGTHS
TSPLX=SPL-PSPLX
TSPLY=SPL-PSPLY
C
C CALCULATE ELEMENTAL WIND AREAS
IF(NWDP.NE.0) GOTO 10
EWAX=0.0
EWAY=0.0
GOTO 20
10 EWAX=TSPLX/(FLOAT(NWDP))*SPD
EWAY=TSPLY/(FLOAT(NWDP))*SPW
GOTO 20
C
C CALCULATE ELEMENTAL CURRENT AREAS
20 IF(NCDP.NE.0) GOTO 30
ECAX=0.0
ECAY=0.0
GOTO 40
30 ECAX=PSPLX/(FLOAT(NCDP))*SPX
ECAY=PSPLY/(FLOAT(NCDP))*SPY
C

```

```

ASB10901
ASB10902
ASB10903
ASB10904
ASB10905
ASB10906
ASB10907
ASB10908
ASB10909
ASB10910
ASB10911
ASB10912
ASB10913
ASB10914
ASB10915
ASB10916
ASB10917
ASB10918
ASB10919
ASB10920
ASB10921
ASB10922
ASB10923
ASB10924
ASB10925
ASB10926
ASB10927
ASB10928
ASB10929
ASB10930
ASB10931
ASB10932
ASB10933
ASB10934
ASB10935
ASB10936

```

ASB10937  
 ASB10938  
 ASB10939  
 ASB10940  
 ASB10941  
 ASB10942  
 ASB10943  
 ASB10944  
 ASB10945  
 ASB10946  
 ASB10947  
 ASB10948  
 ASB10949  
 ASB10950  
 ASB10951  
 ASB10952  
 ASB10953  
 ASB10954  
 ASB10955  
 ASB10956  
 ASB10957  
 ASB10958  
 ASB10959  
 ASB10960  
 ASB10961  
 ASB10962  
 ASB10963  
 ASB10964  
 ASB10965  
 ASB10966  
 ASB10967  
 ASB10968  
 ASB10969  
 ASB10970  
 ASB10971  
 ASB10972

```

C CALCULATE ELEMENTAL WAVE AREAS
  40 IF(NWADP.NE.0) GOTO 50
    EWAAX=0.0
    EWAAY=0.0
    GOTO 60
  50 EWAAX=PSPLX/(FLOAT(NWADP))*SPD
    EWAAY=PSPLY/(FLOAT(NWADP))*SPW
  60 CONTINUE
    RETURN
  END
C *****
C SUBROUTINE CBEAR
C *****
C SUBROUTINE CBEAR(VEL,DIR,DEP,VL,VH,VHGT,DIRV,BEAR)
C IF THERE IS A CURRENT PRESENT AND THE SPAR BUOY HAS AN ORIENTING
C VANE, SUBROUTINE CBEAR DETERMINES THE BEARING OF THE BUOY
C RELATIVE TO MAGNETIC NORTH BY FINDING THROUGH LINEAR
C INTERPOLATION, THE CURRENT DIRECTION AT THE CENTROID
C OF THE VANE.
C
  DIMENSION VEL(501),DIR(501),DEP(501)
  DIMENSION CDIR(501)
  DIMENSION CVX(500),CVY(500)
  COMMON PI,G,DEPTH,RAIR,RWAT,UAIR,UWAT,ICOUNT,AOLX,AOLY
  COMMON NWDP,NCDP,NWADP,NWPD
  NCDPT=NCDP+1
C
C COMPUTE THE TOTAL VANE ELEVATION, THE VANE WIDTH
C CORRECTION FACTOR AND CHECK TO SEE IF THE TOP OF
C THE VANE IS UNDERWATER.
  TVZ=(VHGT+VL)*COS(AOLX*PI/180.)*COS(AOLY*PI/180.)
  VWCP=(VW/2.0)*SIN(AOLX*PI/180.)*SIN(AOLY*PI/180.)*
  1COS(AOLX*PI/180.)*COS(AOLY*PI/180.)
  IF(TVE.GE.DEPTH) GOTO 50
  VD=DEPTH-((VHGT+VL/2.0)*COS(AOLX*PI/180.)*COS(AOLY*PI/180.))+

```



```

1VMCF
  GOTO 60
50 VD=(DEPTH-VHGT*CCS(AOLX*PI/180.)*COS(AOLY*PI/180.))/2.0+VMCF
60 CONTINUE
  C WRITE(6,7777) VD,DEP
  C7777 FORMAT(' ',10(2X,F9.4))
  C
  C DETERMINE BY LINEAR INTERPOLATION THE CURRENT VELOCITY
  C AT THE ORIENTING VANE
    DO 100 I=2,NCDEPT
      IF(DEP(I).GE.VD) GOTO 200
100 CONTINUE
200 DELTD=DEP(I)-DEP(I-1)
    DELTV=DEP(I)-VD
    PCT=DELTVD/DELTD
    IN=I
    IM=I-1
  C
  C COMPUTE CURRENT VELOCITIES AT THE ORIENTING VANE
    DO 300 J=IM,IN
      CVX(J)=VEL(J)*COS(DIR(J)*PI/180.)
      CVY(J)=VEL(J)*SIN(DIR(J)*PI/180.)
300
    DLT VX=CVX(IN)-CVX(IM)
    DLT VY=CVY(IN)-CVY(IM)
    CVXV=CVX(IN)-PCT*DLTVX
    CVYV=CVY(IN)-PCT*DLTVY
    IP=((CVXV.LE.0.001).AND.(CVYV.GE.-0.001)) GOTO 500
    DIRV=ATAN(CVYV/CVXV)*180./PI
    IF(CVXV.LT.0.00) DIRV=DIRV+180.
    GOTO 600
500 IF(CVYV.GE.0.00) DIRV=90.00
    IF(CVYV.LT.0.00) DIRV=-90.00
  C
  C CONVERT BACK TO COMPASS DIRECTION
600 SBEAR=DIRV

```

ASB10973  
 ASB10974  
 ASB10975  
 ASB10976  
 ASB10977  
 ASB10978  
 ASB10979  
 ASB10980  
 ASB10981  
 ASB10982  
 ASB10983  
 ASB10984  
 ASB10985  
 ASB10986  
 ASB10987  
 ASB10988  
 ASB10989  
 ASB10990  
 ASB10991  
 ASB10992  
 ASB10993  
 ASB10994  
 ASB10995  
 ASB10996  
 ASB10997  
 ASB10998  
 ASB10999  
 ASB11000  
 ASB11001  
 ASB11002  
 ASB11003  
 ASB11004  
 ASB11005  
 ASB11006  
 ASB11007  
 ASB11008

```

      BEAR=SBEAR+180.
      IF (BEAR.GT.360.) BEAR=BEAR-360.
      RETURN
      END
C *****
C *          SUBROUTINE RWVEL
C *****
C *****
      SUBROUTINE RWVEL (BEAR, PSPLAW, WSPD, WDIR, ELEV,
      1 WAA, WSP, WVELX, WVELNY, WVELY, WVELNY)
C
C SUBROUTINE RWVEL CALCULATES THE WIND VELOCITIES NORMAL
C TO THE SPAR IN THE X AND Y DIRECTIONS.
C
      DIMENSION ELEV(100), Z(100), WSP(100)
      DIMENSION WVELX(100), WVELY(100), WVELNX(100), WVELNY(100)
      COMMON PI, G, DEPTH, RAIR, RWAT, UAIR, UWAT, ICOUNT, AOLX, AOLY
      COMMON NWDP, NCDP, NWADF, NWDPD
C
C DETERMINE ANGLE OF ATTACK
      WAA=BEAR-WDIR
      IF (WAA.GT.180.0) WAA=360.-WAA
      IF (WAA.LT.-180.0) WAA=360.+WAA
      CPM=0.3048
C
C DETERMINE ELEVATION FROM THE WATER SURFACE TO THE
C CENTER OF THE WIND AREA
      DO 100 I=1, NWDP
        ELEV(I)=PSPLAW/FLOAT(NWDP)*FLOAT(I)-PSPLAW/(2.*FLOAT(NWDP))
        100 Z(I)=ELEV(I)*CPM
C
C COMPUTE THE WIND SPEED AT ANY HEIGHT USING A LOGRITHMIC
C PROFILE AND A KNOWN VELOCITY AT THE 10 METER LEVEL.
      CALL WNDSPD(WSPD, Z, NWDP, WSP)
C
C DETERMINE WIND VELOCITIES RELATIVE TO THE SPAR BUOY
C ORIENTATION IN THE X-Y PLANE

```

```

ASB11009
ASB11010
ASB11011
ASB11012
ASB11013
ASB11014
ASB11015
ASB11016
ASB11017
ASB11018
ASB11019
ASB11020
ASB11021
ASB11022
ASB11023
ASB11024
ASB11025
ASB11026
ASB11027
ASB11028
ASB11029
ASB11030
ASB11031
ASB11032
ASB11033
ASB11034
ASB11035
ASB11036
ASB11037
ASB11038
ASB11039
ASB11040
ASB11041
ASB11042
ASB11043
ASB11044

```

ASB11045  
ASB11046  
ASB11047  
ASB11048  
ASB11049  
ASB11050  
ASB11051  
ASB11052  
ASB11053  
ASB11054  
ASB11055  
ASB11056  
ASB11057  
ASB11058  
ASB11059  
ASB11060  
ASB11061  
ASB11062  
ASB11063  
ASB11064  
ASB11065  
ASB11066  
ASB11067  
ASB11068  
ASB11069  
ASB11070  
ASB11071  
ASB11072  
ASB11073  
ASB11074  
ASB11075  
ASB11076  
ASB11077  
ASB11078  
ASB11079  
ASB11080

```

DO 300 I=1,NWDP
  WVELX(I)=WSP(I)*COS(WAA*PI/180.)
  300 WVELY(I)=WSP(I)*SIN(WAA*PI/180.)

C COMPUTE VELOCITIES NORMAL TO THE BUOY IN
C THE X AND Y DIRECTIONS
DO 400 I=1,NWDP
  WVELNX(I)=WVELX(I)*COS(AOLX*PI/180.)
  400 WVELNY(I)=WVELY(I)*COS(AOLY*PI/180.)
  RETURN
END
C *****
C * SUBROUTINE RCVEL
C *****
C SUBROUTINE RCVEL(BEAR,DIR,VEL,CAA,DEPC,CVX,CVY,CVNX,
1CVNY)
C
C SUBROUTINE RCVEL CALCULATES THE CURRENT VELOCITIES NORMAL
C TO THE SPAR IN THE X AND Y DIRECTIONS.
C
  DIMENSION DIR(501),VEL(501)
  DIMENSION CAA(501),DEPC(500)
  DIMENSION CVX(500),CVY(500),CVNX(500),CVNY(500)
  COMMON PI,G,DEPTH,RAIR,RWAT,UAIR,UWAT,ICOUNT,AOLX,AOLY
  COMMON NWDP,NCDP,NWADE,NWDPD
  NCDPT=NCDP+1
  SBEAR=BEAR-180.

C DETERMINE CURRENT ANGLES OF ATTACK
DO 100 I=1,NCDP
  CAA(I)=SBEAR-DIR(I)
  IF(CAA(I).GT.180.0) CAA(I)=360.-CAA(I)
  IF(CAA(I).LT.-180.0) CAA(I)=360.+CAA(I)
  100 CONTINUE

C COMPUTE AVERAGE (CENTER) CURRENT VELOCITIES RELATIVE TO

```

```

C THE SPAR BUOY ORIENTATION IN THE X-Y PLANE
DO 200 I=1,NCDDP
  CVX(I)=(VEL(I)*COS(CAA(I)*PI/180.))+VEL(I+1)*
  1COS(CAA(I+1)*PI/180.))/2.0
  CVY(I)=(VEL(I)*SIN(CAA(I)*PI/180.))+VEL(I+1)*
  1SIN(CAA(I+1)*PI/180.))/2.0
  200 DEPC(I)=DEPTH/FLOAT(NCDDP)*FLOAT(I)-DEPTH/(2.*FLOAT(NCDDP))

C
C COMPUTE CURRENT VELOCITIES NORMAL TO THE BUOY IN
C THE X AND Y DIRECTIONS
DO 300 I=1,NCDDP
  CVNX(I)=CVX(I)*COS(AOLX*PI/180.)
  300 CVNY(I)=CVY(I)*COS(AOLY*PI/180.)
  RETURN
END
C *****
C * SUBROUTINE RWAVA
C *****
C SUBROUTINE RWAVA(NJADPT,ITHERY,DELTAT,WAMP,SIG,N,WVNO,
  1WAA,C,HWAVX,HWAVY,VWAVX,VWAVY,WAANX,WAANY)
C
C SUBROUTINE RWAVA COMPUTES THE WAVE PARTICLE VELOCITIES AND
C ACCELERATIONS NORMAL TO THE SPAR IN THE X AND Y DIRECTIONS
C USING EITHER LINEAR (AIRY) WAVE THEORY OR STOKES SECOND
C ORDER WAVE THEORY.
C
  DIMENSION Z(501),DEP(500),HYP1(501),HYP2(501),HYP3(501),
  1HYP4(501)
  DIMENSION HWAVX(500),HWAVY(500),VWAVX(500),VWAVY(500)
  DIMENSION WAVNX(500),WAVNY(500)
  DIMENSION HWAAX(500),HWAAY(500),VWAAX(500),VWAAY(500)
  DIMENSION WAANX(500),WAANY(500)
  COMMON PI,G,DEPTH,RAIR,RWAT,UAIR,UMAT,ICOUNT,AOLX,AOLY
  COMMON NWD2,NCDDP,NWADP,NWPPDP
C
  T1=COS(WAA*PI/180.)

```

ASB11081  
 ASB11082  
 ASB11083  
 ASB11084  
 ASB11085  
 ASB11086  
 ASB11087  
 ASB11088  
 ASB11089  
 ASB11090  
 ASB11091  
 ASB11092  
 ASB11093  
 ASB11094  
 ASB11095  
 ASB11096  
 ASB11097  
 ASB11098  
 ASB11099  
 ASB11100  
 ASB11101  
 ASB11102  
 ASB11103  
 ASB11104  
 ASB11105  
 ASB11106  
 ASB11107  
 ASB11108  
 ASB11109  
 ASB11110  
 ASB11111  
 ASB11112  
 ASB11113  
 ASB11114  
 ASB11115  
 ASB11116

```

ASB11117
ASB11118
ASB11119
ASB11120
ASB11121
ASB11122
ASB11123
ASB11124
ASB11125
ASB11126
ASB11127
ASB11128
ASB11129
ASB11130
ASB11131
ASB11132
ASB11133
ASB11134
ASB11135
ASB11136
ASB11137
ASB11138
ASB11139
ASB11140
ASB11141
ASB11142
ASB11143
ASB11144
ASB11145
ASB11146
ASB11147
ASB11148
ASB11149
ASB11150
ASB11151
ASB11152

C
C COMPUTE DEPTH'S OF INTEREST
C NOTE THAT Z HAS ITS ORIGIN AT THE STILL WATER SURFACE
DO 100 I=1,NWADPT
T=FLOAT(I-1)
Z(I)=DEPTH/FLOAT(NWADPT)*T*(-1.00)

C
C CHECK TO SEE IF THE DEPTH OF INTEREST IS ABOVE THE WATER SURFACE
IF (WAMP.LE.Z(I)) GOTO 50
HYP1(I)=COSH(WVNO*(DEPTH+Z(I)))/COSH(WVNO*DEPTH)
HYP2(I)=SINH(WVNO*(DEPTH+Z(I)))/COSH(WVNO*DEPTH)
HYP3(I)=COSH(2.*WVNO*(DEPTH+Z(I)))/(SINH(WVNO*DEPTH)**4.)
HYP4(I)=SINH(2.*WVNO*(DEPTH+Z(I)))/(SINH(WVNO*DEPTH)**4.)
GOTO 100
50 HYP1(I)=0.0
HYP2(I)=0.0
HYP3(I)=0.0
HYP4(I)=0.0
100 CONTINUE

C
C CALCULATE HORIZONTAL AND VERTICAL VELOCITIES USING LINEAR (AIRY)
C WAVE THEORY AT THE TOP AND BOTTOM OF EACH ELEMENTAL AREA AND
C AVERAGE TO GET THE MEAN VELOCITY AT THE CENTER OF EACH
C ELEMENTAL AREA
DO 200 I=1,NWADP
DEP(I)=DEPTH/FLOAT(NWADP)*FLOAT(I)-DEPTH/(2.*FLOAT(NWADP))
HWAUX(I)=WAMP*G*WVNO/SIG*((HYP1(I)+HYP1(I+1))/2.0)*T1
1* COS(-SIGMAT)
HVAUX(I)=WAMP*G*WVNO/SIG*((HYP1(I)+HYP1(I+1))/2.0)*T2
1* COS(-SIGMAT)
HWAUX(I)=WAMP*G*WVNO/SIG*((HYP2(I)+HYP2(I+1))/2.0)*T1
1* SIN(-SIGMAT)
HVAUX(I)=WAMP*G*WVNO/SIG*((HYP2(I)+HYP2(I+1))/2.0)*T2
1* SIN(-SIGMAT)

```

```

C      C COMPUTE HORIZONTAL AND VERTICAL ACCELERATIONS USING LINEAR (AIRY)
C      C WAVE THEORY AT THE TOP AND BOTTOM OF EACH ELEMENTAL AREA AND
C      C AVERAGE TO GET THE MEAN VELOCITY AT THE CENTER OF EACH
C      C ELEMENTAL AREA
      HWAAX(I)=HWAAX(I)*SIG*TAN(-SIGMAT)
      HWAAY(I)=HWAAY(I)*SIG*TAN(-SIGMAT)
      VWAAX(I)=-VWAAX(I)*SIG*COTAN(-SIGMAT)
      VWAAY(I)=-VWAAY(I)*SIG*COTAN(-SIGMAT)

C      C COMPUTE NORMAL VELOCITIES
      WAVNX(I)=HWAAX(I)*COS(AOLY*PI/180.)-VWAAX(I)*SIN(AOLX*PI/180.)
      WAVNY(I)=HWAAY(I)*COS(AOLY*PI/180.)-VWAAY(I)*SIN(AOLY*PI/180.)

C      C COMPUTE NORMAL ACCELERATIONS
      WAANX(I)=HWAAX(I)*COS(AOLX*PI/180.)-VWAAX(I)*SIN(AOLX*PI/180.)
      WAANY(I)=HWAAY(I)*COS(AOLY*PI/180.)-VWAAY(I)*SIN(AOLY*PI/180.)
      200 CONTINUE
      IF(ITHERY.EQ.1) GOTO 400

C      C CALCULATE HORIZONTAL AND VERTICAL VELOCITIES
C      C AT THE TOP AND BOTTOM OF EACH ELEMENTAL AREA
C      C AND AVERAGE TO GET THE MEAN VELOCITY AT THE
C      C CENTER OF EACH ELEMENTAL AREA USING STOKES
C      C SECOND ORDER WAVE THEORY
      DO 300 I=1,NWADP
      HWAAX(I)=HWAAX(I)+0.75*(WVNO*WAMP)**2.*C*((HYP3(I)+HYP3(I+1))
      1/2.0)*T1*COS(-2.*SIGMAT)
      HWAAY(I)=HWAAY(I)+0.75*(WVNO*WAMP)**2.*C*((HYP3(I)+HYP3(I+1))
      1/2.0)*T2*COS(-2.*SIGMAT)
      VWAAX(I)=C*SIG/G*VWAAX(I)+0.75*(WVNO*WAMP)**2.*C*((HYP3(I)
      1+HYP3(I+1))/2.0)*T1*SIN(-2.*SIGMAT)
      VWAAY(I)=C*SIG/G*VWAAY(I)+0.75*(WVNO*WAMP)**2.*C*((HYP3(I)
      1+HYP3(I+1))/2.0)*T2*SIN(-2.*SIGMAT)

C      C COMPUTE HORIZONTAL AND VERTICAL ACCELERATIONS USING STOKES SECOND

```

```

ASB11153
ASB11154
ASB11155
ASB11156
ASB11157
ASB11158
ASB11159
ASB11160
ASB11161
ASB11162
ASB11163
ASB11164
ASB11165
ASB11166
ASB11167
ASB11168
ASB11169
ASB11170
ASB11171
ASB11172
ASB11173
ASB11174
ASB11175
ASB11176
ASB11177
ASB11178
ASB11179
ASB11180
ASB11181
ASB11182
ASB11183
ASB11184
ASB11185
ASB11186
ASB11187
ASB11189

```

```

C ORDER WAVE THEORY AT THE TOP AND BOTTOM OF EACH ELEMENTAL AREA
C AND AVERAGE TO GET THE MEAN VELOCITY AT THE CENTER OF EACH
C ELEMENTAL AREA
      HWAAX(I)=HWAAX(I)+2.*SIG*0.75*(WVNO*WAMP)**2.*C*(HYP3(I)+
      1HYP3(I+1))/2.0*T1*SIN(-SIGMAT)
      HWAAY(I)=HWAAY(I)+2.*SIG*0.75*(WVNO*WAMP)**2.*C*(HYP3(I)+
      1HYP3(I+1))/2.0*T2*SIN(-SIGMAT)
      VWAAAX(I)=C*SIG/G*VWAAAX(I)-2.*SIG*0.75*(WVNO*WAMP)**2.*C*
      1(HYP4(I)+HYP4(I+1))/2.0*T1*COS(-SIGMAT)
      VWAAAY(I)=C*SIG/G*VWAAAY(I)-2.*SIG*0.75*(WVNO*WAMP)**2.*C*
      1(HYP4(I)+HYP4(I+1))/2.0*T2*COS(-SIGMAT)

C
C COMPUTE NORMAL VELOCITIES
      WAVNX(I)=HWAAX(I)*COS(AOLX*PI/180.)-VWAAVX(I)*SIN(AOLX*PI/180.)
      WAVNY(I)=HWAAY(I)*COS(AOLY*PI/180.)-VWAAVY(I)*SIN(AOLY*PI/180.)

C
C COMPUTE NORDAL ACCELERATIONS
      W1ANX(I)=HWAAX(I)*COS(AOLX*PI/180.)-VWAAAX(I)*SIN(AOLX*PI/180.)
      W1AAY(I)=HWAAY(I)*COS(AOLY*PI/180.)-VWAAAY(I)*SIN(AOLY*PI/180.)
      300 WAAANY(I)=W1AAY(I)
      400 RETURN
      END
C *****
C * SUBROUTINE WPV
C * *****
C *****
      SUBROUTINE WPV(WAVNX,WAVNY,CVX,CVY,WPVNX,WPVNY)
      DIMENSION Z(100),WAVNX(100),WAVNY(100),WPVNX(100),WPVNY(100)
      DIMENSION HYP1(100)
      DIMENSION DEP(100),CVX(100),CVY(100)
      COMMON PI,G,DEPTH,RAIR,RWAT,UAIR,UWAT,ICOUNT,AOLX,AOLY
      COMMON NWDP,NCDP,NWADP,NWPDPT
      NCDPT=NCDP+1
      DEP(I)=DEP(I-1)+(DEPTH/FLOAT(NCDP))
      NWFDPT=NWADP
      NWPDPT=NWPDPT+1
      DO 100 I=1,NWPDPT
      T=I-1

```

```

ASB11189
ASB11190
ASB11191
ASB11192
ASB11193
ASB11194
ASB11195
ASB11196
ASB11197
ASB11198
ASB11199
ASB11200
ASB11201
ASB11202
ASB11203
ASB11204
ASB11205
ASB11206
ASB11207
ASB11208
ASB11209
ASB11210
ASB11211
ASB11212
ASB11213
ASB11214
ASB11215
ASB11216
ASB11217
ASB11218
ASB11219
ASB11220
ASB11221
ASB11222
ASB11223
ASE11224

```

ASB11225  
 ASB11226  
 ASB11227  
 ASB11228  
 ASB11229  
 ASB11230  
 ASB11231  
 ASB11232  
 ASB11233  
 ASB11234  
 ASB11235  
 ASB11236  
 ASB11237  
 ASB11238  
 ASB11239  
 ASB11240  
 ASB11241  
 ASB11242  
 ASB11243  
 ASB11244  
 ASB11245  
 ASB11246  
 ASB11247  
 ASB11248  
 ASB11249  
 ASB11250  
 ASB11251  
 ASB11252  
 ASB11253  
 ASB11254  
 ASB11255  
 ASB11256  
 ASB11257  
 ASB11258  
 ASB11259  
 ASB11260

```

C
C CHECK TO SEE IF THE DEPTH OF INTEREST IS BELOW THE STILL WATER DEPTH
  Z(I)=T*(DEPTH+WAMP)/FLOAT(NWDP)
  IF(Z(I).GE.WAMP) GOTO 200
  WPNX(I)=WAVNX(I)
  WPNY(I)=WAVNY(I)
  GOTO 100
200 IF(Z(I).NE.WAMP) GOTO 300
  WPNX(I)=WAVNX(I)+CVX(1)
  WPNY(I)=WAVNY(I)+CVY(1)
  GOTO 100
300 DO 400 J=2,NCDP
  IF(DEP(J)+WAMP.GE.Z(I)) GOTO 500
400 CONTINUE
500 CONTINUE
  DEL1D= DEP(J)-DEP(J-1)
  DEL2D=DEP(J)+WAMP-Z(I)
  DELCX=CVX(J)-CVX(J-1)
  DELCY=CVY(J)-CVY(J-1)
  PCT=DEL2D/DEL1D
  CVZLX=CVX(J)-DELCX*PCT
  CVZLY=CVY(J)-DELCY*PCT
  GOTO 600
600 WPNX(I)=WAVNX(I)+CVZLX
  WPNY(I)=WAVNY(I)+CVZLY
100 CONTINUE
  Z(I)=DEPTH/FLOAT(NWADP)*T*(-1.00)
  IF(PWAMP.LE.Z(I)) GOTO 700
  HYP1(I)=COSH(WVNO*(DEPTH+Z(I)))/COSH(WVNO*DEPTH)
  GOTO 800
700 HYP1(I)=0.0
800 CONTINUE
  DO 900 I=1,NWADPT
  WAVNX(I)=2.0*HYP1(I)
  WAVNY(I)=2.0*HYP1(I)
900 CONTINUE

```



```

      RETURN
      END
C *****
C * SUBROUTINE DRAGC
C *****
C SUBROUTINE DRAGC(WVELNX,WPVNX,SPD,FSPLAW,DEPWP,
  1REH,REWP,CWD,CWPD)
C
C IF THE SPAR HAS A CIRCULAR CROSS-SECTION, THEN
C SUBROUTINE DRAGC CALCULATES REYNOLD'S NUMBERS AND DRAG
C COEFFICIENTS FOR THE WIND AND WATER PARTICLE FORCES ACTING
C ON THE SPAR.
C
  DIMENSION WVELNX(100),WPVNX(500)
  DIMENSION DEPWP(500)
  DIMENSION REW(100),REWP(500),CWD(100),CWPD(500)
  COMMON PI,G,DEPTH,RATL,RZAT,UAIR,UNAT,ICOUNT,AOLX,AOLY
  COMMON NWDP,NCDP,NWADP,NWPD
C
C CALCULATE WIND REYNOLDS NUMBERS
  IF(NWDP.EQ.0) GOTO 350
  DO 100 I=1,NWDP
    REW(I)=2AIR*ABS(WVELNX(I))*SPD/UAIR
    IF(REW(I).GE.5.0E05) GOTO 200
    IF(REW(I).LE.2.0E05) GOTO 300
    CWD(I)=-1.667E-06*REW(I)+1.5334
    GOTO 100
  200 CWD(I)=0.70
    GOTO 100
  300 IF(REW(I).GE.10) GOTO 340
    CWD(I)=0.0
    GOTO 100
  340 CWD(I)=1.2
  100 CONTINUE
  350 IF(NWDP.EQ.0) GOTO 700
C
ASB11261
ASB11262
ASB11263
ASB11264
ASB11265
ASB11266
ASB11267
ASB11268
ASB11269
ASB11270
ASB11271
ASB11272
ASB11273
ASB11274
ASB11275
ASB11276
ASB11277
ASB11278
ASB11279
ASB11280
ASB11281
ASB11282
ASB11283
ASB11284
ASB11285
ASB11286
ASB11287
ASB11288
ASB11289
ASB11290
ASB11291
ASB11292
ASB11293
ASB11294
ASB11295
ASB11296

```

```

C CALCULATE WAVE PARTICLE REYNOLDS NUMBERS
DO 400 I=1,NWPD
  DEWP(I)=DEPTH/FLOAT(NWPD)*FLOAT(I)-DEPTH/(2.*FLOAT(NWPD))
  REW(I)=RWAT*ABS(WPVX(I))*SPD/UWAT
  IF(REW(I).GE.5.0E05) GOTO 500
  IF(REW(I).LE.2.0E05) GOTO 600
  CWP(I)=-1.667E-06*REW(I)+1.5334
  GOTO 400
500 CWP(I)=0.70
  GOTO 400
600 IF(REW(I).GE.10) GOTO 640
  CWP(I)=0.0
  GOTO 400
640 CWP(I)=1.2
400 CONTINUE
700 RETURN
END
C *****
C * SUBROUTINE DRAGX *
C *****
SUBROUTINE DRAGX(WVELX,WPVX,SPD,SPW,
1PSPLAW,DEWP,REW,REWP,CWD,CWPD)
C
C IF THE SPAR HAS AN ELLIPTICAL CROSS-SECTION, THEN
C SUBROUTINE DRAGX CALCULATES REYNOLD'S NUMBERS AND DRAG
C COEFFICIENTS FOR THE WIND AND WATER PARTICLE FORCES ACTING
C ON THE SPAR IN THE X DIRECTION.
C
  DIMENSION WVELX(100),WPVX(500),DEWP(500)
  DIMENSION REW(100),REWP(500),CWD(100),CWPD(500)
  COMMON PI,G,DEPTH,RAIR,RWAT,UWAT,ICOUNT,AOLX,AOLY
  COMMON NWDP,NCDP,NWADP,NWPD
  IF(NWDP.EQ.0) GOTO 290
  DO 100 I=1,NWDP
    REW(I)=RAIR*ABS(WVELX(I))*SPD/UWAT

```

```

ASB11297
ASB11298
ASB11299
ASB11300
ASB11301
ASB11302
ASB11303
ASB11304
ASB11305
ASB11306
ASB11307
ASB11308
ASB11309
ASB11310
ASB11311
ASB11312
ASB11313
ASB11314
ASB11315
ASB11316
ASB11317
ASB11318
ASB11319
ASB11320
ASB11321
ASB11322
ASB11323
ASB11324
ASB11325
ASB11326
ASB11327
ASB11328
ASB11329
ASB11330
ASB11331
ASB11332

```

```

C CALCULATE WIND REYNOLDS NUMBER
  IF (REWX(I).LT.10.00) GOTO 220
  IF (REWX(I).LE.6.5E05) GOTO 230

C
C CALCULATE THE TURBULENT COEFFICIENT OF WIND FRICTION
  DO 200 JJ=1,1000000
    CP=FLOAT(JJ)/10000.
    A=.242/SQRT(CP)
    B=A*LOG10(CP*REWX(I))
    IF (B.GE.A) GOTO 210
  200 CONTINUE
    WRITE(6,250) I,REWX(I),CP
  250 FORMAT(' ',//,/,/,/,/,/,/,/,/,43X,
    1'ERROR IN SUBROUTINE DRAGX - CHECK CALCULATIONS',/,/
    2'I = ',I2,10X,
    3'REYNOLDS NUMBER = ',E13.3,10X,
    4'SKIN FRICTION COEFFICIENT = ',E13.3)
    STOP

C
C CALCULATE THE TURBULENT WIND DRAG COEFFICIENT
  210 CWDX(I)=CP*4.+2.*(SPW/SPD)+120.*((SPD/SPW)**2)
    GOTO 100

C
C CHECK FOR ZERO REYNOLDS NUMBER
  220 CWDX(I)=0.00
    GOTO 100

C
C CALCULATE THE LAMINAR WIND DRAG COEFFICIENT
  230 CF=0.0075
    CWDX(I)=2.*CF*(1.+SPW/SPD)+1.1*(SPD/SPW)
  100 CONTINUE
  290 IF (NWPDP.EQ.0) GOTO 500
    DO 300 J=1,NWPDP
      DEPTH(J)=DEPTH/FLOAT(NWPDP)*FLOAT(J)-DEPTH/(2.*FLOAT(NWPDP))
    300 CONTINUE
  500 CONTINUE
  310 CWDX(I)=CWDX(I)+CWDX(J)
    GOTO 100

C
C CALCULATE WATER PARTICLE REYNOLDS NUMBER

```

ASB11333  
 ASB11334  
 ASB11335  
 ASB11336  
 ASB11337  
 ASB11338  
 ASB11339  
 ASB11340  
 ASB11341  
 ASB11342  
 ASB11343  
 ASB11344  
 ASB11345  
 ASB11346  
 ASB11347  
 ASB11348  
 ASB11349  
 ASB11350  
 ASB11351  
 ASB11352  
 ASB11353  
 ASB11354  
 ASB11355  
 ASB11356  
 ASB11357  
 ASB11358  
 ASB11359  
 ASB11360  
 ASB11361  
 ASB11362  
 ASB11363  
 ASB11364  
 ASB11365  
 ASB11366  
 ASB11367  
 ASB11368

```

REWPX(J)=RWAT*ABS(WPVNX(J))*SPD/UWAT
IF(REWPX(J).LT.10.00) GOTO 420
IF(REWPX(J).LE.6.5E05) GOTO 430

```

```

C
C CALCULATE THE TURBULENT COEFFICIENT OF WATER PARTICLE FRICTION
DO 400 JJJ=1,1000000
CF=FLOAT(JJJ)/10000.
A=.242/SQRT(CF)
B=ALOG10(CF*REWPX(J))
IF(B.GE.A) GOTO 410
400 CONTINUE
WRITE(6,250) J,REWPX(J),CF
STOP

```

```

C
C CALCULATE THE TURBULENT WATER PARTICLE DRAG COEFFICIENT
410 CWPDX(J)=CF*4.+2.*(SPW/SPD)+120.*((SPD/SPW)**2)
GOTO 300

```

```

C
C CHECK FOR ZERO REYNOLDS NUMBER
420 CWPDX(J)=0.00
GOTO 300

```

```

C
C CALCULATE THE LAMINAR WATER PARTICLE DRAG COEFFICIENT
430 CF=0.0075
CWPDX(J)=2.*CF*(1.+SPW/SPD)+1.1*(SPD/SPW)
300 CONTINUE
500 RETURN

```

```

END
C *****
C * SUBROUTINE DRAGY
C *****
SUBROUTINE DRAGY(WVELNY,WPVNY,SPD,SPW,PSPLAW,
1REWY,REWPY,CHDY,CWPDY)

```

```

C
C IF THE SPAR HAS AN ELLIPTICAL CROSS-SECTION, THEN
C SUBROUTINE DRAGY CALCULATES REYNOLD'S NUMBERS AND DRAG

```

ASB11369  
 ASB11370  
 ASB11371  
 ASB11372  
 ASB11373  
 ASB11374  
 ASB11375  
 ASB11376  
 ASB11377  
 ASB11378  
 ASB11379  
 ASB11380  
 ASB11381  
 ASB11382  
 ASB11383  
 ASB11384  
 ASB11385  
 ASB11386  
 ASB11387  
 ASB11388  
 ASB11389  
 ASB11390  
 ASB11391  
 ASB11392  
 ASB11393  
 ASB11394  
 ASB11395  
 ASB11396  
 ASB11397  
 ASB11398  
 ASB11399  
 ASB11400  
 ASB11401  
 ASB11402  
 ASB11403  
 ASB11404

```

C COEFFICIENTS FOR THE WIND AND WATER PARTICLE FORCES
C ACTING ON THE SPAR IN THE Y DIRECTION.
C
    DIMENSION WVELNY(100), WPVNY(500)
    DIMENSION REWY(100), REWPY(500), CWDY(100), CWPDY(500)
    COMMON PI, G, DEPTH, RAIR, RWAT, UAIR, UWAT, ICOJNT, AOLX, AOLY
    COMMON NWDP, NCDP, NWADP, NWDPDP
C
C CALCULATE WIND REYNOLDS NUMBER
    IF (NWDP.EQ.0) GOTO 290
    DO 100 I=1, NWDP
        REWY(I) = RAIR * ABS(WVELNY(I)) * SPW / UAIR
    IF (REWY(I).LT.10.00) GOTO 210
C
C CALCULATE THE WIND DRAG COEFFICIENT
    CWDY(I) = 2.00
    GOTO 100
C
C CHECK FOR ZERO REYNOLDS NUMBER
    210 CWDY(I) = 0.00
    GOTO 100
    100 CONTINUE
C
C CALCULATE WATER PARTICLE REYNOLDS NUMBERS
    290 IF (NWDPDP.EQ.0) GOTO 500
    DO 300 J=1, NWDPDP
        REWPY(J) = RWAT * ABS(WPVNY(J)) * SPW / UWAT
    IF (REWPY(J).LT.10.00) GOTO 410
C
C CALCULATE THE TURBULENT WATER PARTICLE DRAG COEFFICIENT
    CWPDY(J) = 2.00
    GOTO 300
C
C CHECK FOR ZERO REYNOLDS NUMBER
    410 CWPDY(J) = 0.00
    GOTO 300

```

```

ASB11405
ASB11406
ASB11407
ASB11408
ASB11409
ASB11410
ASB11411
ASB11412
ASB11413
ASB11414
ASB11415
ASB11416
ASB11417
ASB11418
ASB11419
ASB11420
ASB11421
ASB11422
ASB11423
ASB11424
ASB11425
ASB11426
ASB11427
ASB11428
ASB11429
ASB11430
ASB11431
ASB11432
ASB11433
ASB11434
ASB11435
ASB11436
ASB11437
ASB11438
ASB11439
ASB11440

```

```

300 CONTINUE
500 RETURN
END
C ***** SUBROUTINE FORCE *****
C *
C ***** SUBROUTINE FORCE (N,NWHPTS,SPD,SPW,CAREA,EWAX,
1EWAY,EMPAX,EMPAY,WVELNX,WVELNY,WVNLX,WVNLNY,WPVNX,WPVNY,WPANX,WPANY,
2CWDX,CWDY,CWPDY,CWPDY,CMX,CMY,WFX,WFY,TWFX,TWFX,TWFX,
3WPDFX,WPDFY,WPIFY,WPIFY,WPFY,WPFY,TWPDFX,TWPDFY,
4TWPIFY,TWPIFY,TWFFX,TWFFY,TFX,TFY,TSBF)
C
C SUBROUTINE FORCE COMPUTES THE WIND AND WATER PARTICLE
C FORCES ACTING ON EACH ELEMENTAL AREA OF THE SPAR. IF
C WAVES ARE PRESENT, THEN BOTH DRAG AND INERTIA FORCES ARE
C COMPUTED FOR EACH ELEMENT. IN ADDITION, THIS SUBROUTINE
C SUMS ALL OF THE INDIVIDUAL FORCES TO DETERMINE THE TOTAL
C FORCE ACTING ON THE SPAR.
C
C DIMENSION WVELNX(100),WVELNY(100)
C DIMENSION WPVNX(500),WPVNY(500),WPANX(500),WPANY(500)
C DIMENSION CWDX(100),CWDY(100),CWPDY(500),CWPDY(500)
C DIMENSION WFX(100),WFX(100)
C DIMENSION WPDFX(500),WPDFY(500),WPIFY(500),WPIFY(500)
C DIMENSION WPFY(500),WPFY(500)
C DIMENSION TSBF(100)
C
C COMMON PI,G,DEPTH,RAIR,RWAT,UAIR,UWAT,ICOUNT,AOLX,AOLY
C COMMON NWDP,NCDP,NWADP,NWPDP
C W=SPW/2.0
C D=SPD/2.0
C
C COMPUTE HYDRODYNAMIC MASS COEFFICIENTS
C CMX=1.0+W/D
C CMY=1.5
C CMY=1.0+D/W

```

ASB11441  
 ASB11442  
 ASB11443  
 ASB11444  
 ASB11445  
 ASB11446  
 ASB11447  
 ASB11448  
 ASB11449  
 ASB11450  
 ASB11451  
 ASB11452  
 ASB11453  
 ASB11454  
 ASB11455  
 ASB11456  
 ASB11457  
 ASB11458  
 ASB11459  
 ASB11460  
 ASB11461  
 ASB11462  
 ASB11463  
 ASB11464  
 ASB11465  
 ASB11466  
 ASB11467  
 ASB11468  
 ASB11469  
 ASB11470  
 ASB11471  
 ASB11472  
 ASB11473  
 ASB11474  
 ASB11475  
 ASB11476

ASB11477  
ASB11478  
ASB11479  
ASB11480  
ASB11481  
ASB11482  
ASB11483  
ASB11484  
ASB11485  
ASB11486  
ASB11487  
ASB11488  
ASB11489  
ASB11490  
ASB11491  
ASB11492  
ASB11493  
ASB11494  
ASB11495  
ASB11496  
ASB11497  
ASB11498  
ASE11499  
ASE11500  
ASE11501  
ASE11502  
ASE11503  
ASE11504  
ASE11505  
ASE11506  
ASE11507  
ASE11508  
ASE11509  
ASE11510  
ASE11511  
ASE11512

```

      CMY=1.5
      TWFX=0.0
      TWFY=0.0
      IF(NWDP.EQ.0) GOTO 150

C
C  CALCULATE WIND DRAG FORCES ON THE SPAR BUOY
      DO 100 I=1,NWDP
        WFX(I)=0.5*RAIR*EWAX*WVELNX(I)*ABS(WVELNX(I))*CWDY(I)
        TWFX=TWFX+WFX(I)
        WFY(I)=0.5*RAIR*EWAY*WVELNY(I)*ABS(WVELNY(I))*CWDY(I)
        TWFY=TWFY+WFY(I)
      100
C
C  CALCULATE WATER PARTICLE DRAG, INERTIA AND TOTAL FORCES
C  ON THE SPAR BUOY
      150 TWPDFX=0.0
          TWPIFX=0.0
          TWPDFY=0.0
          TWPIFY=0.0
          TWPDFX=0.0
          TWPDFY=0.0
          IF(NWDP.EQ.0) GOTO 300
      DO 200 I=1,NWDP
        WPDFX(I)=0.5*RWAT*EWPAX*WPNX(I)*ABS(WPNX(I))*CWPDX(I)
        TWPDFX=TWPDFX+WPDFX(I)
        WPIFX(I)=RWAT*CAREA*WPNX(I)*CMX
        TWPIFX=TWPIFX+WPIFX(I)
        WPDFX(I)=WPDFX(I)+WPIFX(I)
        TWPDFX=TWPDFX+WPDFX(I)
        WPDFY(I)=0.5*RWAT*EWPAY*WPNY(I)*ABS(WPNY(I))*CWPDY(I)
        TWPDFY=TWPDFY+WPDFY(I)
        WPIFY(I)=RWAT*CAREA*WPNY(I)*CMY
        TWPIFY=TWPIFY+WPIFY(I)
        WPDFY(I)=WPDFY(I)+WPIFY(I)
        TWPDFY=TWPDFY+WPDFY(I)
        TWFX=TWFX+TWPDFX
        TWFY=TWFY+TWPDFY
      200

```

```

      TSBP(N)=SQRT(TFX**2+TFY**2)
      300 RETURN
      END
C ***** SUBROUTINE OTHOM *****
C *
C ***** SUBROUTINE OTHOM *****
C ***** SUBROUTINE OTHOM (WFX,WFY,WPFY,PSPLAW,WAMP,CAREA,SPL,
      1SWWD,VL,VHGT,VNWD,IVSUB,VNWD,TBWGT,TSWGT,ANCHX,ANCHY,IEND,
      2WOTMX,WOTMY,WPOTMX,WPOTHY,OTMONX,OTMOMY)
C
C SUBROUTINE OTHOM
C
      DIMENSION WFX(100),WFY(100),WPFY(500),WPFY(500)
      DIMENSION WMA(100),WMA(500)
      COMMON PI,G,DEPTH,RAIR,RWAT,UAIR,UWAT,ICOUNT,AOLX,AOLY
      COMMON NWDP,NCDP,NWADE,NWDPD
C
C COMPUTE WIND OVERTURNING MOMENTS
      WOTMX=0.0
      WOTMY=0.0
      IF(NWDP.EQ.0) GOTO 100
      DELTL=(PSPLAW/FLOAT(NWDP))/2.0
      DO 200 I=1,NWDP
        WMA(I)=PSPLAW/FLOAT(NWDP)*FLOAT(I)-DETL
        WOTMX=WOTMX+WFX(I)*WMA(I)
        200 WOTMY=WOTMY+WFY(I)*WMA(I)
C
C COMPUTE WATER PARTICLE OVERTURNING MOMENT
      100 WPOTMX=0.0
      WPOTHY=0.0
      IF(NWDP.EQ.0) GOTO 300
      DELTL=(DEPTH/FLOAT(NWDP))/2.0
      DO 400 II=1,NWDP
        T=DETL*2.0*FLOAT(II-1)
        WMA(II)=DEPTH-T-DETL
        WPOTMX=WPOTMX+WPFY(II)*WMA(II)

```

```

ASB11513
ASB11514
ASP11515
ASB11516
ASB11517
ASB11518
ASE11519
ASE11520
ASE11521
ASE11522
ASE11523
ASE11524
ASE11525
ASE11526
ASE11527
ASR11528
ASB11529
ASE11530
ASB11531
ASB11532
ASE11533
ASE11534
ASE11535
ASE11536
ASB11537
ASE11538
ASE11539
ASB11540
ASB11541
ASB11542
ASB11543
ASB11544
ASB11545
ASB11546
ASB11547
ASB11548

```



```

400 WPOTHY=WPOTHY+WPY (II)*WPHA (II)
C
C CALCULATE THE SUBMERGED SPAR LENGTH AND THE HEIGHT OF THE
C WATER DISPLACED BY THE SPAR
    SSPL=(DEPTH+WAMP)/(COS(AOLX*PI/180.)*COS(AOLY*PI/180.))
    IVSUB=0
    VMAX=(VHGT+VL/2.)/(COS(AOLX*PI/180.)*COS(AOLY*PI/180.))
    IF(SSPL.GT.VMAX) IVSUB=1
    VWWD=VHWD
    IF(IVSUB.NE.1) VWWD=VWWD/VL*((DEPTH+WAMP)-(VHGT-VL/2.))/
    1(COS(AOLX*PI/180.)*COS(AOLY*PI/180.))
    SHWD=CAREA*SSPL*RWAT*G
    TBWGT=SHWD+VWWD
C
C COMPUTE OVERTURNING MOMENT DUE TO OFF-CENTER
C ANCHOR ATTACHMENT POINT
    300 AARMX=ANCHY*COS(AOLX)
    AARMY=ANCHY*COS(AOLY)
    AOTMX=AAARMX*(TBWGT-TSWGT)
    AOTMY=AAARMY*(TBWGT-TSWGT)
    IF(IEND.EQ.1) GOTO 500
    ECOTMX=0.0
    ECOTMY=0.0
    GOTO 600
C
C COMPUTE OVERTURNING MOMENT DUE TO END CAP
    500 ECOTMX=7.5*SPL*SIN(AOLX*PI/180.)
    ECOTMY=7.5*SPL*SIN(AOLY*PI/180.)
C
C SUM OVERTURNING MOMENTS TO COMPUTE TOTAL OVERTURNING MOMENT
    600 OTMOMX=OTMX+WPOTMX+AOTMX+ECOTMX
    OTMONY=OTMY+WPOTMY+AOTMY+ECOTMY
    RETURN
END
C ***** SUBROUTINE RMOM *****
C *

```

ASB11549  
 ASB11550  
 ASB11551  
 ASB11552  
 ASB11553  
 ASB11554  
 ASB11555  
 ASB11556  
 ASB11557  
 ASB11558  
 ASB11559  
 ASB11560  
 ASB11561  
 ASB11562  
 ASB11563  
 ASB11564  
 ASB11565  
 ASB11566  
 ASB11567  
 ASB11568  
 ASB11569  
 ASB11570  
 ASB11571  
 ASB11572  
 ASB11573  
 ASB11574  
 ASB11575  
 ASB11576  
 ASB11577  
 ASB11579  
 ASB11579  
 ASB11580  
 ASB11581  
 ASB11582  
 ASB11583  
 ASB11584

```

C *****
SUBROUTINE RMOM (SPL,SPW,VW,VL,VHGT,SWGT,WAMP,SWND,VHWD,
1IVSUB,WOMX,WOMY,BMOMX,BMOMY,RMOMX,RMOMY)
C *****
C SUBROUTINE RMOM CALCULATES THE RIGHTING MOMENT OF THE
C SPAR USING ARCHIMEDES PRINCIPLE
C
COMMON PI,G,DEPTH,RAIR,RWAT,UAIR,UWAT,ICOUNT,AOLX,AOLY
COMMON NWDP,NCDP,NWADF,NWDPD
C
C CALCULATE WEIGHT MOMENT ARMS
SARNX=SPL/2.0*SIN(AOLY*PI/180.)
SARNY=SPL/2.0*SIN(AOLY*PI/180.)
VARNX=VHGT*TAN(AOLX*PI/180.)+((VH/2+SPW/2)*COS(AOLX*PI/180))
VARNY=VHGT*TAN(AOLY*PI/180.)
C
C CALCULATE THE WEIGHT MOMENTS
WOMX=SWGT*SARNX+VWGT*VARNX
WOMY=SWGT*SARNY+VWGT*VARNY
C
C CALCULATE THE BUOYANT MOMENT ARMS
SBARNX=(DEPTH+WAMP)/2.0*TAN(AOLX*PI/180.)
SBARNY=(DEPTH+WAMP)/2.0*TAN(AOLY*PI/180.)
VBARNX=VARNX
VBARNY=VARNY
IF (IVSUB.EQ.1) GOTO 100
VLSUB=(DEPTH+WAMP)-(VHGT-VL/2.)
VBARFX=(DEPTH+WAMP-VLSUB/2.)*TAN(AOLX*PI/180.)
VBARFY=(DEPTH+WAMP-VLSUB/2.)*TAN(AOLY*PI/180.)
C
C CALCULATE THE BUOYANT MOMENTS
100 BSMOMX=SWND*SBARNX
BSMOMY=SWND*SBARNY
BVMOMX=VHWD*VBARNX
BVMOMY=VHWD*VBARNY
BMOMX=BSMOMX+BVMOMX

```

ASB11585  
 ASB11586  
 ASB11587  
 ASB11588  
 ASB11589  
 ASB11590  
 ASB11591  
 ASB11592  
 ASB11593  
 ASB11594  
 ASB11595  
 ASB11596  
 ASB11597  
 ASB11598  
 ASB11599  
 ASB11600  
 ASB11601  
 ASB11602  
 ASB11603  
 ASB11604  
 ASB11605  
 ASB11606  
 ASB11607  
 ASB11608  
 ASB11609  
 ASB11610  
 ASB11611  
 ASB11612  
 ASB11613  
 ASB11614  
 ASB11615  
 ASB11616  
 ASB11617  
 ASB11618  
 ASB11619  
 ASB11620

```

ASB11621
ASB11622
ASB11623
ASB11624
ASB11625
ASB11626
ASB11627
ASB11628
ASB11629
ASB11630
ASB11631
ASB11632
ASB11633
ASB11634
ASB11635
ASB11636
ASB11637
ASB11638
ASB11639
ASB11640
ASB11641
ASB11642
ASB11643
ASB11644
ASB11645
ASB11646
ASB11647
ASB11648
ASB11649
ASB11650
ASB11651
ASB11652
ASB11653
ASB11654
ASB11655
ASB11656

```

```

      BMOHY=BSMOHY+BVMCMY
      C
      C CALCULATE RIGHTING MOMENTS
      RMOMX=BMOHX-WMOHX
      RMOMY=BMOHY-WMOHY
      RETURN
      END
      *****
      * SUBROUTINE INOUT1
      *****
      C
      C *****
      C SUBROUTINE INOUT1(ELEV, WAA, WSP, WVELX,
      1 WVELY, WVELNX, WVELNY, DEPC, DEWP, VEL, DIR, CAA, CVX, CVY, CVNX, CVNY,
      2 DEP, WAMP, HMAVX, HMAVY, VMAVX, VMAVY, WMAVX, WMAVY, WPMVX, WPMVY,
      3 SPW, SPD, RENX, RENY, REMPX, REMPY, CMDX, CMDY, CWPDX, CWPDY)
      C
      C WHEN THE INTERMEDIATE OUTPUT NUMBER (ION) HAS BEEN SET TO 1,
      C THIS SUBROUTINE WRITES OUT ALL OF THE INTERMEDIATE VALUES
      C CALCULATED BY THE VARIOUS SUBROUTINES IN THIS PROGRAM, USED
      C TO DETERMINE THE TOTAL FORCE ON THE SPAR.
      C
      C
      C DIMENSION ELEV(100), WSP(100)
      C DIMENSION WVELX(100), WVELY(100), WVELNX(100), WVELNY(100)
      C DIMENSION VEL(500), DIR(500), CAA(500)
      C DIMENSION DEP(500), DEPC(500), DEWP(500)
      C DIMENSION CVX(500), CVY(500), CVNX(500), CVNY(500)
      C DIMENSION WPMVX(500), WPMVY(500)
      C DIMENSION HMAVX(500), HMAVY(500), VMAVX(500), VMAVY(500)
      C DIMENSION WMAVX(500), WMAVY(500), WMAVX(500), WMAVY(500)
      C DIMENSION XREL(500), YREL(500), AX(500), AY(500), BX(500), BY(500)
      C DIMENSION WAAVX(500), WAAVY(500)
      C DIMENSION REMX(100), RENY(100), REMPX(500), REMPY(500)
      C DIMENSION CMDX(100), CMDY(100), CWPDX(500), CWPDY(500)
      C COMMON PI, G, DEPTH, RAIR, RWAT, UAIR, UWAT, ICOUNT, AOLX, AOLY
      C COMMON NWDP, NCDDP, NWADP, NWPDY
      C DATA SYD/'X - ' /, SYD/'Y - ' /

```

C

```

IF (NWDP.EQ.0) GOTO 200
WRITE(6,105)
105 FORMAT('1',53X,'WIND VELOCITY INFORMATION',/,/,59X,
1'X - DIRECTION',/,/,10X,'ELEVATION',10X,
2'WIND ANGLE',9X,'WIND SPEED',9X,'WIND VELOCITY',9X,
3'LIST ANGLE',10X,'WIND VELOCITY',/,29X,'OF ATTACK',68X,
4'NORMAL TO THE BUOY',/,11X,'(FEET)',12X,'(DEGREES)',10X,
6'(FT./SEC.)',12X,'(FT.SEC.)',11X,'(DEGREES)',11X,
7'(FT./SEC.)')
DO 110 I=1,NWDP
110 WRITE(6,115) ELEV(I),WAA,WSP(I),WVELX(I),AOLX,WVELNX(I)
115 FORMAT('0',11X,F5.2,14X,F5.1,12X,F7.2,14X,F7.3,14X,F7.2,
11X,F7.2)
WRITE(6,125)
125 FORMAT('1',53X,'WIND VELOCITY INFORMATION',/,/,59X,
1'Y - DIRECTION',/,/,10X,'ELEVATION',10X,
2'WIND ANGLE',9X,'WIND SPEED',9X,'WIND VELOCITY',9X,
3'LIST ANGLE',10X,'WIND VELOCITY',/,29X,'OF ATTACK',68X,
4'NORMAL TO THE BUOY',/,11X,'(FEET)',12X,'(DEGREES)',10X,
5'(FT./SEC.)',12X,'(FT.SEC.)',11X,'(DEGREES)',11X,
6'(FT./SEC.)')
DO 130 I=1,NWDP
130 WRITE(6,115) ELEV(I),WAA,WSP(I),WVELY(I),AOLY,WVELNY(I)
200 IF (NCDP.EQ.0) GOTO 300
WRITE(6,205)
205 FORMAT('1',51X,'CURRENT VELOCITY INFORMATION',/,/,7X,
1'DEPH',9X,'CURRENT SPEED',9X,'CURRENT',9X,
2'CURRENT ANGLE',9X,'CURRENT VELOCITY',9X,
3'CURRENT VELOCITY',/,42X,'DIRECTION',9X,
4'OF ATTACK',12X,'X - DIRECTION',12X,
5'Y - DIRECTION',/,6X,'(FEET)',10X,
6'(FT./SEC.)',10X,'(DEGREES)',10X,'(DEGREES)',14X,
7'(FT./SEC.)',14X,'(FT./SEC.)')
DO 210 I=1,NCDP
210 WRITE(6,215) DEPC(I),VEL(I),DIR(I),CAA(I),CVX(I),CVY(I)
215 FORMAT('0',5X,F6.2,13X,F5.2,14X,F5.1,13X,F6.1,18X,F6.2,

```

ASB11657  
 ASB11658  
 ASB11659  
 ASB11660  
 ASB11661  
 ASB11662  
 ASB11663  
 ASB11664  
 ASB11665  
 ASB11666  
 ASB11667  
 ASB11668  
 ASB11669  
 ASB11670  
 ASB11671  
 ASB11672  
 ASB11673  
 ASB11674  
 ASB11675  
 ASB11676  
 ASB11677  
 ASB11678  
 ASB11679  
 ASB11680  
 ASB11681  
 ASB11682  
 ASB11683  
 ASB11684  
 ASB11685  
 ASB11686  
 ASB11687  
 ASB11688  
 ASB11689  
 ASB11690  
 ASE11691  
 ASB11692

```

117X,F6.2)
WRITE(6,225)
225 FORMAT('1',45X,'CURRENT VELOCITY INFORMATION (CONTINUED)',/,/,35X,
1'X - DIRECTION',45X,'Y - DIRECTION',/,/,5X,
2'DEPH',5X,'CURRENT VELOCITY',5X,'LIST ANGLE',6X,
3'CURRENT VELOCITY',6X,'CURRENT VELOCITY',5X,
4'LIST ANGLE',6X,'CURRENT VELOCITY',/,/,51X,
5'NORMAL TO THE BUOY',41X,'NORMAL TO THE BUOY',/,4X,
6'(FEET)',8X,'(FT./SEC.)',8X,'(DEGREES)',10X,
7'(FT./SEC.)',12X,'(FT./SEC.)',8X,'(DEGREES)',10X,
8'(FT./SEC.)')
DO 230 I=1,NCDP
230 WRITE(6,235) DEPC(I),CVX(I),AOLX,CVN(X(I),CVY(I),AOLY,CVNY(I)
235 FORMAT('0',4X,F6.2,2(10X,F6.2),13X,F6.2,15X,F6.2,13X,F6.2,
113X,F6.2)
300 IF(NWADP.EQ.0) GOTO 400
WRITE(6,310) SXD,WAMP,AOLX,ICOUNT
310 FORMAT('1',49X,
1'WAVE PARTICLE VELOCITY INFORMATION',/,/,59X,
2A4,'DIRECTION',/,/,40X,
3'WAVE AMPLITUDE = ',23X,F6.3,' FEET',/,/,40X,
4'LIST ANGLE = ',27X,F7.3,' DEGREES',/,/,60X,
5'ICOUNT = ',I3,/,/,9X,
6'ABSOLUTE',9X,'HORIZONTAL PARTICLE',9X,
7'VERTICAL PARTICLE',9X,'RELATIVE PARTICLE',9X,
8'RELATIVE PARTICLE',/,10X,'DEPTH',16X,
9'VELOCITY',19X,'VELOCITY',18X,'VELOCITY',18X,
X'DIRECTION',/,10X,'(FEET)',14X,
1'(FT./SEC.)',17X,'(FT./SEC.)',16X,'(FT./SEC.)',17X,
2'(DEGREES)')
DO 320 I=1,NWADP
320 WRITE(6,330) DEP(I),HWAVX(I),VWAVX(I),XREL(I),BX(I)
330 FORMAT('0',9X,F6.3,15X,F7.3,20X,F7.3,19X,F7.3,20X,F7.3)
WRITE(6,340) SXD,WAMP,AOLX,ICOUNT
340 FORMAT('1',43X,
1'WAVE PARTICLE VELOCITY INFORMATION (CONTINUED)',/,/,59X,

```

```

ASB11693
ASB11694
ASB11695
ASB11696
ASB11697
ASB11698
ASB11699
ASB11700
ASB11701
ASB11702
ASB11703
ASB11704
ASB11705
ASB11706
ASB11707
ASB11708
ASB11709
ASB11710
ASB11711
ASB11712
ASB11713
ASB11714
ASB11715
ASB11716
ASB11717
ASB11718
ASB11719
ASB11720
ASB11721
ASB11722
ASB11723
ASB11724
ASE11725
ASE11726
ASE11727
ASE11728

```

ASB11729  
ASB11730  
ASB11731  
ASB11732  
ASB11733  
ASB11734  
ASB11735  
ASB11736  
ASB11737  
ASB11738  
ASB11739  
ASB11740  
ASB11741  
ASB11742  
ASB11743  
ASB11744  
ASB11745  
ASB11746  
ASB11747  
ASB11748  
ASB11749  
ASB11750  
ASB11751  
ASB11752  
ASE11753  
ASE11754  
ASE11755  
ASE11756  
ASE11757  
ASE11758  
ASE11759  
ASB11760  
ASB11761  
ASE11762  
ASB11763  
ASE11764

```

2A4, 'DIRECTION', //, //, 40X,
3' WAVE AMPLITUDE = ', 23X, F6.3, ' FEET', //, //, 40X,
4' LIST ANGLE = ', 27X, F6.3, ' DEGREES', //, //, 60X,
5' ICOUNT = ', I3, //, 14X,
6' ABSOLUTE', 13X,
7' RELATIVE PARTICLE', 14X, ' PARTICLE VELOCITY', 15X,
8' PARTICLE VELOCITY', //, 15X, ' DEPTH', 16X,
9' ANGLE OF ATTACK', 14X, ' NORMAL TO THE BUOY', 13X,
X' TANGENTIAL TO THE BUOY', //, 15X, ' (FEET)', 18X,
1' (DEGREES)', 22X, ' (FT./SEC.)', 22X,
2' (FT./SEC.)')
DO 350 I=1, NWADP
350 WRITE(6, 355) DEP(I), AX(I), WAVNX(I), WAVTX(I)
355 FORMAT('0', 14X, F6.3, 18X, F7.3, 23X, F9.3, 23X, F9.3)
WRITE(6, 310) SYD, WAMP, AOLY, ICOUNT
DO 370 I=1, NWADP
370 WRITE(6, 330) DEP(I), HWAVY(I), VNAVY(I), YRLE(I), BY(I)
WRITE(6, 340) SYD, WAMP, AOLY, ICOUNT
DO 395 I=1, NWADP
395 WRITE(6, 355) DEP(I), AY(I), WAVNY(I), WAVTY(I)
400 IF (SPH.NE.SPD) GOTO 600
IF (NWDP.EQ.0) GOTO 500
WRITE(6, 410) RAIR, UAIR
410 FORMAT('1', 49X, ' WIND DRAG COEFFICIENT INFORMATION', //, //, 59X,
1' X - DIRECTION', //, //, 17X,
2' AIR DENSITY = ', F7.5, ' SLUGS/FT. ** 3', 17X,
3' AIR VISCOSITY = ', F12.10, ' SLUGS/FT. * SEC.', //, //, 13X,
4' ELEVATION', 16X, ' WIND', 16X, ' CHARACTERISTIC', 14X,
5' REYNOLDS', 17X, ' DRAG', //, 36X, ' VELOCITY', 17X,
6' DIAMETER', 18X, ' NUMBER', 15X, ' COEFFICIENT', //, 14X,
7' (FEET)', 15X, ' (FT./SEC.)', 17X, ' (FEET)')
DO 420 I=1, NWDP
420 WRITE(6, 430) ELEV(I), WVELNX(I), SPD, REMX(I), CWDX(I)
430 FORMAT('0', 13X, F5.2, 18X, F6.3, 20X, F5.3, 17X, E12.6, 15X, F5.3)
WRITE(6, 460) RAIR, UAIR
460 FORMAT('1', 49X, ' WIND DRAG COEFFICIENT INFORMATION', //, //, 59X,

```

ASB11765  
ASB11766  
ASB11767  
ASB11768  
ASB11769  
ASB11770  
ASB11771  
ASB11772  
ASB11773  
ASB11774  
ASB11775  
ASB11776  
ASB11777  
ASB11778  
ASB11779  
ASB11780  
ASB11781  
ASB11782  
ASB11783  
ASB11784  
ASB11785  
ASB11786  
ASB11787  
ASB11788  
ASB11789  
ASB11790  
ASB11791  
ASB11792  
ASB11793  
ASB11794  
ASB11795  
ASB11796  
ASB11797  
ASB11798  
ASB11799  
ASB11800

```

1'Y - DIRECTION',/,/,17X,
2'AIR DENSITY = ',P7.5,' SLUGS/FT. ** 3',17X,
3'AIR VISCOSITY = ',P12.10,' SLUGS/FT. * SEC.',/,/,13X,
4'ELEVATION',16X,'WIND',16X,'CHARACTERISTIC',14X,
5'REYNOLDS',17X,'DRAG',/,36X,'VELOCITY',17X,
6'DIAMETER',18X,'NUMBER',15X,'COEFFICIENT',/,14X,
7'(FEET)',15X,'(FT./SEC.)',19X,'(FEET)')
  DO 470 I=1,NWDP
470 WRITE(6,430) ELEV(I),HVELNX(I),SPD,REHY(I),CWDY(I)
500 IF(NWDP.EQ.0) GOTO 800
  WRITE(6,510) RWAT,UWAT
510 FORMAT('1',4X,
1'WATER PARTICLE DRAG COEFFICIENT INFORMATION',/,/,59X,
2'X - DIRECTION',/,/,16X,
3'WATER DENSITY = ',P7.5,' SLUGS/FT. ** 3',15X,
4'WATER VISCOSITY = ',P12.10,' SLUGS/FT. * SEC.',/,/,15X,
5'DEPTH',13X,'WATER PARTICLE',11X,'CHARACTERISTIC',14X,
6'REYNOLDS',17X,'DRAG',/,36X,'VELOCITY',17X,
7'DIAMETER',18X,'NUMBER',15X,'COEFFICIENT',/,14X,
8'(FEET)',15X,'(FT./SEC.)',17X,'(FEET)')
  DO 520 I=1,NWDP
520 WRITE(6,530) DEHP(I),WPVNX(I),SPD,REWPX(I),CWPDX(I)
530 FORMAT('0',13X,P6.2,17X,P6.3,20X,P5.3,16X,E12.6,15X,P5.3)
  WRITE(6,560) RWAT,UWAT
560 FORMAT('1',4X,
1'WATER PARTICLE DRAG COEFFICIENT INFORMATION',/,/,59X,
2'Y - DIRECTION',/,/,16X,
3'WATER DENSITY = ',P7.5,' SLUGS/FT. ** 3',15X,
4'WATER VISCOSITY = ',P12.10,' SLUGS/FT. * SEC.',/,/,15X,
5'DEPTH',13X,'WATER PARTICLE',11X,'CHARACTERISTIC',14X,
6'REYNOLDS',17X,'DRAG',/,36X,'VELOCITY',17X,
7'DIAMETER',18X,'NUMBER',15X,'COEFFICIENT',/,14X,
8'(FEET)',15X,'(FT./SEC.)',17X,'(FEET)')
  DO 570 I=1,NWDP
570 WRITE(6,530) DEHP(I),WPVNY(I),SPD,REWPY(I),CWPDY(I)
  GOTO 800

```

ASB11801  
ASB11802  
ASB11803  
ASB11804  
ASB11805  
ASB11806  
ASB11807  
ASB11808  
ASB11809  
ASB11810  
ASB11811  
ASB11812  
ASB11813  
ASB11814  
ASB11815  
ASB11816  
ASB11817  
ASB11818  
ASB11819  
ASB11820  
ASB11821  
ASB11822  
ASB11823  
ASB11824  
ASB11825  
ASB11826  
ASB11827  
ASB11828  
ASB11829  
ASB11830  
ASB11831  
ASB11832  
ASB11833  
ASB11834  
ASB11835  
ASB11836

```

600 IF (NWDP.EQ.0) GOTO 700
    WRITE(6,610) RAIR,UAIR
610 FORMAT('1',49X,'WIND DRAG COEFFICIENT INFORMATION',/,/,59X,
    1'X - DIRECTION',/,/,17X,
    2'AIR DENSITY = ',F7.5,' SLUGS/FT. ** 3',17X,
    3'AIR VISCOSITY = ',F12.10,' SLUGS/FT. * SEC.',/,/,13X,
    4'ELEVATION',16X,'WIND',16X,'CHARACTERISTIC',14X,
    5'REYNOLDS',17X,'DRAG',/,36X,'VELOCITY',17X,
    6'DIAMETER',18X,'NUMBER',15X,'COEFFICIENT',/,14X,
    7'(FEET)',15X,',(FT./SEC.)',17X,',(FEET)')
    DO 620 I=1,NWDP
620 WRITE(6,630) ELEV(I),WVELNX(I),SPD,REHX(I),CWDX(I)
630 FORMAT('0',13X,F5.2,18X,F6.3,20X,F5.3,17X,F12.6,15X,F5.3)
    WRITE(6,660) RAIR,UAIR
660 FORMAT('1',49X,'WIND DRAG COEFFICIENT INFORMATION',/,/,59X,
    1'X - DIRECTION',/,/,17X,
    2'AIR DENSITY = ',F7.5,' SLUGS/FT. ** 3',17X,
    3'AIR VISCOSITY = ',F12.10,' SLUGS/FT. * SEC.',/,/,13X,
    4'ELEVATION',16X,'WIND',16X,'CHARACTERISTIC',14X,
    5'REYNOLDS',17X,'DRAG',/,36X,'VELOCITY',17X,
    6'DIAMETER',18X,'NUMBER',15X,'COEFFICIENT',/,14X,
    7'(FEET)',15X,',(FT./SEC.)',19X,',(FEET)')
    DO 670 I=1,NWDP
670 WRITE(6,630) ELEV(I),WVELNY(I),SPW,REHY(I),CWDY(I)
700 IF (NWDP.EQ.0) GOTO 800
    WRITE(6,710) RWAT,UWAT
710 FORMAT('1',44X,
    1'WATER PARTICLE DRAG COEFFICIENT INFORMATION',/,/,59X,
    2'X - DIRECTION',/,/,16X,
    3'WATER DENSITY = ',F7.5,' SLUGS/FT. ** 3',15X,
    4'WATER VISCOSITY = ',F12.10,' SLUGS/FT. * SEC.',/,/,15X,
    X'DEPTH',13X,'WATER PARTICLE',11X,'CHARACTERISTIC',14X,
    5'REYNOLDS',17X,'DRAG',/,36X,'VELOCITY',17X,
    6'DIAMETER',18X,'NUMBER',15X,'COEFFICIENT',/,14X,
    7'(FEET)',15X,',(FT./SEC.)',17X,',(FEET)')
    DO 720 I=1,NWDP

```



```

720 WRITE(6,730) DEWP(I),WPVNX(I),SPD,REWPX(I),CWPDX(I)
730 FORMAT('0',13X,F6.2,17X,F6.3,20X,F5.3,16X,E12.6,15X,F5.3)
      WRITE(6,760) RWAT,UMAT
760 FORMAT('1',44X,
1'WATER PARTICLE DRAG COEFFICIENT INFORMATION',/,/,59X,
2'Y - DIRECTION',/,/,16X,
3'WATER DENSITY = ',F7.5,' SLUGS/FT. ** 3',15X,
4'WATER VISCOSITY = ',F12.10,' SLUGS/FT. * SEC.',/,/,15X,
5'DEPTH',13X,'WATER PARTICLE',11X,'CHARACTERISTIC',14X,
6'REYNOLDS',17X,'DRAG',/,36X,'VELOCITY',17X,
7'DIAMETER',18X,'NUMBER',15X,'COEFFICIENT',/,14X,
8'(FEET)',15X,'(FT./SEC.)',17X,'(FEET)')
      DO 770 I=1,NWDP
770 WRITE(6,730) DEWP(I),WPVNY(I),SPW,REWPY(I),CWPDY(I)
800 RETURN
      END
C ***** SUBROUTINE INOUT2 *****
C *
C ***** SUBROUTINE INOUT2 *****
C ***** SUBROUTINE INOUT2(SHAX,EWAY,CAREA,CMX,CHY,ELEV,
1WFX,WFY,TWFX,TWFY,ENPAX,ENPAY,DEWP,WPDX,WPDPY,WPIFX,WPIFY,
2WPPX,WPPY,TWPPX,TWPPY,TWPIFX,TWPIFY,TWPPY,TWPMX,
3WOTMY,WPOTHY,WPOTHY,OTMOMX,OTMOMY,IART,WOMX,WOMY,
4BOMX,BOMY,RMOMX,RMOMY)
C
C WHEN THE INTERMEDIATE OUTPUT NUMBER (ION) HAS BEEN SET EQUAL TO 1,
C THIS SUBROUTINE WRITES OUT THE WIND AND WAVE PARTICLE FORCES ON
C EACH ELEMENTAL AREA AS WELL AS THE TOTAL FORCE ON THE SPAR. IN
C ADDITION, ALL OVERTURNING AND RIGHTING MOMENTS IN BOTH THE X AND
C Y DIRECTIONS ARE WRITTEN OUT.
C
      DIMENSION ELEV(100)
      DIMENSION WFX(100),WFX(100)
      DIMENSION DEWP2(500)
      DIMENSION WPDX(500),WPDPY(500),WPIFX(500),WPIFY(500)
      DIMENSION WPPX(500),WPPY(500)

```

ASB11837  
 ASB11838  
 ASB11839  
 ASB11840  
 ASB11841  
 ASB11842  
 ASB11843  
 ASB11844  
 ASB11845  
 ASB11846  
 ASB11847  
 ASB11848  
 ASB11849  
 ASB11850  
 ASB11851  
 ASB11852  
 ASB11853  
 ASB11854  
 ASB11855  
 ASB11856  
 ASB11857  
 ASB11858  
 ASB11859  
 ASB11860  
 ASB11861  
 ASB11862  
 ASB11863  
 ASB11864  
 ASB11865  
 ASB11866  
 ASB11867  
 ASB11868  
 ASB11869  
 ASB11870  
 ASB11871  
 ASB11872

ASB11873  
 ASB11874  
 ASB11875  
 ASB11876  
 ASB11877  
 ASB11878  
 ASB11879  
 ASB11880  
 ASB11881  
 ASB11882  
 ASB11883  
 ASB11884  
 ASB11885  
 ASB11886  
 ASB11887  
 ASB11888  
 ASB11889  
 ASB11890  
 ASB11891  
 ASB11892  
 ASB11893  
 ASB11894  
 ASB11895  
 ASB11896  
 ASB11897  
 ASB11898  
 ASB11899  
 ASB11900  
 ASB11901  
 ASB11902  
 ASB11903  
 ASB11904  
 ASB11905  
 ASB11906  
 ASB11907  
 ASB11908

COMMON PI,G,DEPTH,RAIR,RWAT,UAIR,UWAT,ICOUNT,AOLX,,OLY  
 COMMON NWDP,NCDP,NWADP,NWPDF

C

```

IP(NWDP,EQ.0) GOTO 900
WRITE(6,810) RAIR,EWAY,CAREA,CMX
810 FORMAT('1',55X,'WIND FORCE INFORMATION',/,/,59X,
1'X - DIRECTION',/,/,40X,
2'MASS DENSITY OF AIR = ',19X,F6.4,' SLUGS/FT * 3',/,/,40X,
3'ELEMENTAL AREA = ',23X,F6.3,' FEET ** 2',/,/,40X,
4'CROSS-SECTIONAL AREA = ',17X,F6.3,' FEET ** 2',/,/,40X,
5'HYDRODYNAMIC MASS COEFFICIENT = ',9X,F4.2,/,/,39X,
6'AVERAGE',37X,'TOTAL WIND',/,38X,
7'ELEVATION',38X,'FORCE',/,40X,'(FEET)',38X,'(POUNDS)')
DO 820 I=1,NWDP
820 WRITE(6,830) ELEV(I),WFX(I)
830 FORMAT('0',36X,F6.2,27X,F12.2)
WRITE(6,840) TWFX
840 FORMAT('0',43X,'TOTAL = ',F12.2)
WRITE(6,860) RAIR,EWAY,CAREA,CMX
860 FORMAT('1',55X,'WIND FORCE INFORMATION',/,/,59X,
1'X - DIRECTION',/,/,40X,
2'MASS DENSITY OF AIR = ',19X,F6.4,' SLUGS/FT * 3',/,/,40X,
3'ELEMENTAL AREA = ',23X,F6.3,' FEET ** 2',/,/,40X,
4'CROSS-SECTIONAL AREA = ',17X,F6.3,' FEET ** 2',/,/,40X,
5'HYDRODYNAMIC MASS COEFFICIENT = ',9X,F4.2,/,/,39X,
6'AVERAGE',37X,'TOTAL WIND',/,38X,
7'ELEVATION',40X,'FORCE',/,40X,'(FEET)',38X,'(POUNDS)')
DO 870 I=1,NWDP
870 WRITE(6,830) ELEV(I),WPY(I)
WRITE(6,840) TWPY
900 IF(NWDP,EQ.0) GOTO 1000
WRITE(6,910) RWAT,EWPAX,CAREA,CMX
910 FORMAT('1',50X,'WATER PARTICLE FORCE INFORMATION',/,/,59X,
1'X - DIRECTION',/,/,40X,
2'MASS DENSITY OF WATER = ',17X,F6.4,' SLUGS/FT * 3',/,/,40X,
3'ELEMENTAL AREA = ',23X,F6.3,' FEET ** 2',/,/,40X,
  
```

```

4 CROSS-SECTIONAL AREA = ,17X,F6.3, FEET ** 2',/,40X,
5 HYDRODYNAMIC MASS COEFFICIENT = ,9X,F4.2,/,20X,
6 AVERAGE',21X,'DRAG',22X,'INERTIA',21X,'TOTAL WAVE',/,21X,
7 DEPTH',21X,'FORCE',23X,'FORCE',20X,'PARTICLE FORCE',/,20X,
8 (FEET)',20X,'(PCUNDS)',20X,'(POUNDS)',21X,'(POUNDS)')
DO 920 I=1,NWPD
920 WRITE(6,930) DEHP(I),WPDFX(I),WPIFX(I),WPFY(I)
930 FORMAT('0',19X,F6.2,16X,F12.2,16X,F12.2,18X,F12.2)
WRITE(6,940) TWPDFX,TWPIFX,TWPFY
940 FORMAT('0',33X,'TOTAL = ',F12.2,8X,'TOTAL = ',F12.2,11X,
1 'TOTAL = ',F12.2)
WRITE(6,960) RWAT,EWPAY,CAREA,CMY
960 FORMAT('1',50X,'WATER PARTICLE FORCE INFORMATION',/,/,59X,
1 'Y - DIRECTION',/,/,40X,
2 'MASS DENSITY OF WATER = ',17X,F6.4,' SLUGS/FT * 3',/,40X,
3 'ELEMENTAL AREA = ',23X,F6.3,' FEET ** 2',/,40X,
4 'CROSS-SECTIONAL AREA = ',17X,F6.3,' FEET ** 2',/,40X,
5 'HYDRODYNAMIC MASS COEFFICIENT = ',9X,F4.2,/,20X,
6 AVERAGE',21X,'DRAG',22X,'INERTIA',21X,'TOTAL WAVE',/,21X,
7 DEPTH',21X,'FORCE',23X,'FORCE',20X,'PARTICLE FORCE',/,20X,
8 (FEET)',20X,'(POUNDS)',20X,'(POUNDS)',21X,'(POUNDS)')
DO 970 I=1,NWPD
970 WRITE(6,930) DEHP(I),WPDFY(I),WPIFY(I),WPFY(I)
WRITE(6,940) TWPDFY,TWPIFY,TWPFY
1000 CONTINUE
WRITE(6,1010) WOTMX,WOTMY,WPOTMX,WPOTY,OTMOMX,OTMOMY
1010 FORMAT('1',52X,'TABLE OF OVERTURNING MOMENTS',/,/,65X,
1 'X-MOMENT',26X,'Y-MOMENT',/,/,25X,
2 'WIND MOMENT',26X,F10.2,24X,F10.2,/,25X,
3 'WATER PARTICLE MOMENT',16X,F10.2,24X,F10.2,/,25X,
4 'TOTAL MOMENT',25X,F10.2,24X,F10.2)
IF(IART.NE.1) GOTO 1200
WRITE(6,1110) WMOMX,WMOMY,BMOMX,BMOMY,RMOMX,RMOMY
1110 FORMAT('1',54X,'TABLE OF RIGHTING MOMENTS',/,/,65X,
1 'X-MOMENT',26X,'Y-MOMENT',/,/,25X,
2 'WEIGHT MOMENT',24X,F10.2,24X,F10.2,/,25X,

```

ASB11909  
 ASB11910  
 ASB11911  
 ASB11912  
 ASB11913  
 ASB11914  
 ASB11915  
 ASB11916  
 ASB11917  
 ASB11918  
 ASB11919  
 ASB11920  
 ASB11921  
 ASB11922  
 ASB11923  
 ASB11924  
 ASB11925  
 ASB11926  
 ASB11927  
 ASB11928  
 ASB11929  
 ASB11930  
 ASB11931  
 ASB11932  
 ASB11933  
 ASB11934  
 ASB11935  
 ASB11936  
 ASB11937  
 ASB11938  
 ASE11939  
 ASE11940  
 ASB11941  
 ASB11942  
 ASB11943  
 ASB11944

ASB11945  
ASB11946  
ASB11947  
ASB11948  
ASB11949  
ASB11950  
ASB11951  
ASB11952  
ASB11953  
ASB11954  
ASB11955  
ASB11956  
ASB11957  
ASB11958  
ASB11959  
ASB11960  
ASB11961  
ASB11962  
ASB11963  
ASB11964  
ASB11965  
ASB11966  
ASB11967  
ASB11968  
ASB11969  
ASB11970  
ASB11971  
ASB11972  
ASB11973  
ASB11974  
ASB11975  
ASB11976  
ASB11977  
ASB11978  
ASB11979  
ASB11980

```

3 BUOYANT MOMENT',23X,F10.2,24X,F10.2,/,/,25X,
4 TOTAL MOMENT',25X,F10.2,24X,F10.2)
1200 RETURN
END
C ***** SUBROUTINE ANCHOR *****
C *
C ***** SUBROUTINE ANCHOR(NWHPTS,TSWGT,SBWGT) *****
C
C SUBROUTINE ANCHOR DETERMINES THE RESERVE BUOYANCY OF THE
C SPAR AND THEN MATCHES THIS WITH A STANDARD COAST GUARD SINKER.
C NOTE THAT THE COAST GUARD SINKERS ARE SPECIFIED BY THEIR WEIGHT
C IN AIR BUT ARE MATCHED WITH THE RESERVE BUOYANCY OF THE SPAR BY
C THEIR WEIGHT IN WATER.
C
C DIMENSION SBWGT(100)
C COMMON PI,G,DEPTH,RAIR,RWAT,UAIR,UWAT,ICOUNT,AOLY,AOLY
C COMMON NWDP,NCDDP,NWADE,NWPDP
C
C DEFINE MASS DENSITY OF CONCRETE
C RCON=4.476
C
C CALCULATE WEIGHTS IN WATER OF STANDARD COAST GUARD SINKERS
C S1=20.*20.*8./1728.*(RCON-RWAT)*G
C S2=24.*24.*10./1728.*(RCON-RWAT)*G
C S3=32.*32.*12./1728.*(RCON-RWAT)*G
C S4=40.*40.*15./1728.*(RCON-RWAT)*G
C S5=45.*45.*18./1728.*(RCON-RWAT)*G
C S6=50.*50.*19./1728.*(RCON-RWAT)*G
C S7=54.*54.*21./1728.*(RCON-RWAT)*G
C S8=58.*58.*23./1728.*(RCON-RWAT)*G
C S9=60.*60.*28./1728.*(RCON-RWAT)*G
C S10=60.*60.*42./1728.*(RCON-RWAT)*G
C
C CALCULATE THE MAXIMUM TOTAL BUOYANT WEIGHT
C TBMX=0.0

```

```

DO 100 I=1,NWHPTS
100 TBNMAX=AMAX1(TBNMAX,SBWGT(I))
C
C CALCULATE THE RESERVE BUOYANCY OF THE SPAR
RB=TBNMAX-TSWG
C
C DETERMINE THE APPROPRIATE ANCHOR SIZE
IF(RB.LT.S1) GOTO 200
IF(RB.LT.S2) GOTO 300
IF(RB.LT.S3) GOTO 400
IF(RB.LT.S4) GOTO 500
IF(RB.LT.S5) GOTO 600
IF(RB.LT.S6) GOTO 700
IF(RB.LT.S7) GOTO 800
IF(RB.LT.S8) GOTO 900
IF(RB.LT.S9) GOTO 1000
IF(RB.LT.S10) GOTO 1100
C
C WRITE OUT APPROPRIATE ANCHOR SIZE
WRITE(6,1205) RB
1205 FORMAT('1',44X,'MINIMUM REQUIRED ANCHOR SIZE IS ',F8.2,
1' LBS.',//,18X,
2'THIS BUOY DESIGN CANNOT BE SECURED TO THE BOTTOM WITH JUST A SINGL
3E COAST GUARD SINKER')
GOTO 1200
200 FS=S1/RB
WRITE(6,1215) RB,FS
1215 FORMAT('1',//,18X,'MINIMUM REQUIRED ANCHOR SIZE IS ',F7.2,
1'MINIMUM REQUIRED ANCHOR SIZE IS ',F7.2,
2' LBS.',//,27X,'A 250 LB. STANDARD COAST GUARD ANCHOR WILL PROVI
3DE A FACTOR OF SAFETY OF ',F4.1)
GOTO 1200
300 FS=S2/RB
WRITE(6,1225) RB,FS
1225 FORMAT('1',//,18X,'MINIMUM REQUIRED ANCHOR SIZE IS ',F7.2,
1'MINIMUM REQUIRED ANCHOR SIZE IS ',F7.2,

```

ASB11981  
ASB11982  
ASB11983  
ASB11984  
ASB11985  
ASB11986  
ASB11987  
ASB11988  
ASB11989  
ASB11990  
ASB11991  
ASB11992  
ASB11993  
ASB11994  
ASB11995  
ASB11996  
ASB11997  
ASB11998  
ASB11999  
ASB12000  
ASB12001  
ASB12002  
ASB12003  
ASB12004  
ASB12005  
ASB12006  
ASB12007  
ASB12008  
ASB12009  
ASB12010  
ASB12011  
ASB12012  
ASB12013  
ASB12014  
ASB12015  
ASB12016

```

2' LBS',./././,27X,'A 500 LB. STANDARD COAST GUARD ANCHOR WILL PROVI
3DE A FACTOR OF SAFTEY OF ',F4.1)
GOTO 1200
400 FS=S3/RB
WRITE(6,1235) RB,FS
1235 FORMAT('1',./././,././,././,././,././,././,././,./,44X,
1'MINIMUM REQUIRED ANCHOR SIZE IS ',F7.2,
2' LBS',./././,27X,'A 1000 LB. STANDARD COAST GUARD ANCHOR WILL PROV
3IDE A FACTOR OF SAFTEY OF ',F4.1)
GOTO 1200
500 FS=S4/RB
WRITE(6,1245) RB,FS
1245 FORMAT('1',./././,././,././,././,././,././,././,./,44X,
1'MINIMUM REQUIRED ANCHOR SIZE IS ',F7.2,
2' LBS',./././,27X,'A 2000 LB. STANDARD COAST GUARD ANCHOR WILL PROV
3IDE A FACTOR OF SAFTEY OF ',F4.1)
GOTO 1200
600 FS=S5/RB
WRITE(6,1255) RB,FS
1255 FORMAT('1',./././,././,././,././,././,././,././,./,44X,
1'MINIMUM REQUIRED ANCHOR SIZE IS ',F7.2,
2' LBS',./././,27X,'A 3000 LB. STANDARD COAST GUARD ANCHOR WILL PROV
3IDE A FACTOR OF SAFTEY OF ',F4.1)
GOTO 1200
700 FS=S6/RB
WRITE(6,1265) RB,FS
1265 FORMAT('1',./././,././,././,././,././,././,././,./,44X,
1'MINIMUM REQUIRED ANCHOR SIZE IS ',F7.2,
2' LBS',./././,27X,'A 4000 LB. STANDARD COAST GUARD ANCHOR WILL PROV
3IDE A FACTOR OF SAFTEY OF ',F4.1)
GOTO 1200
800 FS=S7/RB
WRITE(6,1275) RB,FS
1275 FORMAT('1',./././,././,././,././,././,././,././,./,44X,
1'MINIMUM REQUIRED ANCHOR SIZE IS ',F7.2,
2' LBS',./././,27X,'A 5000 LB. STANDARD COAST GUARD ANCHOR WILL PROV

```

ASB12017  
 ASB12018  
 ASB12019  
 ASB12020  
 ASB12021  
 ASB12022  
 ASB12023  
 ASB12024  
 ASB12025  
 ASB12026  
 ASB12027  
 ASB12028  
 ASB12029  
 ASB12030  
 ASB12031  
 ASB12032  
 ASB12033  
 ASB12034  
 ASB12035  
 ASB12036  
 ASB12037  
 ASB12038  
 ASB12039  
 ASB12040  
 ASB12041  
 ASB12042  
 ASB12043  
 ASB12044  
 ASB12045  
 ASB12046  
 ASB12047  
 ASB12048  
 ASB12049  
 ASB12050  
 ASB12051  
 ASB12052



## APPENDIX B

User Manual for the Computer Model, ASB1



## USERS MANUAL FOR THE COMPUTER MODEL, ASB1

### Introduction

A program has been developed which computes the total force, resultant moment and if articulated, the list angle on a spar device being acted upon by wind, current and wave forces. Consisting of a main program, MAIN, and 19 internally called subroutines, this program written in Fortran IV has been run successfully on the University of Rhode Island's ITELAS 5 digital computer. Every effort has been made to make this program as general as possible. Consequently, a wide variety of input data as outlined below may be used. Because of the large number of arrays which may be used during computation, it is necessary to allocate 320k bytes of core to execute this program. Unfortunately, as a result of the wide range of possible input data as well as the iterative nature of the program, it is not possible to estimate the amount of time required to compile and execute this analytical model.

This program may be thought of as having two distinct phases: a control phase and a computational phase. Program MAIN acts in a control capacity, reading input data, checking its validity and calling the appropriate subroutines. During the computational procedure, program MAIN keeps track of the internal counters present in the program and ensures that the iterative technique used to determine the spar list angle converges. Once the appropriate force, moment and list angle information has been computed for a given case, program MAIN, checks to see if there are more cases and if so resets all counters to their initial value.

The computational phase of the program consists of the subroutines. All of the actual calculations take place in these subroutines, there being at least one subroutine for each of the major steps shown in the

flowchart (Figure II-3). These computational operations are repeated in a cyclical manner until the convergence criteria specified in the main program, MAIN, is satisfied.

#### Input Data

The English system of units (pounds-mass, feet, seconds) is assumed for all input data unless otherwise specified. Since most of the environmental and structural data available to users of this program is described using this system of units, it was chosen to make running this program as easy as possible. All of the input data is read by the main program, MAIN, where it is checked to ensure that each value is within its allowable range. Should an input value be specified outside of this range, a message to this effect is printed out and the program is terminated. Input data may be grouped into three categories; general information, spar structural information, and force information and should be read into the program in the following order. Unless otherwise specified, an F10.0 format is assumed for all input variables.

Program: MAIN

#### Input Variables

##### General Information

NCASE	Number of cases contained in the input data set (Integer *3)
IWAT	Water type. This value is used to define the fluid density and viscosity. It should be set equal to 1 if the buoy is to be located in salt water or 0 if this is not the case. (Integer * 1)

DEPTH            Still water depth.

#### Spar Structural Information

SPL,SPW,SPD    Spar length; spar width; spar depth.

SM,SMD,SWT    Spar material (Alpha-numeric \* 10); spar material density;  
spar wall thickness. If the spar is a solid structure,  
then the spar wall thickness value should be set equal to  
0.00.

IVANE           Orienting vane flag. This value should be set equal to 1  
if an orienting vane is present, otherwise this value  
should be set equal to 0 and the next three vane informa-  
tion data cards omitted. (Integer \* 1).

VL,VHT,VT      Vane length; vane height; vane thickness.

VM,VMD          Vane material (Alpha-numeric \* 10); vane material density.

VHGT            Vane height. This is the height from the bottom of the  
spar to the bottom edge of the orienting vane.

IART            Articulation flag. If the buoy is articulated about its  
base then this value should be set equal to 0. If this  
value is not equal to 1, then it is assumed that the spar  
acts as a pile structure which is aligned perpendicular to  
the bottom and, therefore, no list angles or righting  
moments are computed. (Integer \* 1).

ANCHX,ANCHY    Coordinates of the anchor attachment point relative to the  
center of the bottom face of the spar.

#### Force Information

NWDP            Number of wind data points. This value establishes the  
number of elemental areas into which that portion of the  
spar which is above the still water surface is divided.

Because of dimension limitations on the wind arrays, this value should always be less than 100. If this value is set equal to 0, then the next wind information data card must be omitted. (Integer \*3)

WSPD,WDIR      Wind speed (in miles per hour); wind direction (in degrees magnetic)

WLEEV,FETCH    elevation at which the wind speed was measured; fetch length.

NCOP           Number of current data points. This value establishes the number of elemental areas into which the submerged portion of the spar is divided for the purpose of computing current velocity information. This value should not exceed 500 because of dimension limitations on the current arrays. If this value is set equal to 0, it is assumed that no current forces are present and thus the next three current information data cards must be omitted. (Integer \* 3)

ICUR           Uniform current flag. This value determines whether a single set of variables or an array of current information are the next input avariables. This value indicates whether the current velocity profile is uniform or not. If this value is set to 1 then the following data card should contain the variables UCVEL and UCDir. If this value is 0 then the subsequent data cards should contain the current velocity profile VEL, DIR, DEP. (Integer \* 1)

UCVEL,UCDir    Uniform current velocity; uniform current direction. These array elements are read in only when the ICUR value has been set equal to 1.

VEL,DIR,DEP Current velocity; current direction; current depth. These array values are read in when the ICUR variable has been set equal to a value other than 1. Having a length equal to NCDP + 1, each row of this array contains the current speed and direction at an associated depth. Beginning with a water depth of 0.00, this current profile information must be supplied at equally spaced depth increments.

NWADP Number of wave data points. This value establishes the number of elemental areas into which the submerged portion of the spar (as measured from the still water surface) is divided for the purpose of computing wave particle velocity and acceleration information. Because of dimension limitations on the wave arrays, this value cannot exceed 500. Further, if both wave and current forces are present in an analysis, this value must be less than or equal to NCDP. If the NWADP value specified is non-zero and less than NCDP then it is increased to equal NCDP and a message to the effect is printed. If NWADP is set to 0, no wave forces are present and the next four wave data cards must be omitted. (Integer \* 1)

IWAVE Wave flag. If the significant and average wave heights and wave periods are to be supplied, this value should be set to 1. If this value is other than 1 then this wave information is internally calculated in subroutine WAVSMB and, therefore, the next wave data card should be omitted. (Integer \* 1)

TSIG,TAVG, Significant wave period; average wave period;

HGTSIG,HGTAVG significant wave height; average wave height. These values are read in only when the IWAVE parameter is equal to 1.

ITIME Time step increment. This value establishes the number of time increments into which the average wave period is divided. The total force on the spar and its resulting list angle is computed at each of these time steps.  
(Integer \* 3)

ITHERY Wave theory flag. This value should be set equal to 1 if linear, (Airy) wave theory is to be used to compute the wave particle motions and surface profile. A value of 2 is used to specify that Stokes second order wave theory is to be used to compute these wave parameters. (Integer \* 1)

ION Integer output number. This value should be set equal to 1 if a listing of all of the intermediate calculations used to compute the resultant list angle is desired. If this value is other than 1, no such listing will be produced.  
(Integer \* 1)

#### Additional General Information

NEWPD New physical data. This value is only read in when the number of cases in the input data set is greater than 1. If new general and spar structural information is to be forthcoming then this value should be set to 1, otherwise it is assumed that only the force information is to be varied and the value read in is assigned to the variable NWDP.

## THE SUBROUTINES

The subroutines described below are listed in the order in which they are called by the program, MAIN. The first four subroutines are called only once by the main program because the calculations involved are independent of the spar's list angles.

### Subroutine WEIGHT

The WEIGHT subroutine computes the weight of the entire spar device in both air and water. If the spar has been previously identified by the LIST parameter as being articulated then its total buoyancy is determined. Based upon this information, a check is then made to ensure that the specified spar design acting as a free body in the absence of any environmental forces will float. Should the dimensions of the spar have been specified so that a particular design will not float, a message to this effect is printed and the program terminated.

### Subroutine WNDSPO

The WNDSPO subroutine computes the wind speed profile from the wind velocity input data based upon the Prandtl-von Karman universal distribution law.

### Subroutine WAVSMB

The significant wave height and significant wave period of a wave is computed in subroutine WAVSMB using the S.M.B. method. Assuming that the wave height and the square of the wave period are both Rayleigh distributed, average values for these two parameters are also determined. (Ippen, 1965). These average values are subsequently used in the wave force calculations.

#### Subroutine WAVE

Subroutine WAVE is called by the program, MAIN, to compute basic information about the waves acting on the spar including the wavelength, wave celerity, wave frequency and the wave number. A wave amplitude value based upon the previously selected wave theory is also computed.

#### Subroutine AREAS

In this analysis, the total area exposed to wind forces is determined by the distance from mean sea level to the top of the spar; the total current area is determined by the distance from mean sea level to the bottom of the spar and the total area exposed to wave particle forces is determined by the distance from the free surface to the bottom of the spar. These distances, which are computed in subroutine AREAS, vary as a function of the spar's list angle. Further, since the distribution of the driving force velocities and accelerations may have large spatial variations in the vertical, subroutine AREAS divided these three areas into many equal elemental areas. The exact number of elemental areas into which an area exposed to a driving force is divided is equal to one less than the number of data points assigned to that force (i.e., one less than NWDP, NCDPAND, NWADP).

#### Subroutine CBEAR

Because the environmental forces in this model are defined with respect to a fixed reference point (i.e., magnetic north), it is necessary to define the orientation of the spar in relationship to this point in order that the relative forces acting on the spar be established. Subroutine CBEAR is called to compute this orientation when the buoy configuration under study has a splitter plate or other vane. This



subroutine assumes that a buoy's orientation is defined by the current direction at the centroid of its vane.

#### The Velocity Subroutines

Once the orientation of the spar has been established with respect to magnetic north, the driving force velocities normal to the spar in the X and Y directions are determined.

#### Subroutine RWVEL

Subroutine RWVEL calculates the wind velocities normal to the spar in the X and Y directions. In this subroutine, velocities are computed at the center of each elemental wind area.

#### Subroutine RCVEL

Current velocities normal to the spar in the X and Y directions are computed in subroutine RCVEL. These velocities are computed at the top and bottom of each elemental current area and then averaged linearly to determine the velocity at the center of each area.

#### Subroutine RWAVA

In subroutine RWAVA the water particle velocities and accelerations normal to the spar in the X and Y directions are computed. These values are computed at the top and bottom of each elemental wave particle area and then averaged linearly to determine the velocity and acceleration terms at the center of each area.

#### Subroutine WPV

In order to properly compute the total force due to current and waves acting on the spar, it is necessary to compute the total water particle velocity by summing these individual components at each depth of interest.

"When current is present, fluid forces may still be evaluated according to Morrison's formula (Myers, 1969). This is achieved by considering fluid particle velocity as the vector sum current velocity and wave induced particle velocity. Since the drag force is non-linear, it cannot be regarded as a simple superposition of current and wave drag forces." (Wu and Tung, 1975)

Subroutine WPV combines these current and wave particle velocities to determine the water particle velocity and associated water particle area at each depth of interest.

#### The Drag Coefficient Subroutines

##### Subroutine DRAGC

Subroutine DRAGC is called by program MAIN when the spar being studied has a cylindrical cross-section (i.e.,  $SPW = SPD$ ). In this subroutine, drag coefficients are computed at each elemental area from Reynolds number determinations according to the U.S. Army Corps of Engineers Recommended Design Curve. (U.S. Army Corps of Engineers, 1973).

##### Subroutine DRAGX

If the spar under study does not have a cylindrical cross-section then drag coefficients for driving force velocities in the X-direction to each elemental area are calculated in subroutine DRAGX based upon empirically derived relationships. (Hoerner, 1965)

#### Subroutine DRAGY

No empirical relationship describing the drag coefficient on an elliptical body whose major axis was normal to the flow could be found in the literature. Consequently, this subroutine assumes that such a shape may be considered a flat plate and, therefore, assigns a drag coefficient value of 2.0 to driving force components acting in this direction.

#### Subroutine FORCE

The wind and water particle normal forces on each of these elemental areas is computed in subroutine FORCE using the Morison equation and velocity, acceleration, area and drag coefficient information from previous subroutines. Subsequently, the total wind and water particle normal force on the spar is determined by summing each set of these elemental forces.

#### Subroutine OTMOM

Subroutine OTMOM computes the total wind and water particle overturning moments acting on the spar in the X and Y directions. These values are subsequently added together so that the total overturning in each of these directions is known.

#### Subroutine RMOM

This subroutine calculates the total righting moment acting on a spar in the X and Y directions based upon buoyancy considerations and the total spar weight.

### The Intermediate Output Subroutines

For the purpose of checking the final output or the computations performed in a subroutine, the intermediate output subroutines when called by program MAIN print the results of all significant calculations used to determine the total force, resulting moment and list of angle of a spar.

#### Subroutine INOUT 1

This subroutine prints the results of all the significant calculations performed in the following subroutines: AREAS, CBEAR, RWVEL, RCVEL, RWAVA, DRAGC, DRAGX, and DRAGY.

#### Subroutine INOUT 2

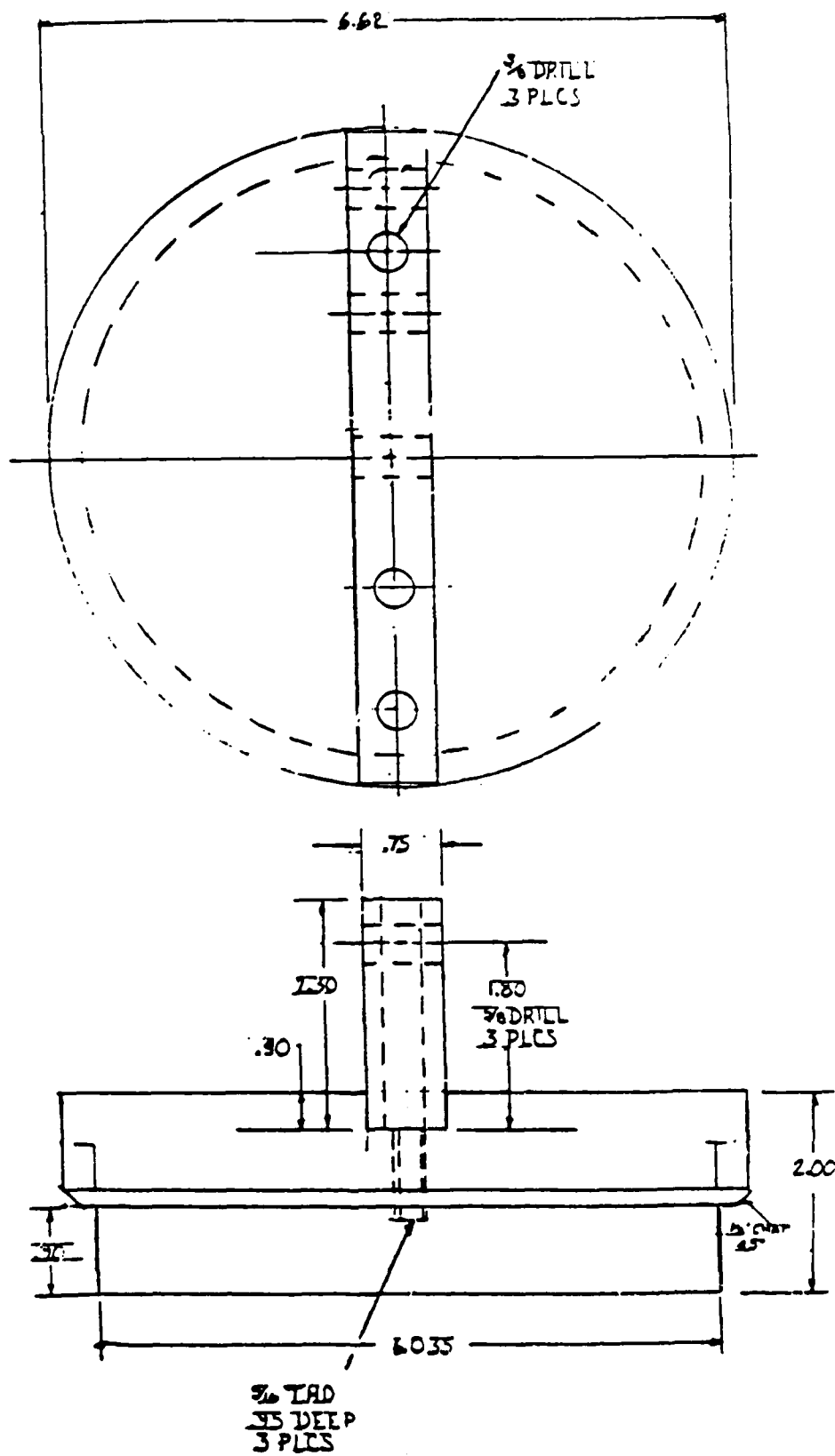
This subroutine prints the results of all the significant calculations performed in the following subroutines: FORCE, OTMOM, AND RMOM.

#### Subroutine ANCHOR

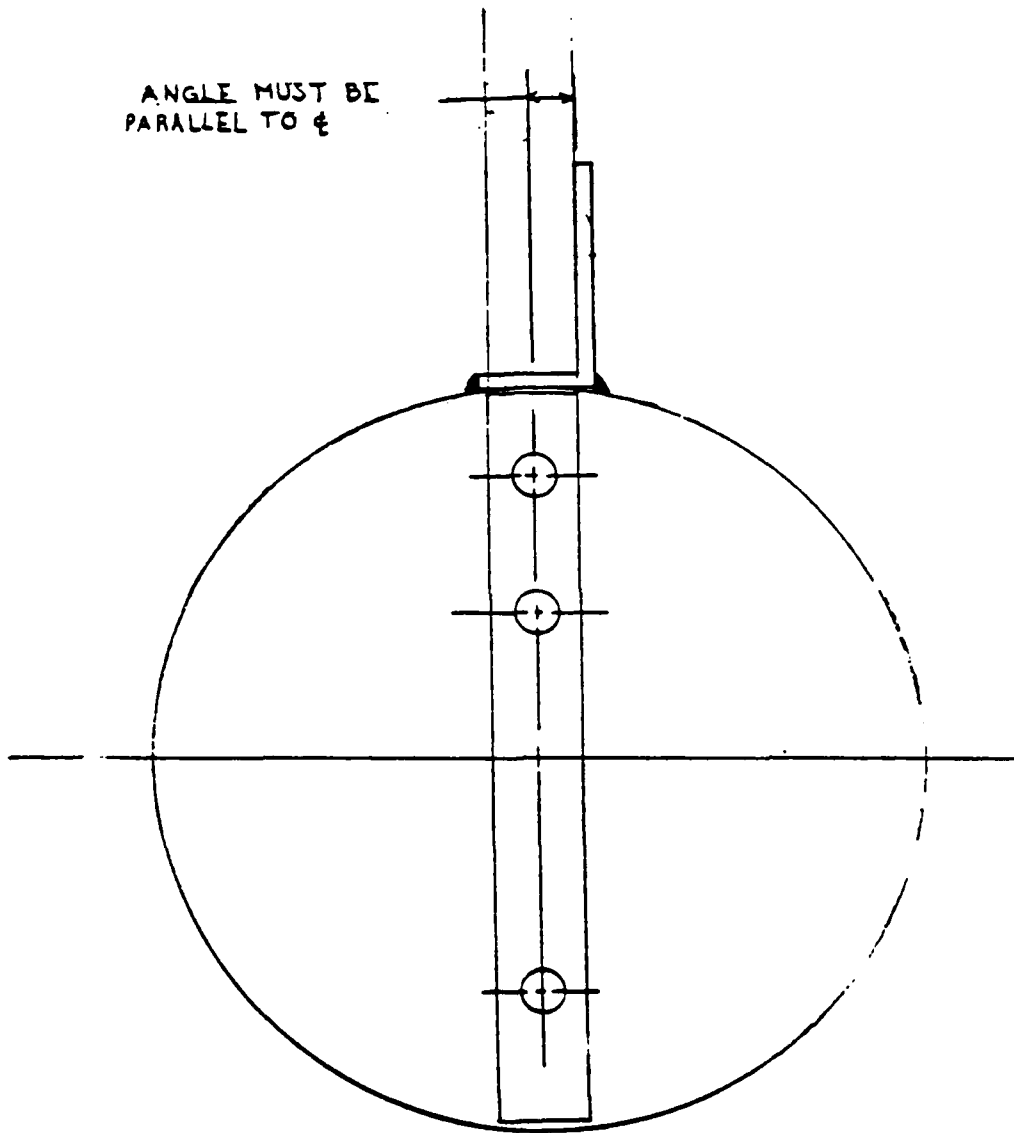
Subroutine ANCHOR determines the maximum buoyant force acting on the spar during one wave period. Subsequently, the minimum standardized anchor size needed to resist this buoyant force is determined and the factor of safety associated with this anchor selection is computed.

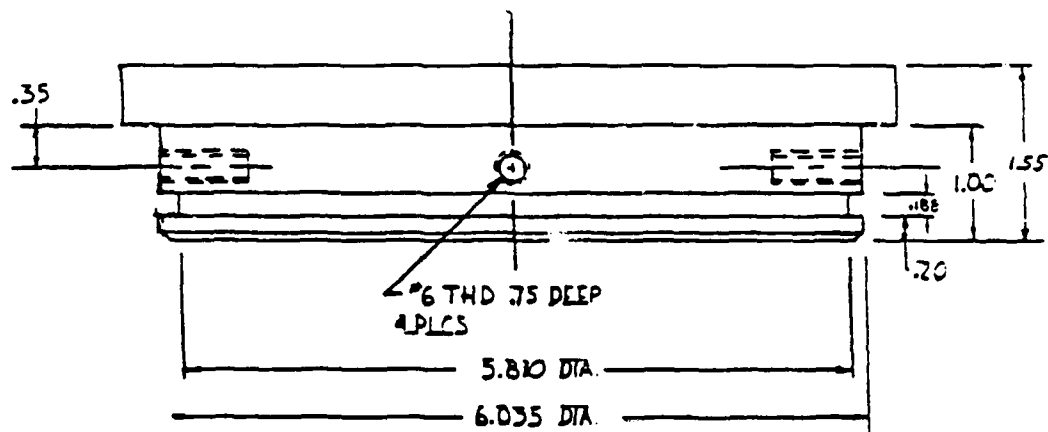
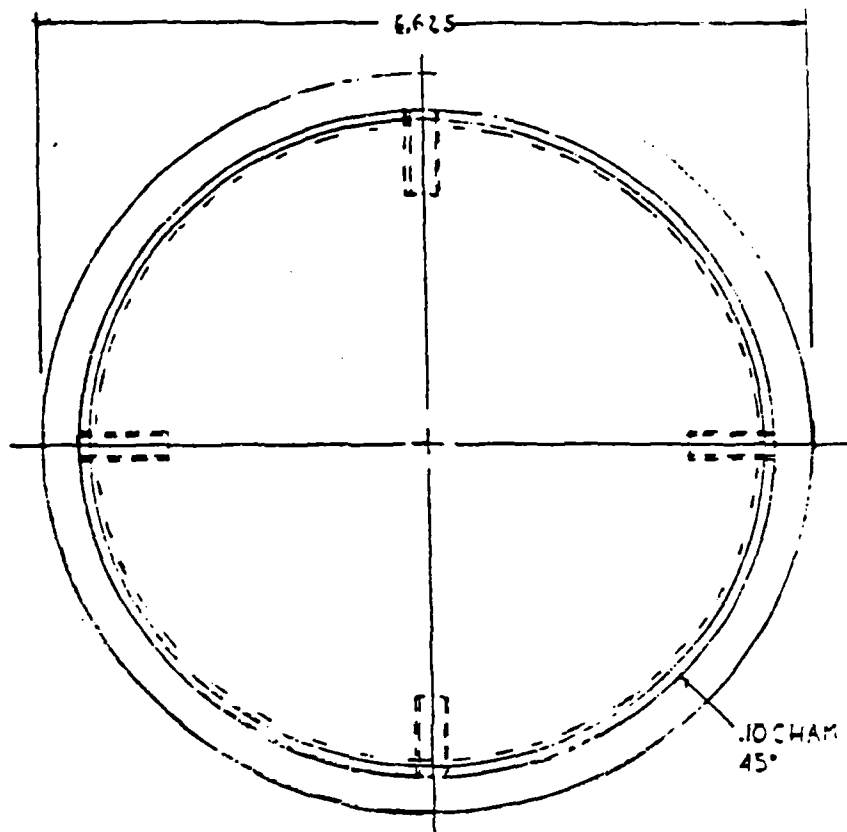
APPENDIX C

Design Drawings of the Field Test



ANGLE MUST BE  
PARALLEL TO  $\phi$







**DAT**  
**ILMI**